Department of Mechanical and Aerospace Engineering

Integrating Photovoltaic Panels and Wind Turbines for Low-Cost District Heating Systems - A Case Study of Queen's Quay District Heating Network"

Author: Ihsane Gabel

Supervisor: Dr. Paul Tuohy

A thesis submitted in partial fulfilment for the requirement of degree in

Master of Science in *Renewable Energy Systems and the Environment*

2024

Copyright Declaration

Signed: Ihsane Gabel Date: 12/08/2024

Abstract

The electricity industry is undergoing rapid changes as the pressing demand to shift from limited fossil fuels to renewable energy sources is driving substantial growth in the renewable energy industry. Hybrid Renewable Power Systems (HRPS) play a vital role in this transition by integrating renewable with traditional energy sources or the grid.

This dissertation investigates the integration and modelling of HRPS comprising photovoltaic (PV) panels and wind turbines (WT), within the Queen's Quay District Heating Network (DHN) using HOMER PRO software. The primary objective is to assess the economic and energy efficiency of three hybrid systems that are connected to the grid, comparing them to a baseline model dependent on grid electricity, with the aim of making the DHN more appealing for wider community connectivity.

The study begins with a review of Scotland's energy landscape and the goal of reaching carbon neutrality by 2045. It underscores the evolution of DHNs and the pivotal role of renewable energy technologies like heat pumps, PV systems, and wind turbines, in fostering sustainable energy solutions.

Following this review, the methodology involves selecting the study location, assessing renewable resource potential, evaluating load demand, and simulating the proposed systems. Assumptions were made regarding input parameters, including solar and wind potential, system components costs, and performance metrics as per 2024. Scenario simulations were conducted for configurations such as grid-connected PV, grid-connected WT, and a combination of WT and PV with the grid, focusing on economic viability.

Key findings based on these input parameters indicate that integrating solar and wind into the existing DHN system significantly improves economic metrics across all setups. The grid-connected wind turbine scenario proved to be the most cost-effective, achieving a 70% improvement in Net Present Cost (NPC) and an 81% improvement in the Levelized Cost of Electricity (LCOE) and the Levelized cost of Heat (LCOH). Combining both PV panels and wind turbines with the grid provides the best overall balance, ensuring a reliable energy supply with a 62% improvement in NPC and a 74% improvement in LCOE and LCOH.

While the thesis demonstrates significant achievements, it also acknowledges several limitations, including reliance on models and input data assumptions, the exclusion of certain renewable technologies, and the lack of energy storage technology modelling. Future research should prioritise incorporating extensive real-world data, explore additional renewable technologies, and enhance financial models to improve both robustness and scalability.

Acknowledgements

I sincerely thank Almighty Allah for granting me the strength, perseverance, and wisdom throughout this journey. His guidance and blessings have been a constant source of inspiration and assistance.

I am profoundly thankful to my family, particularly my parents, for their unconditional love, prayers, and support. Your confidence in my abilities has consistently driven me to aim for excellence. I would also like to extend special appreciation to my siblings and friends Abdullah, Asma, and Abdulrahman, for their continuous encouragement and understanding during the difficult moments of this journey.

I extend my heartfelt thanks to my supervisor, Dr. Paul Tuohy for his outstanding support and guidance throughout this research. His insightful feedback and steadfast patience have been crucial to the successful completion of this thesis.

I also wish to acknowledge the support and resources provided by the University of Strathclyde, which facilitated the completion of this research successfully. The access to the necessary tools, libraries, and research facilities has been crucial for my work.

I am immensely grateful to all my lecturers for their enthusiasm and expertise throughout this year of study. Your dedication has made the course far more informative, enjoyable, and fulfilling than I could have ever imagined.

Lastly, I am grateful to everyone who has directly or indirectly contributed to this thesis. Your support and encouragement have been vital in helping me achieve this milestone. Thank you all for being part of this incredible journey.

Table of Contents

List of Figure

List of Tables

Nomenclature

Symbol	Description	Units
DHN	District Heating Network	
GHG	Greenhouse Gas	
HRPS	Hybrid Renewable Power System	
QQ	Queen's Quay	
WWHC	West Whitlawburn Housing Co-operative	
COP	Coefficient of Performance	
HP	Heat Pump	
WSHP	Water Source Heat Pump	
GSHP	Ground Source Heat Pump	
ASHP	Air Source Heat pump	
PV	Photovoltaic	
WT	Wind Turbine	£/kWh
DG	Diesel Generator	£/kWh
LCOE	Levelized Cost of Energy	£
LCOH	Levelized Cost of Heat	£
NPC	Net Present Cost	£
OC	Operation Cost	
O&M	Operation and Maintenance	

1.0 Introduction

1.1 Background

Energy plays a crucial role in upholding a good standard of living in today's civilisation (Oyedepo, 2012). Nonetheless, countries worldwide are facing significant energy issues such as increasing greenhouse gas emissions, energy usage, and growing reliance on energy imports. Burning fossil fuels is the main cause of carbon dioxide (CO2) emissions, a vital GHG that greatly influences climate change. This issue is commonly seen as one of the most urgent challenges in today's world (Oyedepo, 2012).

The Scottish Government has established ambitious targets to combat the climate change, with a goal of reaching a zero-carbon footprint by 2045 (SNP, 2022). Considerable progress has been made in decarbonising the electricity sector, with low-carbon sources accounting for 83.1% of total electricity generation by 2018. However, natural gas continues to be the primary fuel for heating in Scotland, with gas boilers powering 78% of all homes. The most used and affordable way to heat a space is through natural gas. However, it accounts for most the country's CO2 emissions. In response, the government has set a target to fulfil 50% of the country's energy need with renewable sources by 2030 (SNP, 2022).

Although heat networks now meet about 2-3% of the heating demand in the UK, research shows that there is great room for expansion. The UK Government aims to increase this to about 20% by 2050 as part of its broader decarbonisation strategy. These networks are particularly efficient at reducing CO2 emissions from buildings by using low-carbon technologies and integrating multiple heat sources (Department for Energy Security and Net Zero, 2024). In March 2020, Scotland became the first country in the UK to legislate for the establishment of heat networks, setting regulations for their provision, construction, and operation. By 2020, It had over 830 functioning heat networks and aimed to deliver 1.5 TWh of heat. The District Heating Loan Fund was created to address financial and technical challenges, avoiding issues associated with commercial borrowing (Slaihem, 2021).

The concept of District Heating (DH) emerged in the 1880s. DH systems transfer thermal power from a central source to nearby consumers, providing both heating and cooling (Ewing, 2020). These systems perform well in areas with considerable heat

demand, like cities. They offer heating for buildings and hot water for households using geothermal or waste energy from power production methods like waste incineration or industrial processes (Ewing, 2020).

District heating networks (DHNs) have evolved through various generations, each reflecting the dominant energy sources and government policies of its time (McKeown, 2020). The initial generation, utilised steam generated by coal combustion or waste heat from industrial processes. High steam distribution temperatures in these systems led to considerable thermal losses and safety concerns, including the potential for hazardous steam explosions. The second generation made its debut in the 1930s and maintained temperatures close to 100°C by using hot water instead of steam. Concurrent with the widespread industrial electrification, this shifts enhanced security and made it possible to use heat from combined heat and power plants (CHP) more effectively (McKeown, 2020). Although these developments, the price volatility of fuels, especially oil, continued to be a significant worry. Introduced in Nordic countries in the 1980s, the third generation represented a major change by combining heat pumps with biomass and conventional fossil fuels. These systems were distinguished by a diverse array of energy sources, prefabricated insulated pipes to reduce heat loss, and lower distribution temperatures (McKeown, 2020).

The fourth generation, one of the recent generations of DHNs emphasises decarbonising the heating sector through renewable energy integration, lower temperature distribution, and smart energy systems (Lund et al., 2018). The fifth generation further advances these concepts by using ambient temperature networks with individual heat pumps, significantly improving efficiency and sustainability (Lund et al., 2018). DHNs in Scotland utilise various heat sources, including water source heat pumps (WSHP), biomass, CHP plants, and ground source heat pumps (GSHP). These developments align with Scotland's strategic objectives, which include decarbonising its heat supply, lowering overall energy consumption, and guaranteeing energy security for consumers at a reasonable price (Slaihem, 2021).

Heat pumps are a low-carbon alternative that require little work energy to transform low-grade, low-value heat sources into higher-grade, higher-value heat sources (Millar, 2022). Heat pumps are essential components of renewable heating technologies, but the source of the electricity they consume determines how sustainable they are overall. Air, ground, and water are the three primary types of

thermal resources for heat pumps. Every variety has a unique set of benefits and drawbacks (Millar, 2022).

To access stable heat sources, Ground Source Heat Pumps (GSHP) are usually installed tens or even hundreds of metres underground. To maximise heat absorption, some GSHP systems run close to the surface, anywhere from one to five metres deep, using vast pipe networks. For instance, pipes are used in Sohnius-Weide, Germany's district heating system (Millar, 2022).

Water Source Heat Pumps (WSHP) employ variety of water bodies, including lakes, rivers, seas, and groundwater (Ewing, 2020). Groundwater systems necessitate excavation to reach water stored between rock layers, which may be naturally occurring or found in abandoned mine shafts. The DHN in Heerlen, Netherlands, is one example of this, as it uses three different mines for various temperature heat sources. River source heat pumps are also popular due to successful implementations, such as the Drammen DHN in Norway, which draws energy from a hydroelectric dam, and another system under construction on the Clyde River in Glasgow (Ewing, 2020).

The Coefficient of Performance (COP) for heat pumps measures the efficiency of converting electricity into heat (Hedegaard, 2013). For example, if the COP is 3, it shows that the heat pump requires 1 kWh of electricity and 2 kWh of heat from the source to generate an output of 3 kWh of heat. The COP depends on the temperature lift, which is the difference between the heat source temperature and the output temperature. Higher temperature lifts lead to lower COP values (Hedegaard, 2013).

The Queens Quay District Heating Network (DHN) situated in the former John Brown Shipyard in Clydebank near Glasgow, is a pioneering project led by West Dunbartonshire Council, and funded by the Scottish Government's Low Carbon Infrastructure Investment Programme, is an essential component of a £250 million regeneration initiative (Moran, 2021). It is designed to be scalable, with the intention to link upcoming projects such as a health centre, library, town hall, and approximately 1,200 residences (Moran, 2021). Two ammonia heat pumps, each with a capacity of 2.65 MWth are at the heart of this network and were designed by Star Renewable Energy. They utilise water from the River Clyde to heat water to 80°C, this heated water is then distributed via a 5 km underground pipe network, providing low-carbon heating to several buildings.

The system has a 130 m³ thermal storage unit to improve heat supply and gas boilers that provide another 15 MW for high demand, ensuring Stability. This project showcases the outstanding efficiency of WSHPs and benefits from the ongoing decarbonisation of the electricity grid, resulting in significant reductions in both energy costs and carbon emissions (Queens Quay: Water Source Heat Pump Scheme in Scotland, no date).

Figure 1: Energy centre of Queen's Quay DHN (Queens Quay: Water Source Heat Pump Scheme in Scotland, no date).

Solar and wind energy are widely recognised as non-depleting, location-specific, and environmentally friendly renewable energy sources. Since the 1970s oil crisis, their importance and cost-effectiveness have risen significantly (Soloha et al., 2017). Nevertheless, both energy sources face the issue of intermittency. Solar power is reliant on variable sunlight hours, whereas wind power requires relatively high cut-in wind speeds, resulting in inefficient use and misalignment with demand (Soloha et al., 2017). Consequently, standalone systems frequently require overestimation to ensure reliability, increasing costs. Despite higher initial installation costs, solar and wind systems have much lower operating and maintenance costs than diesel generators (Deshmukh, and Deshmukh, 2008). In DHNs, solar energy can be integrated through

solar thermal collectors or PV systems, directly heating water for distribution. While Wind energy can be converted to heat in DHNs, beneficial in grid-congested scenarios or where wind power is curtailed, as demonstrated by projects like the Drammen DHN in Norway (Soloha et al., 2017).

1.2 Aim and Deliverables

Aim

This thesis aims to investigate the advantages of incorporating wind and solar technologies into the 4th generation DHN at Queen's Quay. The focus is on enhancing both the Levelized Cost of Electricity (LCOE) and the Levelized Cost of Heat (LCOH), crucial metrics for assessing the long-term economic viability and efficiency of energy systems. By improving these costs, the study aims to promote economic efficiency and boost consumer connectivity to the DHN and diversify the energy mix for heat pumps, ensuring they draw electricity from the grid, wind turbines, or PV systems to achieve the lowest LCOE and LCOH.

Deliverables

- Conduct a comprehensive evaluation of the current DHN system at Queen's Quay
- Analyse the study location solar and wind energy resources' availability
- Conduct parametric study and develop system models
- Perform an economic and technical assessment of the hybrid systems
- Improve the system configuration to achieve the lowest possible LCOE and LCOH
- Provide zip folders of the simulation models as separate files along with the dissertation

1.3 Methodological Approach

The methodological approach encompasses crucial steps to effectively integrate and simulate a PV/Wind Hybrid Renewable Power System (HRPS) within the Queen's Quay DHN. The process begins with a comprehensive literature review to establish a solid foundation of existing knowledge. Following this, the most suitable energy

microgrid software is selected, based on the specific requirements and the depth of the study desired.

Next, a baseline model is established using existing grid data. The study then progresses to the analysis of three primary datasets: selecting the study location, evaluating the available solar and wind resources, and calculating the electrical load required for heat pumps.

Subsequently, the new electricity supply components are integrated d to model three distinct system configurations: grid-connected PV, grid-connected WT, and a combination of both PV and WT along with the grid.

The findings are then analysed and compared to determine the most advantageous scenario, focusing on minimising economic costs and enhancing energy autonomy. Finally, the approach considers the study's limitations, suggesting areas for further research, and ends with a summary of the results.

Scope In and Scope Out

<u>The study includes:</u>

- Detailed evaluation of the load demand of the heat pumps
- Comprehensive evaluation of solar and wind energy resources in QQ
- Implementation of WT and PV systems at QQ DHN
- Assessing economic feasibility through LCOE, LCOH, and NPC calculations

<u>The study excludes:</u>

- The energy storage technologies in-depth analysis and model
- A comprehensive policy and regulatory analysis
- A completed lifecycle environmental assessment
- A Sensitivity analysis

2.0 Literature Review

This chapter offers an in-depth review of the current literature and tools for incorporating solar and wind energy within DHNs. This review will gather key information for the thesis's subsequent sections, highlighting both the strengths and limitations of previous studies. The goal is to establish the foundation for the analysis and methodology used in the project, ensuring a comprehensive understanding of the current state of research and technology.

2.1 Renewable Energy Overview

2.1.1 Global and Regional Developments

Renewable energy uses naturally replenishing resources like solar, geothermal, wind, biomass, and hydropower. The need to address environmental pollution caused by fossil fuels and their costs fluctuation, has caused a move towards renewable energy sources (Lund et al., 2007). Therefore, this energy has become an essential approach for reducing environmental impact and reducing and promoting long term energy development (Lund et al., 2007). The capacity for renewable electricity has consistently risen from 2009 to 2020, averaging more than 700 MW of growth per year since late 2009 (Scottish Renewables, n.d.), as depicted in figure 2.

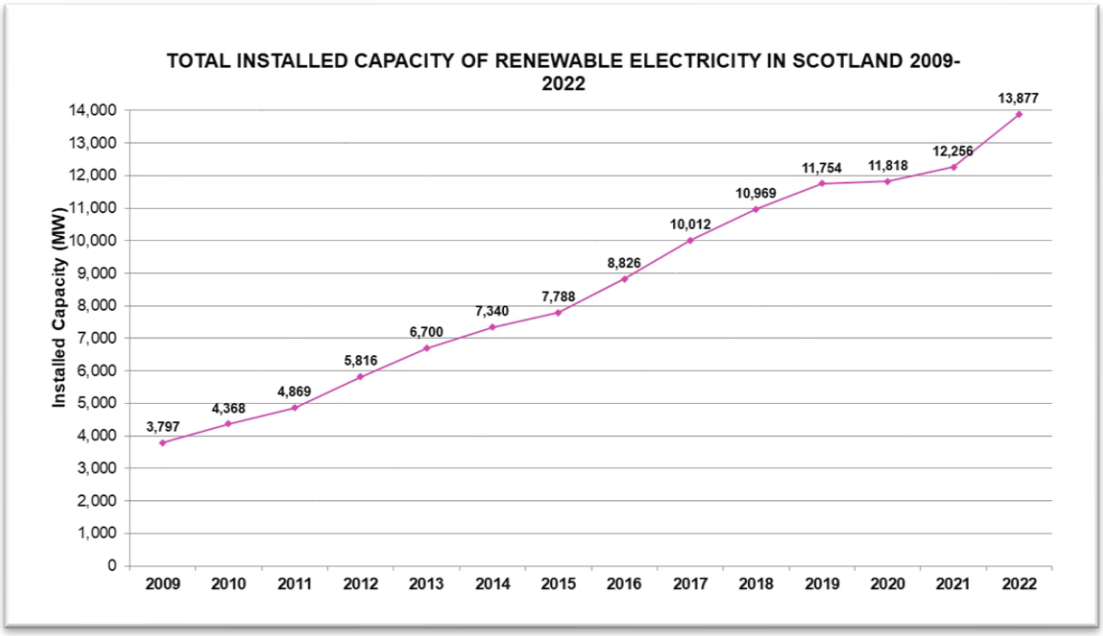

Figure 2:Total Installed Capacity of Renewable Electricity in Scotland 2009-2022 (Scottish renewables, no date).

2.1.2 Renewable Electricity Supply in Scotland

In the year 2022, there was a significant increase in renewable electricity production in Scotland, with a total output of 35.3 TWh. Multiple sources contributed to this significant increase: onshore wind energy produced 21,788 GWh, offshore wind generated 5,755 GWh, hydro produced 4,866 GWh, solar PV contributed 455 GWh, wave and tidal energy added 10 GWh, and biomass and waste provided 2,379 GWh. This represented a 28.1% rise from 2021 and a 9.8% boost from 2020, reaching a new record for yearly renewable energy generation, exceeding the previous high set in 2020. (figure 3) (Scottish renewables, no date).

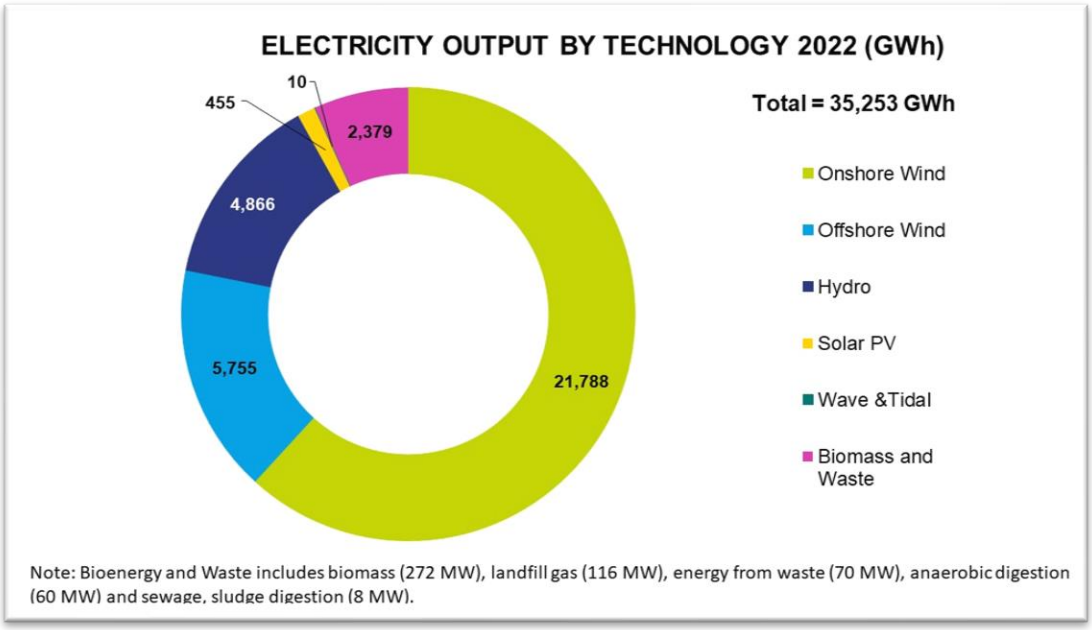

Figure 3: 2022 Renewable Electricity Output by Technology (Scottish renewables, no date).

Solar power is a sustainable and CO2-neutral source, utilised both for producing hot water and heating spaces (Ghenai and Bettayeb, 2020). Scotland saw a substantial rise in solar PV capacity during the early 2010s, from 2 MW in 2010 to 326 MW in 2016. Nevertheless, there has been a decrease in the growth rate in the past few years, as capacity reached 522 MW by March 2023. The slowdown is most likely caused by the end of Renewables Obligation accreditation for solar projects in March 2017. In 2022, Scotland had over 61,100 solar PV installations that generated 394 GWh of electricity, enough to power over 90,000 homes for a year. Furthermore, 28 MW of solar projects are scheduled for development by March 2023 (Scottish renewables, no date).

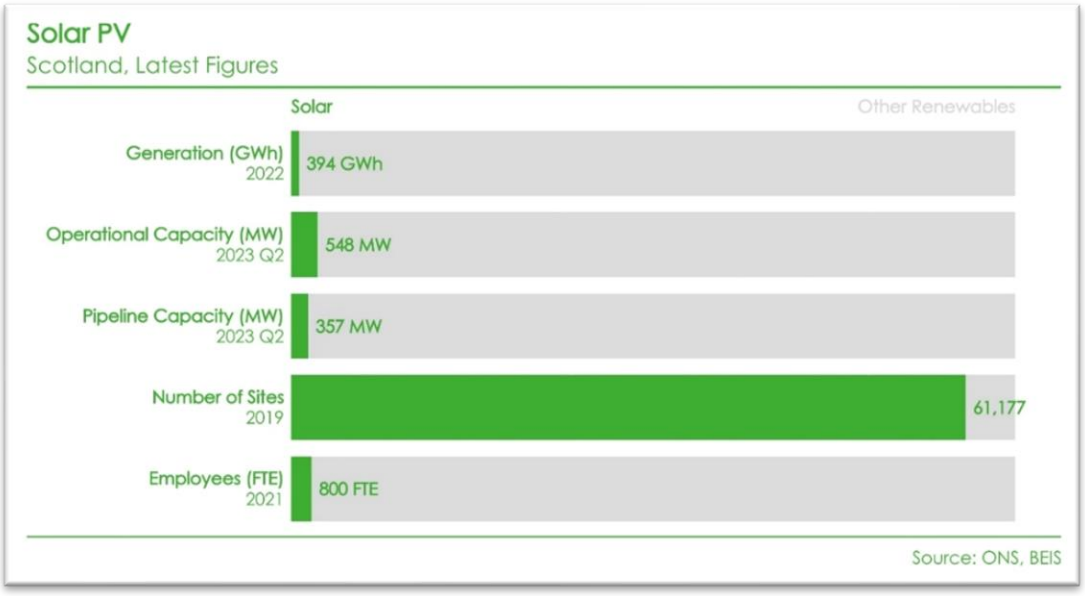

Figure 4: Solar PV, Scotland Latest Figures (Scottish Energy Statistics Hub, 2024).

Wind energy is acknowledged worldwide as a crucial form of renewable energy necessary for cutting down on GHG emissions and decrease reliance on conventional power, mainly because of its economic viability (Hedegaard, 2013). This fact is clear from the substantial planned expansions of wind energy capacities in different countries. In contrast to dispatchable energy sources like biomass-fired power plants, wind power is unpredictable and inconsistent, which makes it difficult to seamlessly integrate into the energy grid. The variable character of wind may result in scenarios where wind power generation surpasses the need for electricity, requiring enforced electricity export (Hedegaard, 2013).

In Scotland, onshore wind power is the primary renewable energy source for generating electricity (figure 5). In the year 2022, the nation produced 21,975 GWh of electricity from land-based wind sources, making up 61.5% of its renewable energy and sufficient to supply power to all homes in Scotland for nearly two years (Scottish Energy Statistics Hub, 2024). By March 2023, there are 3,500 operational sites with a total onshore wind capacity of 9.3 GW. Since 2009, this industry has experienced significant growth, with both its capacity and output increasing more than four times. In 2021, approximately 3,300 full-time jobs were created by onshore wind, leading to a turnover of £1.98 billion. The onshore wind industry in Scotland is still growing, with 10.3 GW of projects currently being developed (Scottish Energy Statistics Hub, 2024).

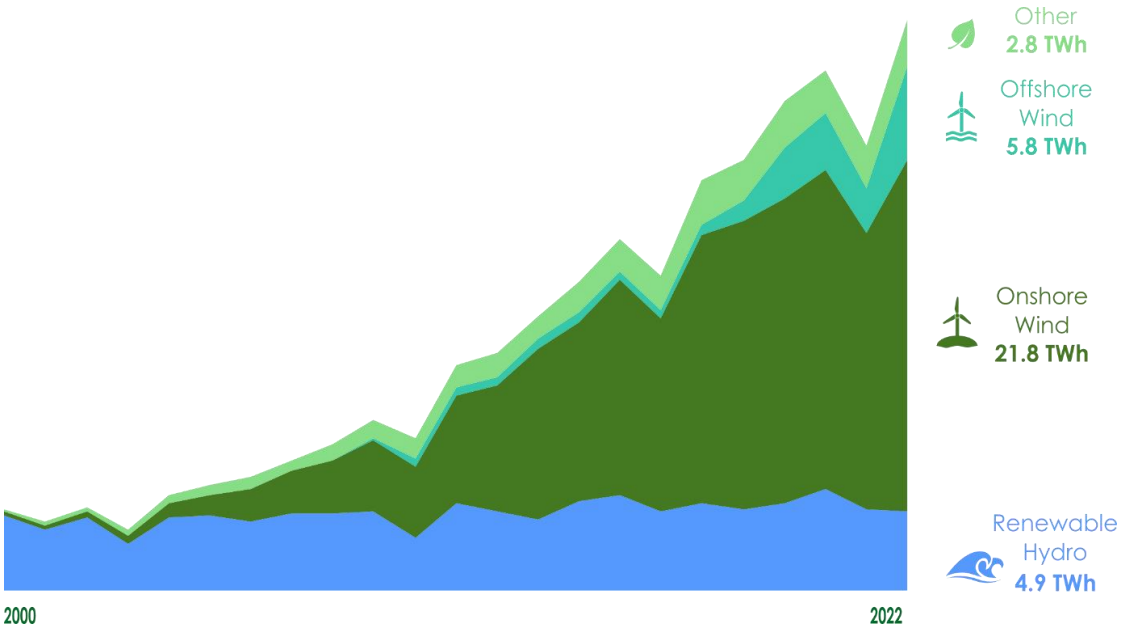

Figure 5:Onshore and offshore Wind Energy Generation (Scottish Energy Statistics Hub, 2024).

As of March 2023, offshore wind played a significant role in Scotland's renewable energy sector, accounting for a capacity of 2.4 GW. In 2022, there was a slight decrease in offshore wind electricity generation to 5.8 TWh from 3.5 TWh in 2020 as illustrated in figure 6. In 2021, the offshore wind industry produced £2.59 billion in revenue and sustained around 3,100 full-time equivalent positions (Scottish Energy Statistics Hub, 2024).

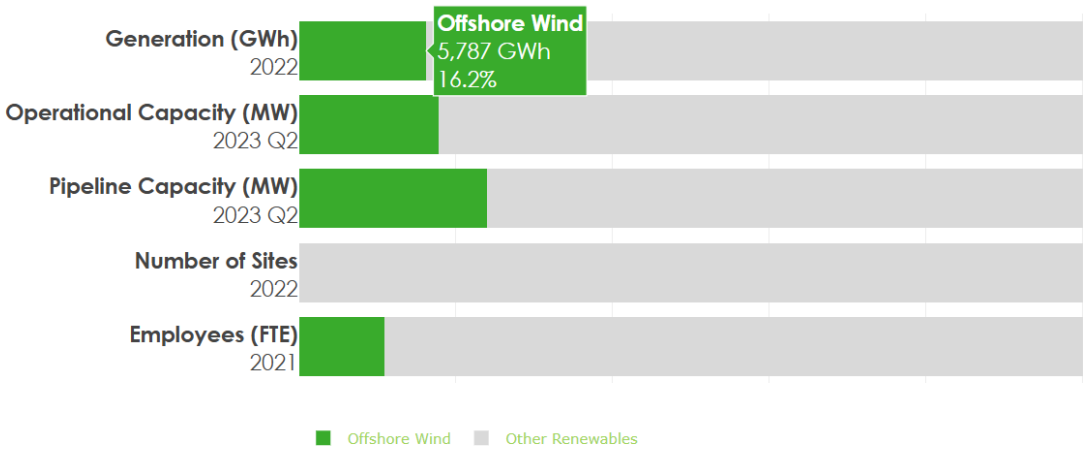

Figure 6:Offshore wind generation 2022 in Scotland (Scottish Energy Statistics Hub, 2024).

2.1.3 Scotland’s Carbon Footprint

Over the last twenty years, there has been a notable reduction in Scotland's carbon footprint, which calculates the GHG emissions linked to Scottish consumer activity. Impacted by different industries like transportation, commerce, farming, energy, housing, waste management, government, manufacturing, and urban planning (Scotland’s carbon footprint 1998-2020, 2024). From 1998 to 2020, Scotland saw a 33.3% drop in its carbon footprint. The trend of Scotland's carbon footprint did not always decrease consistently during this timeframe. It increased steadily from 2001 to a high point of 81.2 MtCO2e in 2007. Nonetheless, following 2007, in conjunction with the worldwide economic downturn, there was a significant decrease. After that, other than small rises in 2012 and 2018, the carbon footprint has gone down every year. In 2020, 76.1% of Scotland's overall carbon footprint was due to CO2, up from 73.6% in 1998. This shows that even though there has been a general decrease in emissions, the percentage of CO2 in the mixture has slightly gone up (Scotland’s carbon footprint 1998-2020, 2024).

It is crucial to mention that the year 2020 stood out as unconventional because of the COVID-19 pandemic. The consumption-based emissions were notably affected by national lockdowns and travel restrictions, especially in areas like transportation, leisure, and hospitality. In 2020, emissions from transportation directly produced by households decreased by 24.4%, for example. The Scottish Government (Scotland’s carbon footprint 1998-2020, 2024).

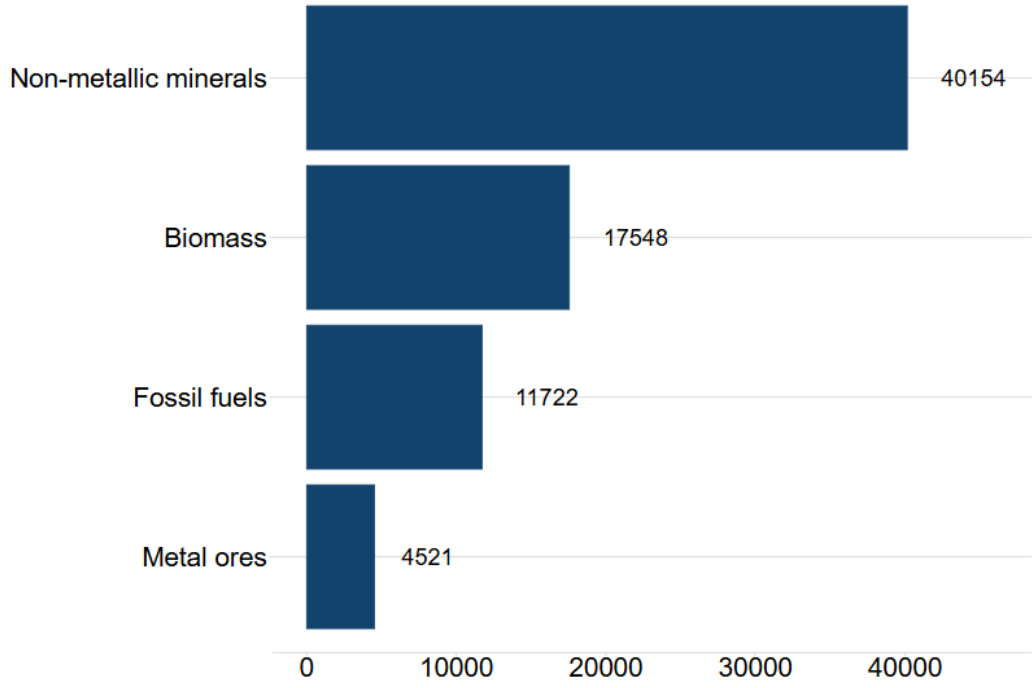

Figure 7: Material footprint of Scotland by type, 2020. Quantities expressed in thousand tonnes (The carbon footprint of Scotland, 1998–2020, 2024).

2.2 District Heating Network

2.2.1 Overview, Types and Evolution of the District Heating Network (DHN)

District heating is a proven technology that has the potential to significantly decrease carbon emissions and improve energy efficiency. Recently, it has become more popular as a substitute for single natural gas boilers, providing heat to various buildings from central generation locations (Buffa et al., 2019).

DHNs can effectively supply regions with high heat concentration, as long as there is a suitable heat source accessible (Millar, 2022). These systems take advantage of cost savings from operating at a larger scale, providing a lot of flexibility and improved supply security with no local emissions. On the other hand, remote or sparsely populated areas usually have to depend on separate heating systems because the costs of installing and running a district heating system would be too high (Millar, 2022).

DHNs are categorised according to criteria including the type of heat transfer fluid, source of energy, and when they were installed, with definitions potentially differing depending on the source (McKeown, 2020).

To fully comprehend DHNs, it is crucial to analyse specific schemes instead of just depending on general generational descriptions. In the past, DHNs have transitioned from high enthalpy, simple systems (1st Generation) (figure 8) to complex systems with various technological integrations (3rd and 4th Generations) (McKeown, 2020). DH scheme designs are evolving to reflect changes in societal heat usage. As buildings become more energy-efficient and there is an emphasis on decarbonising heat supply, there is a shift from 3rd generation networks to 4th generation networks. These newer systems are decentralised and operate at lower distribution temperatures (McKeown, 2020).

DHNs supply heat to several buildings in a specific area using different heat sources based on local accessibility. According to Millar (2022), there are several different sources, including nuclear power, biomass, fossil fuels, waste heat, solar thermal energy, cogenerated heat, and ground source heat pumps. The Monterusciello system, which effectively uses geothermal energy in Italy, is a significant example in Europe. An underground network of well-insulated pipes effectively transfers heat by transferring hot water to buildings and returning chiller water to the heat source, all while minimising heat loss (Millar, 2022).

Conventional DH systems use centralised power plants to distribute hot water or steam to urban areas via a network of pipes. These high-temperature systems frequently face substantial heat losses and expensive installation expenses (McKeown**,** 2020). In the summer, DH systems usually only work for heating water, and up to 30% of the energy provided can be lost through heat due to water being kept in the network for a long time. McKeown (2020) state that the economic sustainability of traditional high-temperature DH systems may face challenges due to these issues, along with reduced heating demand from renovated buildings. In conventional heating and cooling system, users cannot exchange energy within the network and are reliant on a market driven solely by consumption. To tackle these obstacles, ongoing research is concentrating on the advancement of 4th and 5th Generation District Heating and Cooling (DHC) networks, which improve efficiency by operating at reduced temperatures (Brown et al., 2022).

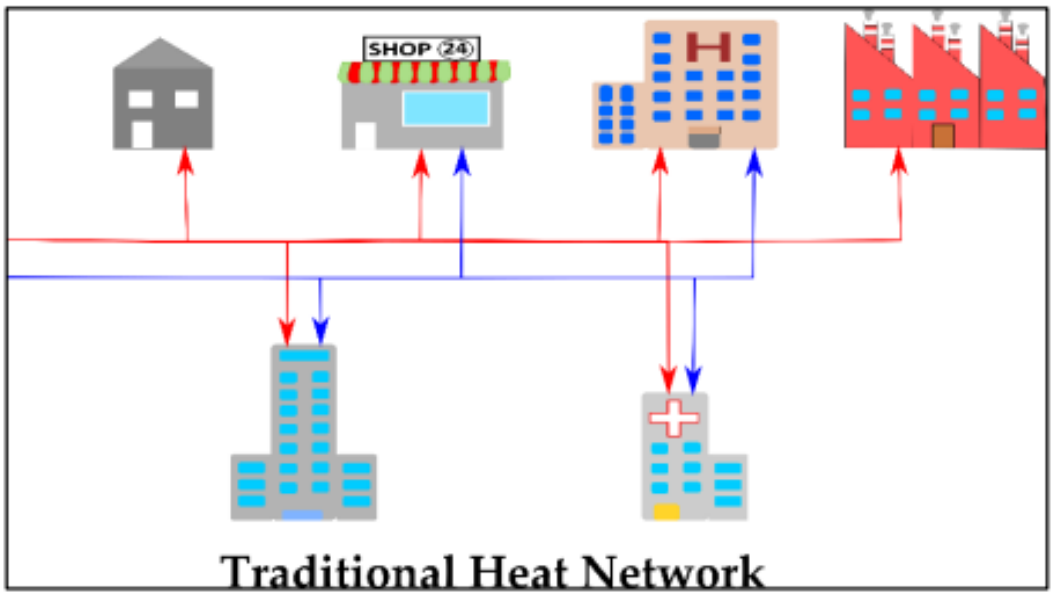

Figure 8:Traditional Heat Network (Millar et al., 2020).

Lund et al. (2014) emphasise the importance of 4GDH systems for the future of district heating (refer to figure 9). These networks play a crucial role in sustainable energy frameworks by integrating renewable energy sources, enhancing energy efficiency, and utilising combined heat and power (CHP) generation.

4GDH systems successfully tackle problems such as infrastructure incompatibility and low heat demand density through aligning energy sources with user demand. They assist in capturing extra heat and incorporating renewable energy sources. However, one limitation is that 4GDH pipes cannot provide simultaneous heating and cooling services for multiple buildings (Lund et al., 2014).

5GDH, in contrast to earlier versions, combines the heating needs of users with the cooling needs of others by utilising sources of low-grade heat such as excess heat from supermarket refrigeration units or industrial waste heat. This leads to a decentralised prosumer market (Millar et al., 2020). 5GDH systems function at temperatures that are lower (10–40°C), This requires the use of heat pumps for elevation. The market viability and pricing strategies of 5GDH are still under scrutiny, despite its potential to enhance efficiency and lower capital costs when compared to traditional systems (Millar et al., 2020).

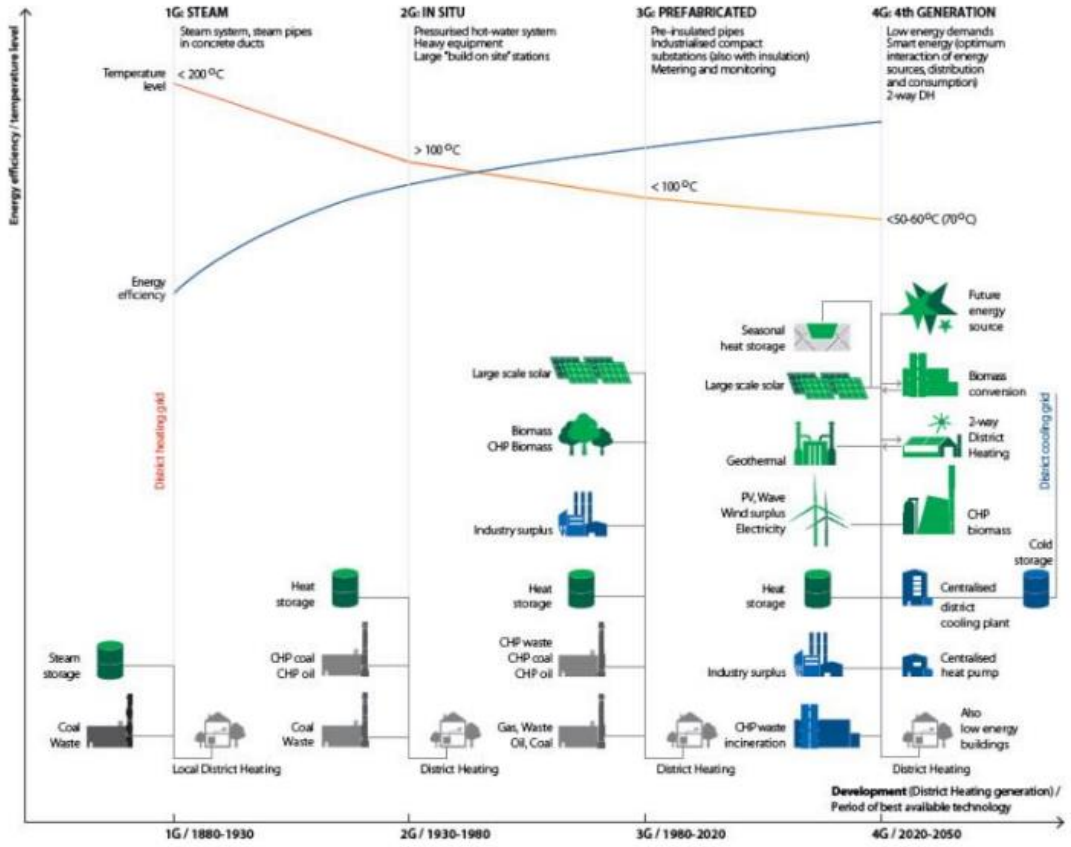

Figure 9: District Heating System Development: The Path to 4th Generation Solutions (Lund et al., 2014)

2.2.2 Case studies on Integrating HPs into District Heating Networks

Heat pump DH systems can either be incorporated into current setups or created as fresh installations, frequently with peak boilers included to ensure efficiency and dependability (Auer, 2019). These systems differ in their intended use (heating and cooling, heating, cooling), heat source (sewage water, industrial waste heat, geothermal, solar), heat pump placement (central, central with decentralised boosters, fully decentralised), and distribution temperature (high >80°C, low >50°C, ultra-low >35°C, ambient >5°C) (Ewing, 2020).

Utilising surplus heat from a nearby river and a CHP plant, Wien Energie HP integrates excess heat into Vienna's existing high-temperature DH system (Figure 10). Friotherm produces a sizable heat pump that can supply the DHN at temperatures as high as 95°C

by using waste heat that ranges from 6°C to 27°C. The system's estimated seasonal performance factor is 3, and its capacity is 40 MW (Auer, 2019).

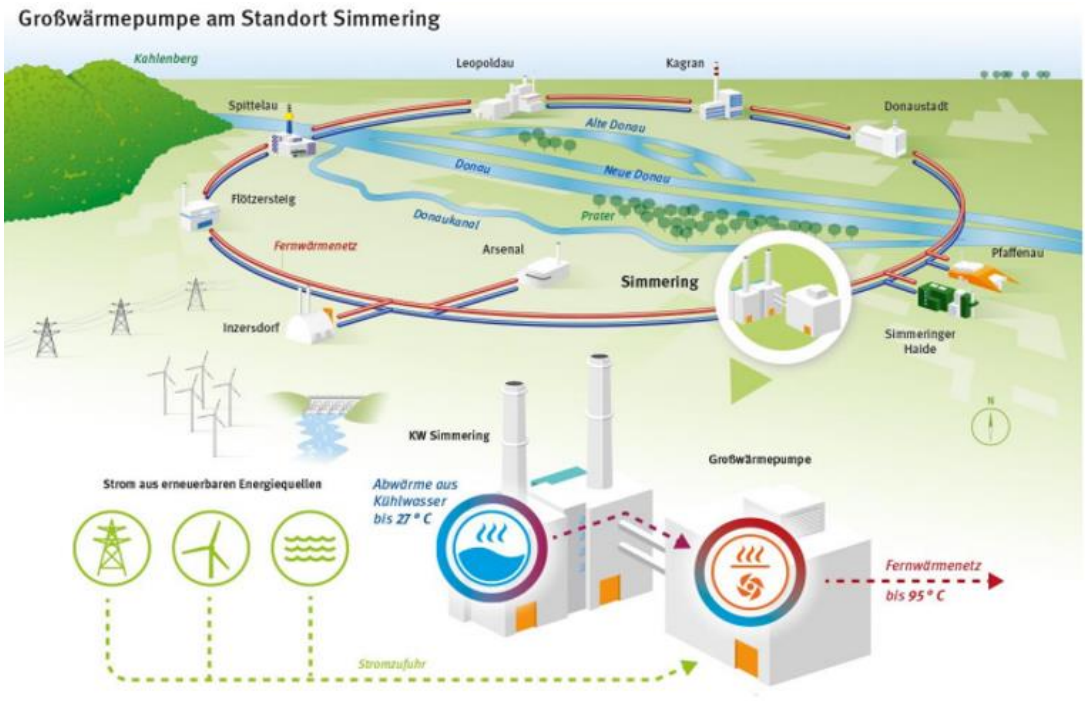

Figure 10: Wien energy schematic of large-scale heat pump integration (Auer, 2019)

The Glasgow Housing Association (GHA) at Hillpark Drive initiated a retrofit project to address fuel poverty and reduce carbon emissions by replacing costly electric storage heaters with a district heating network powered by an ASHP. Other options for heating were investigated but ultimately turned down: biomass was not selected because of worries about air pollution, GSHPs were not viable because of limited space, and WSHPs were not feasible due to a lack of appropriate water source (Jures, 2016; McKeown, 2020).

Figure 11: ASHP deployed at Hillpark Drive DHN (UK's largest residential air -source heat pump halves the cost of energy for flats in hillpark, no date).

Copenhagen DHN that uses renewable energy sources like biomass, waste incineration, and geothermal energy is another successful case study. It highlights the transition to 4th and 5th generation systems aimed at improving efficiency and reducing heat loss through lower distribution temperatures (Jensen et al., 2017). The case study examines the design and implementation of a serially connected ammonia-water hybrid absorption-compression heat pump (HACHP) for the Greater Copenhagen DH network. This system utilises a geothermal heat source at 73°C to generate 7.2 MW of heat at 85°C, supporting Copenhagen's 2025 CO2-neutral heating target (Jensen et al., 2017).

Figure 12: Copenhill: Copenhagen's Iconic Waste-to-Energy Facility by Bjarke Ingels Group (Danish district heating – The heat of the moment. 2020).

2.3 Heat pumps

2.3.1 Overview and Types

Interest in heat pumps (HPs) has increased due to the rising prices of fuel and growing worries about global warming. By recycling waste and ambient heat back into the heat generation process, they offer a very efficient way to combat the greenhouse effect (Chua et al., 2010).

HPs utilise ambient heat from the environment that is constantly replenished by a renewable heat source that conventional heat production technologies do not access. Typically, they rely on external energy sources like the electric grid, with their environmental impact being determined by the carbon intensity of the electricity they use (Cutting, 2020). Three primary heat pump categories include ground (GSHP), air (ASHP), and water (WSHP), are distinguished by their heat sources.

GSHPs utilise underground exchangers to extract ground heat. Typically, these systems use deep boreholes or extensive piping to maintain stable underground temperatures (Olabi et al., 2023). Failure to accurately estimate the necessary heating

can deplete the heat reservoir due to poor design. Water found in sealed mine shafts is occasionally repurposed for different uses. In Heerlen, Netherlands, a DHN utilises three separate mines as heat sinks operating at various temperatures (Olabi et al., 2023).

ASHPs are commonly used in a mix of heating applications because they can draw heat from the surrounding air using open heat exchangers. In Glasgow, a 400 kW ASHP is employed in DHNs as an illustration of their application (Carroll et al., 2020).

WSHPs are placed underwater to remove heat from water with consistent temperatures. They can be linked to multiple bodies of water, like lakes, rivers, seas, and groundwater. Every category of WSHP has its own benefits and drawbacks, which make them appropriate for various uses (Reiners et al., 2021).

2.3.2 Mechanics of Heat Pumps

Heat pumps work by using electricity to power a refrigeration process that moves heat from a ground, air, or water source to a destination. This procedure results in producing more heat than the energy put in, achieving high efficiencies (COP of 3 or higher) (Cutting, 2020**).**

Heat pumps are sorted into different groups depending on various qualities. One way to categorise heat pumps is by the thermodynamic cycle they use, and the fluids involved, leading to two primary types: vapor compression and absorption heat pumps (Grassi, 2017). Vapor compression heat pumps work on a reverse thermodynamic process with a compressor driven by an electric motor or engine, using environmentally safe, inert, chemically stable, non-flammable, non-toxic refrigerants with low freezing points. Absorption heat pumps do not have a mechanical compressor and rely on a combination of two fluids with varying vapor pressures, like water-lithium bromide or water-ammonia mixtures (Grassi, 2017).

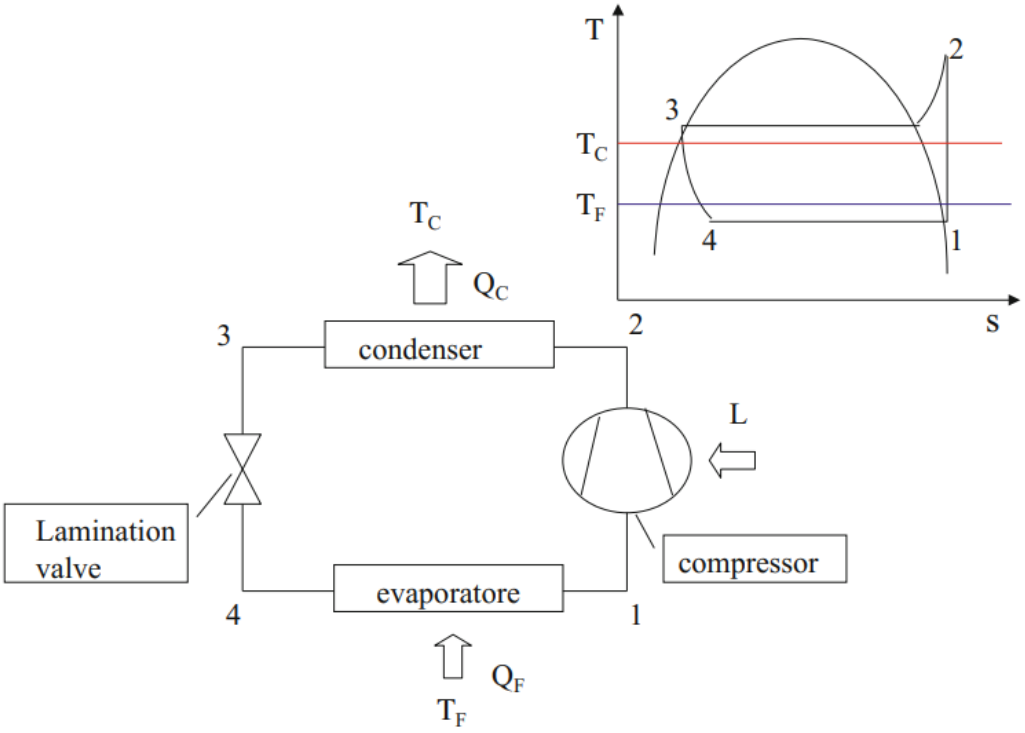

Figure 13: Heat pump diagram paired with an ideal T-s diagram positioned in the top left corner (Grassi, 2017).

2.3.3 Coefficient of Performance (COP) of Heat Pumps

The COP is used to determine how efficiently a heat pump operates. It is the ratio of energy needed for heating or cooling to the amount of effective heating or cooling given (Ewing, 2020).

$$COP = \frac{Heat\ Output\ (Q)}{Heat\ Input\ (W)}$$

Mathematically speaking, a greater COP signifies a heat pump that is more effective in delivering heating or cooling for the energy it consumes. The COP of heat pumps in the UK remains consistent at a range of 2 to 3 all year long (Moran, 2021). Seasonal coefficient of performance (SCOP) is an alternative term for evaluating heat pump efficiency, indicating the heating season's mean COP (Ewing, 2020).

Employing various techniques to estimate COP in energy planning can greatly affect economic and environmental results (Pieper et al., 2020). For example, the Constant COP Method utilises a consistent COP value year-round, usually determined by design conditions and not adjusted for changes in operating conditions. Moreover, the Lorenz Efficiency Method calculates COP by considering the ideal Lorenz cycle, modified

with a fixed Lorenz efficiency factor, using the logarithmic mean temperatures of the heat source and sink. Additionally, the Exergy Efficiency Method evaluates COP by considering the energy streams' useful work potential, which is commonly associated with Lorenz efficiency, and employs the exergy efficiency ratio. The Jensen et al. Method provides a thorough calculation considering variables such as isentropic efficiency, temperature differences in heat exchangers, and properties of the refrigerant, leading to precise COP estimates for heat pump designs (Pieper et al., 2020).

2.3.4 Water Source Ammonia HP Case Studies

The use of ammonia (NH3) as a natural refrigerant can greatly decrease emissions, as it has no ozone-depleting or global warming effects (Ayub, 2016). Ammonia heat pumps fuelled by river water provide a sustainable and cost-effective option for district heating systems. By using river water as low as 5°C, these heat pumps produce hot water up to 85°C, benefiting the environment by cooling the river slightly and potentially mitigating global warming effects (Ayub, 2016).

Large Scale

In the Norwegian municipality of Drammen, situated 40 km southwest of Oslo, a notable ammonia heat pump has been installed for district heating. Led by a local utility company, this initiative strives to improve energy efficiency and decrease environmental harm by reducing reliance on fossil fuels. Drammen authorities aimed to decrease fuel-burning boilers for DH by using Ammonia HP technology to generate water/glycol at 90°C. This novel strategy underscores the need to carefully design crucial elements in large heat pumps for effective energy retrieval and distribution at the specified temperature (Ayub, 2016).

This case study showcases the significant benefits of utilising Ammonia HPs for DH particularly in advocating for cleaner energy sources.

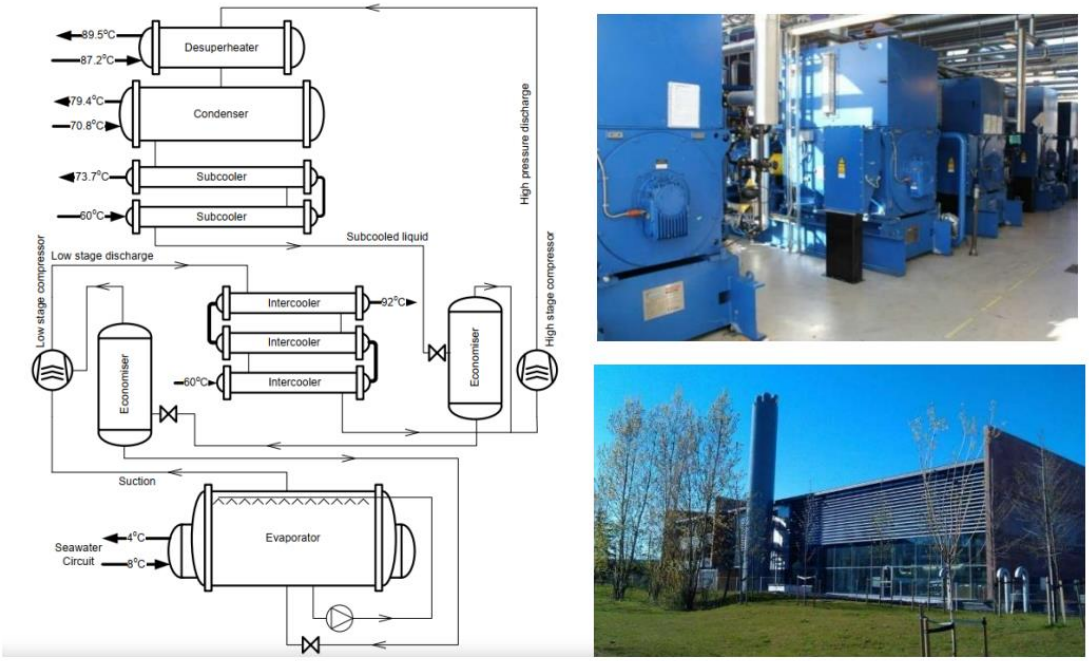

Figure 14: Drammen Heat Pump: Ammonia Cycle Schematic and Installation (Auer, 2019).

Small Scale

A 3.3 MWth HP was installed in Sala, Sweden in June 1981 to extract heat from treated sewage water for the DH system (Lindström, 1985). Initially, the HP, which had a screw compressor, faced considerable maintenance difficulties. Damage in pipes and valves occurred due to vibrations in the slide valve used for capacity control. Once these problems were dealt with, the system met the anticipated levels of performance and availability. This situation emphasises how crucial it is to have precise design considerations and consistent maintenance to guarantee the high availability and optimal performance of heat pump systems (Lindström, 1985).

2.4 Renewable Energy System and technologies: Solar and Wind

Electricity is the most utilised type of energy because it can be transmitted over great distances via cables. Electricity is generated at the power plant, sent to distribution centres through transmission wires, and finally distributed to customers via distribution grids (DeBartolo, 2015). Incorporating renewable energy technologies like photovoltaic (PV) and wind turbine (WT) systems into the current grid infrastructure is essential for promoting sustainable energy options.

2.4.1 Grid Connected Systems

2.4.1.1 Photovoltaic (PV) Systems

Solar cells in PV systems produce electric current by converting sunlight into electricity (Kamel et al., 2015). Typical PV cells are comprised of mono-crystalline and multi-crystalline silicon cells, with efficiency levels of 18-21% and 13-14%, correspondingly. Factors like solar irradiance, packing factor, and cell temperature can affect the performance of PV cells, with higher temperatures resulting in lower efficiency. Efficient cooling is crucial for maintaining productivity and for transforming waste heat into valuable energy (Kamel et al., 2015).

The transition to clean energy requires grid-connected solar energy systems (Amole et al., 2023). As an illustration, integrating solar power with the grid increases energy security through widening g the energy mix and reducing the need for imported fuels. This is especially important for countries looking to become more energy independent or those with high energy import bills (Amole et al., 2023). Grid-connected systems maintain a consistent power supply by supplementing renewable sources with grid power when energy production is low. An example would be how solar PV panels produce electricity throughout the day, with surplus power either stored or sent to the grid to maintain an equilibrium between supply and demand (Sarbu et al., 2022). Furthermore, connecting to the grid can greatly reduce operational costs by selling excess energy produced by PV systems back to the grid, offering a financial motivation for the uptake of renewable energy (Pürlü and Ozkan, 2023). Therefore, the expenses for installation and configuration can be significant, particularly when incorporating advanced features such as tracking systems and battery storage (Liu et al., 2012).
Hossain and Sadrul (2011) conducted research to investigate the financial viability and long-term reliability of grid-connected solar PV systems in Bangladesh. They concluded that implementing these systems can greatly help decrease reliance on fossil fuels, which will lessen greenhouse gas emissions and tackle the current power shortage. Nonetheless, solar energy, which is a renewable source, is naturally inconsistent and can cause fluctuations in the production of electricity. This may create difficulties in maintaining grid stability and necessitates advanced management and storage methods for ensuring a dependable power source (Pamuk, 2024; Mondal and Islam, 2011).

2.4.1.2 Wind Turbine (WT) Systems

Wind energy is extracted using wind turbines, which consist of blades attached to a rotor. As wind rotates the blades, the rotor captures kinetic energy and converts it to electrical power through a generator. The amount of energy produced is primarily dependent on the rotor diameter (Ram, 2017).

Al-Tajer and Poullikkas (2015) claim that incorporating wind power into the grid strengthens the energy supply's resilience (Al-Tajer and Poullikkas, 2015; Olabi et al, 2023). In addition, Fitzgerald et al. (2012) investigated the possibility of combining wind power with smart electric water heating system. By converting excess electricity into thermal energy, which can be stored and used when needed, this approach aims to successfully balance supply and demand. (Fitzgerald et al., 2012; Rahman et al., 2017**)**.

Integrating wind power into the grid offers significant economic and environmental benefits (Fadlallah et al., 2021). On-grid wind power systems can lower electricity costs by generating power from wind and feeding surplus energy back to the grid, thereby reducing fossil fuel reliance and creating economic benefits through savings and potential revenue from selling excess power (Fadlallah et al., 2021). Furthermore, wind is a sustainable and environmentally friendly power that aids in decreasing GHG emissions, ultimately assisting in the fight against climate change (Rehman, 2004).

2.4.1.3 Combined PV and WT Systems

The merging of PV panels with wind turbines and grid improves energy security and reliability by leveraging the complementary characteristics of solar and wind energy (Bazdar and Shirzadi, 2017). This mix guarantees a steady and reliable energy source, addressing the energy needs in a cost-efficient and environmentally friendly manner. These findings are supported by Pamuk (2024) research, which explores the feasibility and best setup of hybrid renewable systems in residential areas. Through capitalising on the synergistic relationship between solar and wind power, the study demonstrates that these systems improve energy security, reliability, and cost efficiency (Pamuk, 2024).

Khalil et al. (2021) employ HOMER Pro software to optimise and establish a hybrid energy system for the Seashore of Baluchistan. The system combines WT, PV arrays, converters, and DG to reduce operating costs, net present cost (NPC), and gas emissions, while also guaranteeing a dependable energy supply. Using the local grid as a backup power source helps decrease the necessity for battery storage, which in turn improves energy usage (Khalil et al., 2021).

This is further confirmed by Said et al. (2024), they examined combining PV, WT, and battery technologies into the present grid infrastructure in remote areas. The study concludes that this configuration is a viable solution for improving the voltage profile and meeting the energy demands. While also supports future growth and sustainability goals and minimising environmental impact (An introduction to river water ammonia heat pumps for district heating, Star Renewable Energy, no date).

2.4.2 Stand-alone Systems

2.4.2.1 Photovoltaic (PV) Systems

Stand-alone systems are effective at providing electricity to rural areas where grid extension is impractical. Tools like HOMER software help design and improve these systems (Mokheimer et al, 2015; Sen and Bhattacharyya, 2014). Hybrid systems mitigate the variability of individual sources. However, maintaining these systems in urban areas poses logistical challenges. Nevertheless, they are frequently a more economical option compared to expanding the grid, particularly considering the decreasing costs of solar PV and subsidies (Mokheimer et al., 2015; Sen and Bhattacharyya, 2014). Additionally, Off-grid solar systems provide a non-polluting alternative to traditional fossil fuel-based energy sources (El-Houari et al., 2019).

2.4.2.2 Wind Turbine (WT) Systems

Li et al. (2020) analyses the economic and technological potential of off-grid hybrid wind/diesel/battery systems in cold regions, with a specific focus on a residential district in Lanzhou, China. The research using HOMER Pro software determines that WT hybrid energy system, including DG and flow batteries is the most affordable setup. These systems offer independence in energy, sustainability in the environment,

and viability in the economy. Yet, substantial challenges exist due to high initial expenses, maintenance needs, and fluctuating levels of wind energy generation (Li et al., 2020).

Similarly, a different research project conducted by Aberilla et al. (2020), investigates the possibility of integrating wind and tidal turbines in a small-scale system to supply energy to isolated coastal settlements in New Zealand. By utilising HOMER and WRPLOT software, the research found that pairing two wind turbines and four tidal turbines with a diesel generator is the best approach to decrease environmental impacts and the overall cost. However, the research acknowledges obstacles like expensive upfront expenses and complicated upkeep tasks (Aberilla et al., 2020).

2.4.2.3 Combined PV and WT Systems

The PV and WT integration addresses the inherent intermittency and fluctuation of each source. They both complement one another, with solar power abundant during the day and wind power frequently higher at night or during different seasons. This complementary nature ensures a more consistent and stable power supply, which is particularly crucial for remote and off-grid areas.

Das et al. (2021) and See et al. (2022) demonstrate the financial and eco-friendly advantages of integrating PV and wind systems in terms of both economic and environmental impacts in remote areas. Das et al. (2021) showed that hybrid PV/Wind/Micro Gas Turbines (MGT)/Battery systems can effectively meet both electricity and thermal demands in different climate zones in Australia.

Furthermore, see et al. (2022) discovered that a hybrid PV/WT/battery/DG configuration is the best option for Malawali Island in Malaysia. Offering dependable and affordable electricity supply while also having notable environmental advantages (Lindström, 1985).

2.4.3 Viability of Grid-connected and Stand-alone HRPS in terms of Energy, Economy and the Environment

A study by Roy (2023) evaluates the energy performance of PV and wind systems in Satna District, Madhya Pradesh, India. The researchers designed grid-connected and off-grid systems to meet a typical daily requirement of 774 kWh. The on-grid system, which includes PV arrays, wind turbines, batteries, and a grid connection, demonstrated a higher renewable fraction, which represents the percentage of energy produced by renewables in relation to the overall energy usage. A higher renewable fraction indicates a greater reliance on renewable energy, allowing for the sale of excess energy, thus optimising energy use and reducing waste (Rahman et al., 2017; Sarbu et al., 2022).

The economic analysis of these systems showed that the grid-connected HRPS was less costly than the off-grid system. Selling surplus energy to the grid greatly boosts the economic viability of the on-grid system by reducing the need for large battery banks, thereby lowering the overall Net Present Cost (NPC) and Levelized Cost of Electricity (LCOE). This is supported by Türkay and Telli (2011), revealed that grid-connected systems have lower NPC and LCOE due to better energy management and the capability to return excess electricity to the grid. Standalone systems, on the other hand, require larger battery storage, resulting in higher costs and complexity (Türkay and Telli, 2011).

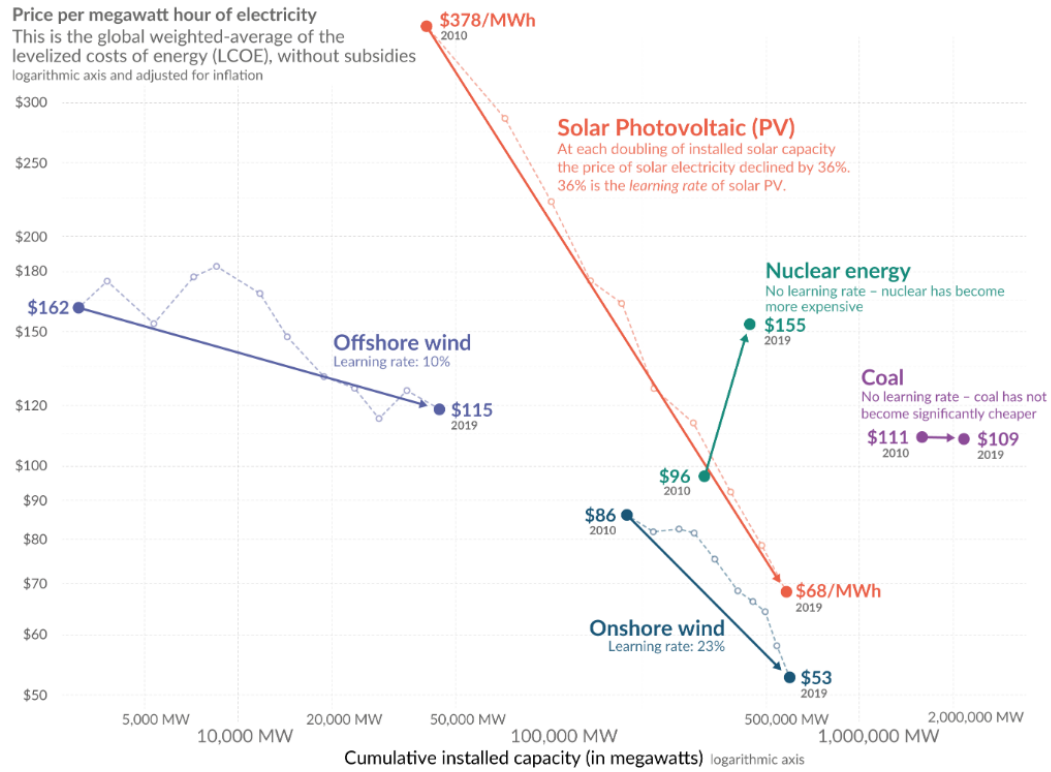

Figure 15: The Accelerating Drop in Renewable Energy Cost (Roser, 2020).

In the past years, the economic feasibility of solar and wind power has greatly improved due to major cost reductions in technology. As per the graph in figure 15, the price of solar photovoltaic (PV) power dropped by 82%, going from $378 per megawatt-hour in 2010 to $68 per megawatt-hour in 2019. In the same way, the price of onshore wind energy dropped from $86 per megawatt-hour in 2010 to $53 per megawatt-hour in 2019, representing a decrease of around 38% (Roser, 2020).

2.5 Software selection

2.5.1 Choice of Software: HOMER

Selecting the right software tools for modelling the integration of renewable energy sources within DHN is crucial for accurately assessing their potential impact. Various methodologies for software selection range from structured approaches to comprehensive analyses by researchers such as Lyden, Pepper, and Tuohy (Lyden et al., 2018).

For this study, it is essential that the software chosen has several key capabilities: time-series simulation for detailed analysis of energy flows over time, hybrid system

modelling to integrate multiple energy sources, comprehensive economic assessment through lifecycle cost analysis, a user-friendly interface for efficient model creation and troubleshooting, and reliable performance to handle complex simulations without frequent crashes. After a comprehensive review of available options and a thorough comparison with other software packages like MERIT and PyLESA, HOMER has been selected for this simulation exercise.

Initially, HOMER was compared with MERIT and was found to be a more comprehensive package. HOMER offers a broader range of technological components, which provides greater flexibility in creating models that can accommodate various energy sources and storage options. Unlike MERIT, HOMER boasts superior reliability, evidenced by its lower crash rate, ensuring consistent performance during complex simulations (Lambert, Gilman and Lilienthal, 2006).

In contrast, PyLESA excels in adaptability, detailed thermal storage modelling, and dynamic market simulations. Its open-source nature and use of model predictive control (MPC) for economic optimisation make it highly suitable for localised and smart power systems (Lyden, Flett and Tuohy, 2021). However, PyLESA tends to be more complex and time-consuming to use. Therefore, for the objectives of this report, HOMER is chosen for its user-friendliness and comprehensive features (figure 16).

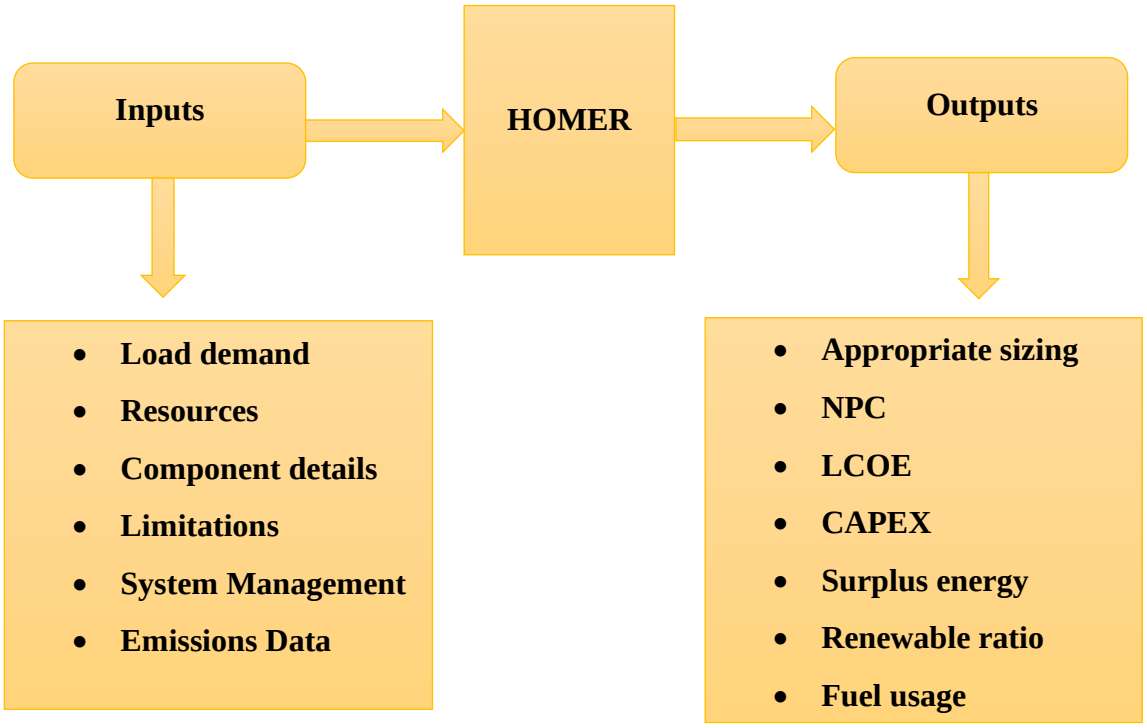

Figure 16: HOMER System (Sinha and Chandel, 2014.)

2.5.2 Limitations of HOMER

When selecting software for modelling HRPS, understanding the constraints and presumptions related to the tools is essential. HOMER, frequently utilised in HRPS investigations, has several recognised limitations.

According to Sinha and Chandel (2014), HOMER is constrained to minimising a single objective, the Net Present Cost (NPC), and cannot address multiple objective problems. Moreover, it has some limitations, such as not accounting for variability within the hour and relying on 1st degree linear equations (Sinha and Chandel, 2014).

Additionally, it cannot import time series data daily, and its resolution for exploring the search space is restricted. Obtaining precise input details for HOMER can also be challenging (DeBartolo, 2015). However, conducting a sensitivity analysis help refine the accuracy of input variables, especially when initial estimates are rough.

Lambert, Gilman, and Lilienthal (2006) suggest that allowing more flexibility in selecting optimisation techniques could strengthen HOMER's resilience and facilitate simple comparison of findings across multiple methods.

2.5.3 Case Study

By conducting micropower analysis, an illustrative example of how HOMER can be applied is seen in its modelling of a hybrid solar-biomass system in rural area of Pakistan. Shahzad et al. (2017) employed HOMER for optimising system size by considering energy balances on hourly basis and minimum NPC goals, showcasing its efficacy in assessing techno-economic feasibility. This case study showcases HOMER's ability to integrate diverse renewable energy sources and enhance their setups for both cost-effectiveness and efficiency (Grassi, 2017).

Likewise, Chmiel and Bhattacharyya (2015) utilised HOMER in order to simulate the stand-alone energy setup for Isle of Eigg. Their goal was to assess the existing system design through simulation and propose different setups to enhance power production and decrease dependence on DGs. The sensitivity analysis conducted showed that the best setup for the existing load, was notably different from the current setup. HOMER suggested using a configuration with 32 kW of PV panels in place of the current 53

kW, and a 40-kW DG instead of the current 80 kW being used. This analysis determined that the existing equipment was slightly oversized but capable of accommodating increased load. Furthermore, it was found that increasing wind penetration tends to benefit the area than increasing solar (Chmiel and Bhattacharyya, 2015).

In summary, HOMER's flexibility, comprehensive optimisation capabilities, and advanced control options position it as a suitable tool for assessing the integration of wind, solar, and storage technologies at Queen’s Quay without redundant repetition of ideas.

3.0 Methodology for Modelling Investigation

To effectively integrate solar and wind renewable energy into the existing District Heating Network (DHN) at Queen's Quay, a systematic approach is employed.

The process begins with selecting the study location and assessing the wind and solar potential in that area. The subsequent step involves determining the load for the heat pumps, which is calculated based on their COP and Queen's Quay heat demand. Following this, a baseline model is established by combining the grid module with the electrical load of the heat pumps (HP).

Three hybrid renewable systems are then configured: PV panels integrated with the grid, wind turbines integrated with the grid, and a combination of PV panels and WT alongside the grid. Each system component and the corresponding equations for their power output are introduced and evaluated through studies examining various prices and sizes. The input data for these setups include assumptions about costs, efficiencies, and other relevant parameters of the components.

Finally, an economic analysis is performed using KPI such as the LCOE, LCOH, and payback period to assess the suggested systems' financial feasibility in relation to the baseline model.

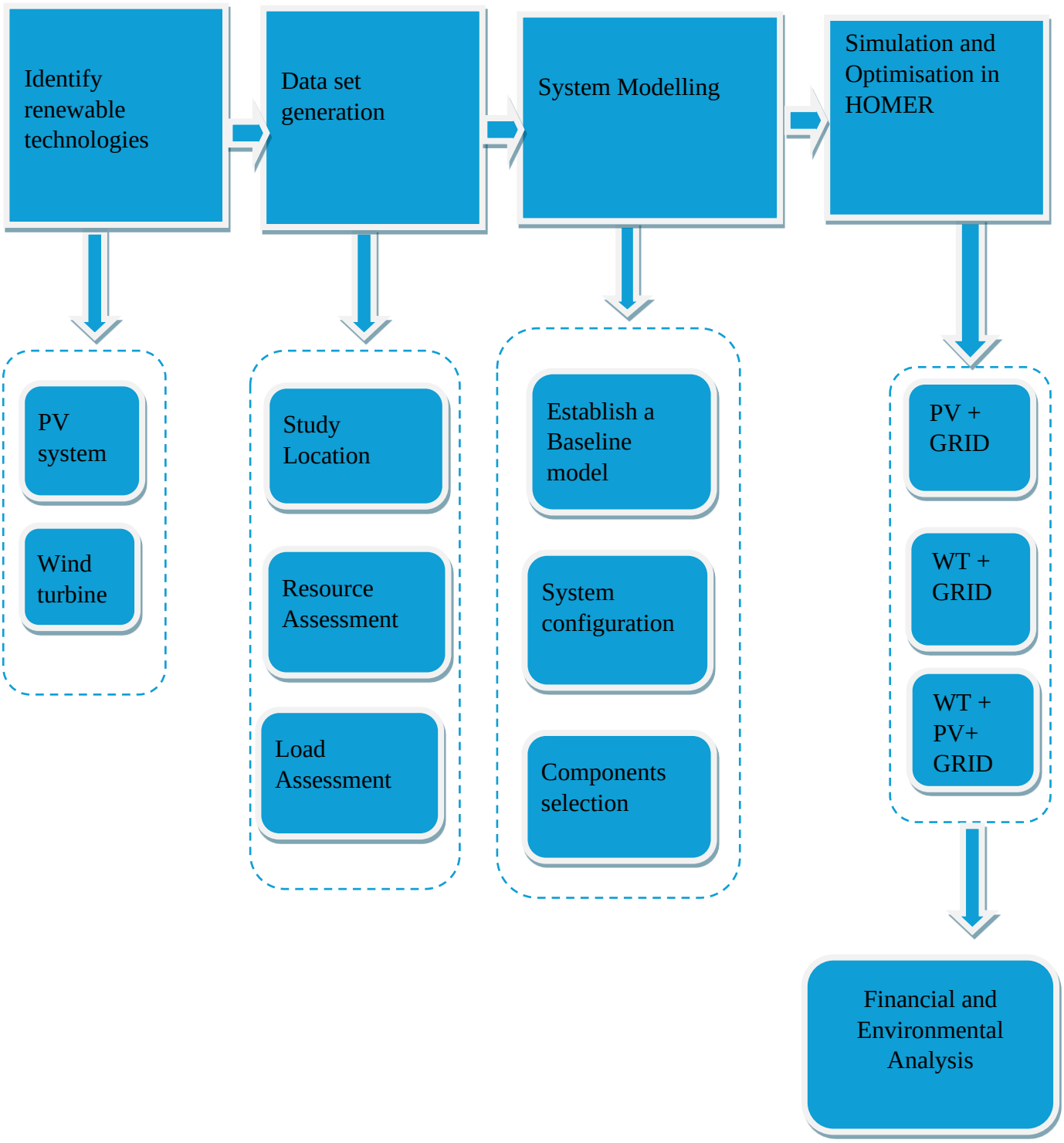

Figure 17: Methodology Flowchart

3.1 Dataset Generation

Lyden and Tuohy (2019) state that building a model for an energy system necessitates three primary datasets. It involves evaluating meteorological resources, analysing component attributes, and assessing loads. The process of finding it is detailed below.

3.1.1 Define Study Location and Weather Data

Queen's Quay DHN in Clydebank is located at a latitude of 55.9045° N and a longitude of 4.4049° W, with an elevation of 6 meters above sea level. Clydebank experiences a temperate maritime climate with moderate solar irradiance of 2.5 to 3.0 kWh/m²/day making it suitable for photovoltaic panels. Daily temperatures range from 1-6°C in winter to 12-18°C in summer, and wind speeds average 4 to 5 meters per second, supporting wind turbine installations. The area receives around 1,200 mm of rainfall annually, with slightly higher amounts in winter. Clydebank has a population of approximately 26,640 characterised by a diverse mix of families, professionals, and retirees (Clydebank (West Dunbartonshire) weather, 2024).

3.1.2 Resources Assessment

The study focuses on harnessing wind and solar resources to generate electricity. HOMER offers the capability to either directly download resource data from the internet via the NASA Surface Meteorology and Solar Energy database or import data from a time series file.

3.1.2.1 Solar Resources

To accurately model a system with a photovoltaic array, it is crucial to input specific solar resource data for the chosen site. For flat plate PV components, global horizontal irradiance data is required.

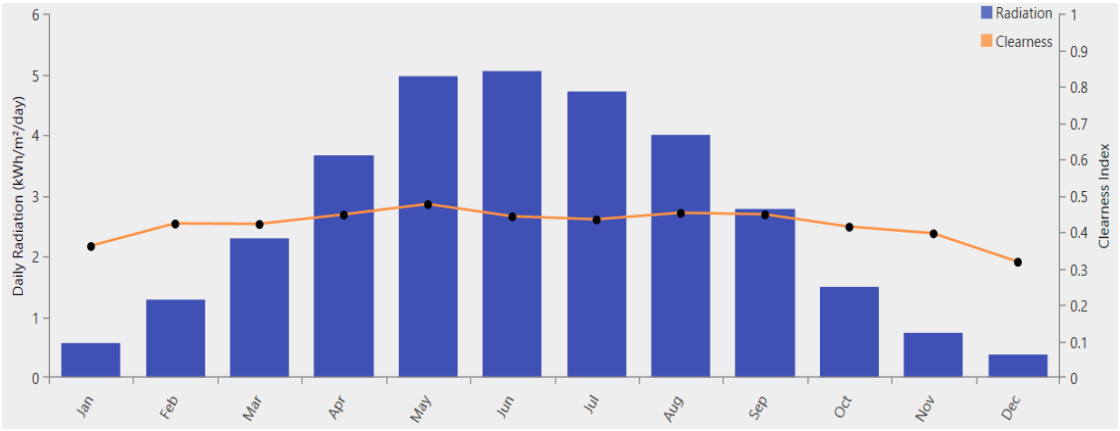

Figure 18:Queen's Quay Solar Radiation Profile

Figure 18 depicts the lowest and highest monthly daily solar radiation values: 0.38 kWh/m²/day in December and 5.06 kWh/m²/day in June. Project location and local meteorological data obtained from HOMER, show 2.66 kWh/m²/day, yearly mean daily solar radiation.

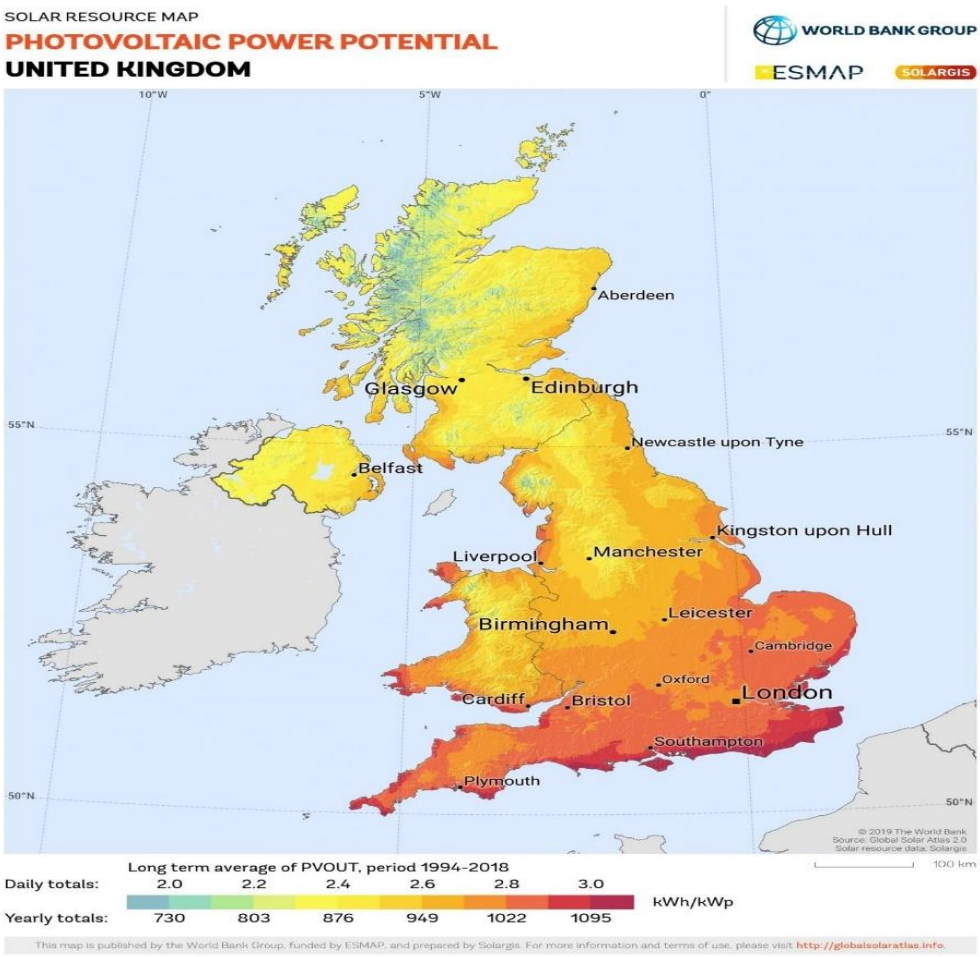

Figure 19:Solar Irradiance in the UK, (Global Solar Atlas, no date)

Figure 19 shows the solar irradiance levels for Glasgow on 'The World Bank Group's Global Solar Atlas' map. The typical daily solar radiation in Glasgow ranges from 2.5

to 2.7 kWh/m²/day. The project's average annual calculation of 2.66 kWh/m²/day falls within the expected range, offering dependable information for designing renewable energy systems (Global solar atlas, No date).

3.1.2.2 Temperature Resource

HOMER uses temperature data directly from the NASA Surface Meteorology and Solar Energy database to generate the temperature profile for Queen's Quay, as depicted in Figure 20. Minimum and maximum monthly average temperature values are observed in January and July, with 2.74 °C and 13.84 °C respectively. The scaled annual average temperature is 7.76°C. These values are consistent with data provided by the 'Met Office' for the Glasgow region, where average temperatures range from about 2°C in January to 14°C in July, with an annual average of around 8°C (Clydebank (West Dunbartonshire) weather, 2024). This ensures accurate and reliable input for renewable energy system planning.

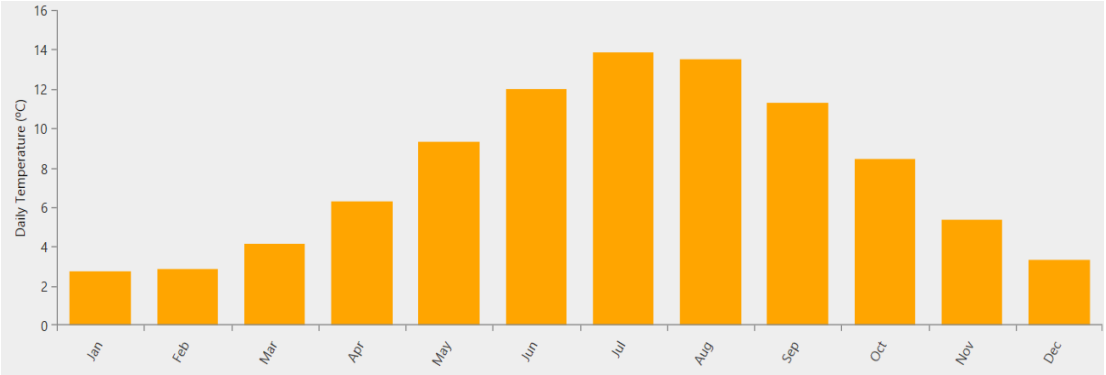

Figure 20:Queen's Quay Temperature Profile

3.1.2.3 Wind Resource

Accurately simulating a wind turbine system in HOMER Pro requires detailed wind resource data that accurately represents the annual wind speed profile of the specific location, as small changes in wind speed can significantly impact turbine output (De Bartolo, 2015).

For Clydebank, the NASA Surface Meteorology database reports an estimated average wind speed of 7.50 m/s annually. Minimum and maximum monthly average wind

speed values are observed in July and January, with 6.15m/s and 9.19 m/s respectively, as shown in figure 21.

This is slightly higher than the 7m/s annual average wind speed provided by the GLOBAL WIND ATLAS for Clydebank (Global wind atlas, no date). To ensure a realistic estimation of the wind park's energy output, advanced inputs detailed in Table 1 are necessary.

Table 1: Advanced Input Data for The Generation of Synthetic Wind Speed Profile

Advanced Input Data	Values
Weibull K	2
1 hour Autocorrelation Factor	0.85
Hour of Peak Wind speed	15

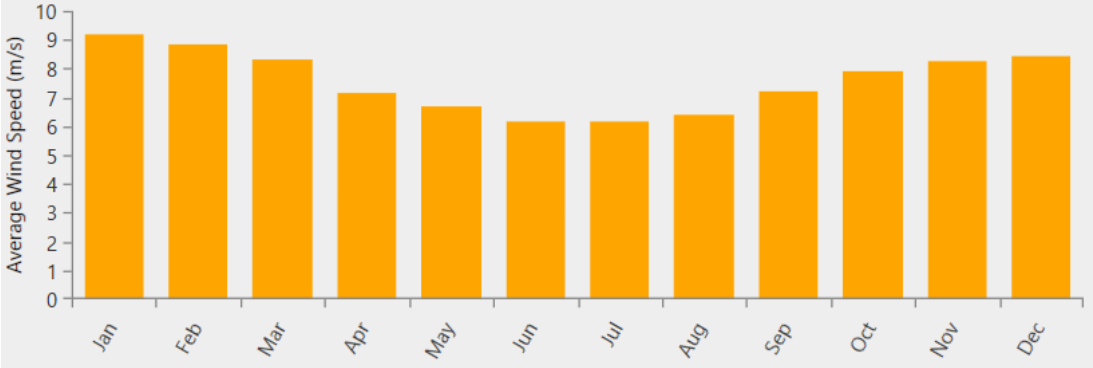

Figure 21:Queen's Quay Wind Speed Profile

3.1.3 Load Assessment

3.1.3.1 Heat Demand Estimation for Queen's Quay DHN

The approach used to estimate the heating demand for the Queen's Quay DHN consists of analysing and accurately scaling the data from the West Whitlawburn Housing Co-operative (WWHC) district heating system (Lyden and Paul, 2022). The baseline data for the WWHC district heating network's hourly heating demand was used to create the graph in figure 22.

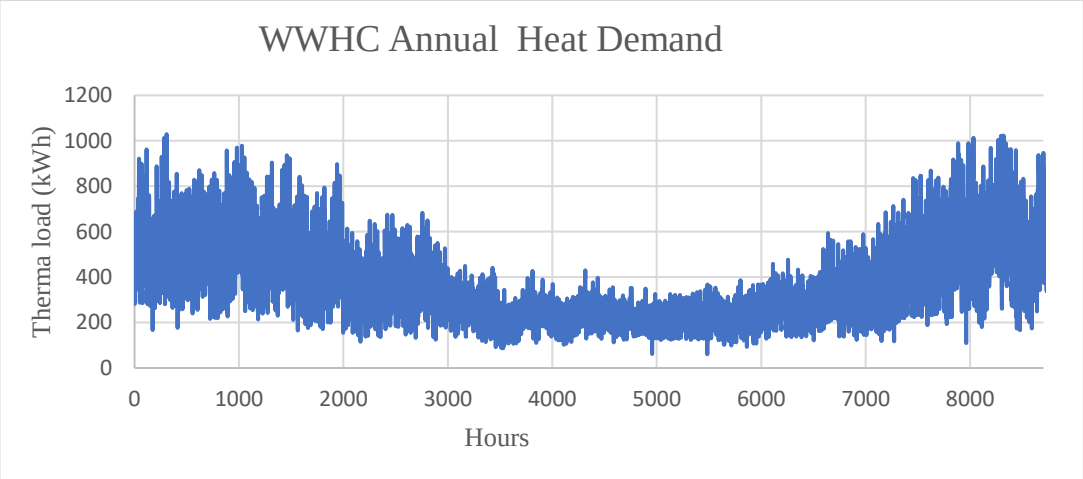

Figure 22:Annual Heating Demand for WWHC District Heating Network

This data indicates an approximate annual thermal demand of 3.2 GWh with a peak load of 1.1 MWh. Despite serving 664 homes, the demand may appear to be low for a DHN. A key reason is that the size of dwellings affects heating demand as larger homes have more surface area for heat loss and greater volumes to heat, potentially offsetting efficiency improvements (Viggers et al., 2017). However, multi-unit buildings benefit from reduced heat loss due to shared walls, unlike standalone houses (Viggers et al., 2017). Additionally, energy efficiency measures such as improved insulation and modern heating systems in these buildings further decrease the overall thermal demand (McKeown, 2020).

Table 2:Load Scaling Ratio in WWHC and Queen's Quay District Heating Networks

Peak Thermal Demand for WWHC	1.1
No. Of heat pumps in QQ	2
QQ Heat Pump capacity	2.65 MWth
Total Capacity (Peak thermal demand QQ)	5.3 MWth
Peak Load Ratio (WWHC/QQ)	4.818

Table 2 compares the peak thermal demand between the WWHC and the Queen's Quay DHNs. The highest thermal demand for WWHC is 1.1 MWh, whereas Queen's Quay has a much higher peak demand of 5.3 MWh because they use two 2.65 MWth heat pumps (Queens Quay Heat Network, no date). To adjust for the difference in size, a peak load ratio of 4.818 is determined then applied to increase the hourly heating demand data from WWHC, representing the heightened demand at Queen's Quay (figure 23).

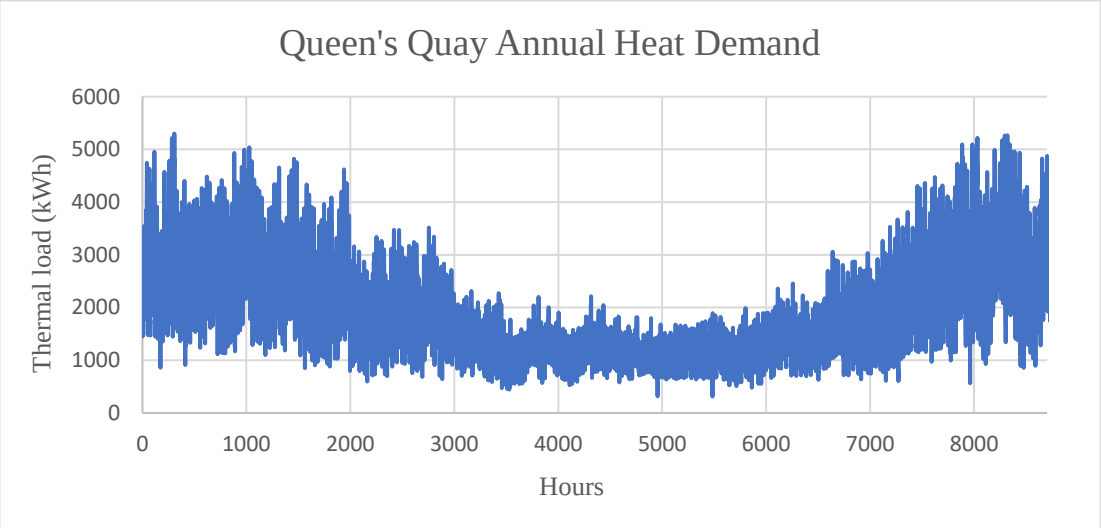

Figure 23:Annual Heating Demand Profile for Queen's Quay DHN

The heat demand exhibits a typical pattern, which is subject to fluctuations due to seasonal changes, along with the habits of users on a daily and weekly basis (Aragon et al., 2022). Peak loads around 5.3 MW occur only briefly, which often leads to the oversizing of heating capacities for both individual properties and district heating systems (Djurić Ilić, 2020). However, district heating benefits from the aggregation of diversified loads, resulting in a reduced overall capacity requirement (Khan et al., 2021).

3.1.3.2 Heat Pump Electrical Demand

The electrical demand is estimated based on the heating demand of Queen's Quay DHN and heat pumps COP. This estimated load will be utilised later to identify any increases in local renewable energy usage that will be incorporated into this project.

COP of the HP Calculation

Several methods exist for calculating a heat pump's Coefficient of Performance (COP), including real-time monitoring, seasonal performance factors (SPF), design-based estimates, laboratory testing, and simulation models (Pieper et al., 2020; Jensen et al., 2018). For the Queen's Quay WSHP, a COP of 3.1 is determined using theoretical methods. This approach aligns with the constant COP method described by Pieper et al. (2020), which uses a fixed COP value to simplify modelling and facilitate effective energy planning.

The calculated COP of 3.1 is then used to estimate the electrical load of the heat pumps, which is in line with typical UK heat pump performance that typically ranges from 2 to 3 throughout the year (Moran, 2021).

Ideal COP Calculation Using Carnot Efficiency (Grassi, 2017):

$$COP = \frac{T_{hot}}{T_{hot} - T_{cold}} \qquad (1)$$

Here, T_{hot} is output temperature in Kelvin, and T_{cold} is source temperature (river) in Kelvin.

Adjusting for Real-World Efficiency (Grassi, 2017):

The ideal Carnot COP is then scaled to reflect real-world efficiency as shown in table 3. An efficiency factor of 61% is used based on typical heat pump performance (Hong et al, 2013).

$$Scaled\ Carnot\ COP = Carnot\ COP \times Efficiency\ Factor \qquad (2)$$

Table 3:Heat Pump Performance Metrics Across Different Seasons

	HP o/p Temperature (T_{hot})	Winter ($T_{cold,W}$)	Summer ($T_{cold,S}$)	Average
Temp (°C)	80	5	17	11
Temp (K)	353	278	290	284
Carnot COP	-	4.7	5.6	3.3
Scaled Carnot COP	-	2.85	3.3	3.1

To simulate how the heat pump's performance fluctuates throughout the year due to temperature changes and other seasonal effects, Equation (3) can be used to estimate the seasonal variations in COP. However, this study will not include this detailed seasonal modelling.

$$COP = Offset + Sin\ Amplitude.\sin\left(\frac{Hours.2\pi}{8760} - \frac{\pi}{2}\right) \qquad (3)$$

Heat pump (HP) electrical load calculation

The electrical load of the heat pump is determined (table 4), using the COP calculated above and Queen's Quay DHN thermal demand, using the following formula (Ewing, 2020):

$$P_{e,HP} = \frac{Q}{COP} \qquad (4)$$

Where, $P_{e,HP}$ is the electrical load (kW), Q is the thermal load (kW).

Table 4:Electrical Peak Load of the Heat Pumps

COP of HP	HP peak thermal load (MWh)	HP peak electrical load (MWh)
3.1	5.3	1.7097

The electrical load of the HPs is entered into HOMER, where it generates five critical data points for each month, which include highest primary load, the mean daily peak primary load, the total average primary load, the average daily lowest primary load, and the lowest primary load (figure 24).

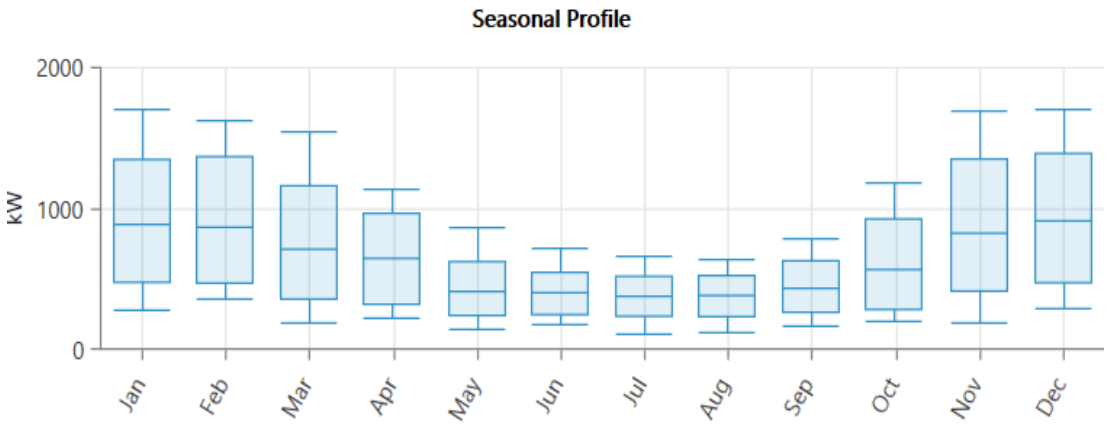

Figure 24:Seasonal Profile of Queen's Quay DHN

Figure 24 illustrates the seasonal profile of the electrical load for the Queen's Quay heat pumps. It shows the variations in electrical demand across different months. January is identified as the peak month with the highest load, while the demand significantly drops during the summer months. The annual average electrical load is 15,026.40 kWh/day, with day-to-day variability assessed at 10.946%.

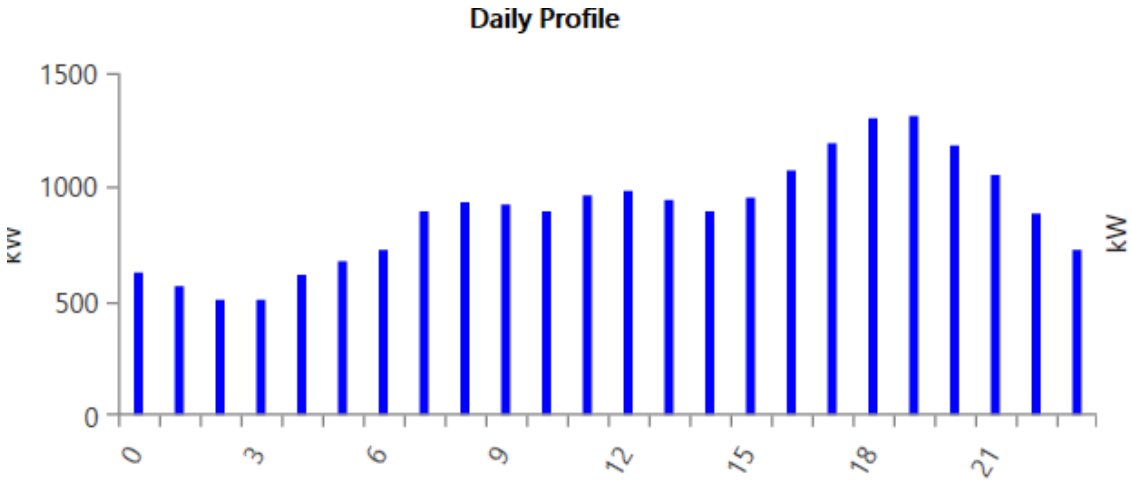

Figure 25: Average Hourly January Demand Profile of QQ

Figure 25 presents the daily profile of the electrical load for the Queen's Quay HPs. It underscores how the electrical demand varies throughout the day, influenced by the activities of people requiring electricity at different times. The maximum average peak load of 1,709.6 kW occurs at 7 PM.

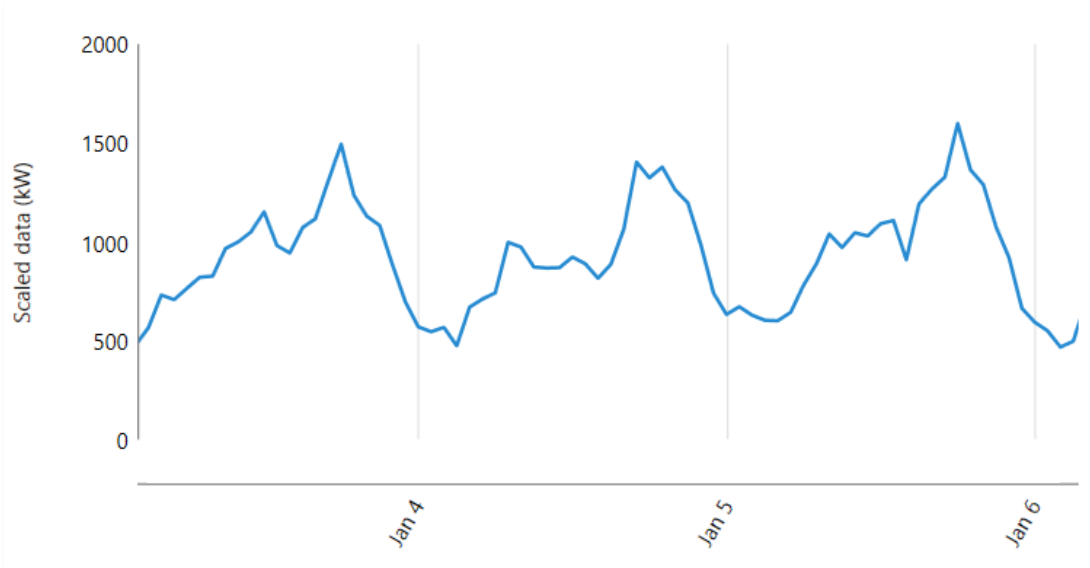

Figure 26: The Electrical Demand over Three days in Winter (January)

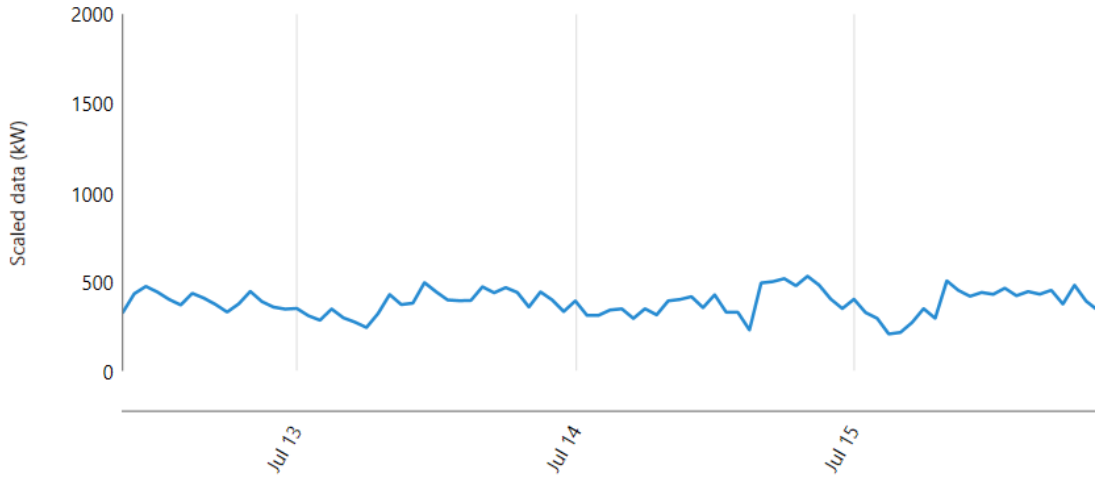

Figure 27: The Electrical Demand over Three Days Summer (July)

Figures 26, 27 represent the electrical load over three days in winter (January) and three days in summer (July), respectively. The data reveals significant seasonal variations, with high demand peaks during the colder months, likely corresponding to winter, and lower demand during the warmer months, reflecting summer conditions.

3.2 Desing and Analysis of the HRPS

The suggested HRPS comprises four main components: the grid, photovoltaic (PV) panels, a converter and a wind turbine (WT). This section offers a detailed description of each component used in simulating and developing the HRPS that operates using a Combined Dispatch (CD) strategy while connected to the grid.

3.2.1 Grid Component and Power Cost Assumptions

The grid is depicted in HOMER Pro as a component that enables the purchase of electricity when the system's production falls short of demand and the sale of excess energy when production exceeds consumption. The software offers a range of advanced functionalities, such as the ability to restrict grid sales and set different tariffs for electricity sales depending on the time of day. For this study, a simple rate function is applied to the grid module.

In this study, the financial modelling aims to accurately reflect the economic conditions faced by large consumers, such as councils. Assumptions include a fixed electricity tariff of 24p/kWh, a compensation rate for returning power to the grid of 0.14 p/kWh, and a fixed gas tariff of 6.06p/kWh, based on the extensive purchasing agreements managed by the Convention of Scottish Local Authorities (COSLA). These agreements enable Scottish councils, including Clydebank, to secure electricity at more favourable rates compared to smaller consumers (COSLA, 2024). Furthermore, typical electricity rates from Scottish Power, set at 28.62p/kWh for 2024, support the assumption of slightly higher rates due to their status as one of the more expensive electricity suppliers (Scottish Power Tariffs, Prices & Reviews, 2024).

According to Ofgem's 2024 standards, the energy price cap plays a crucial role in protecting consumers from excessive charges, by limiting the price per kWh providers can charge. The price cap for variable electricity tariffs is set at 22.36p/kWh (Get energy price cap standing charges and unit rates by region, no date).

Given the bulk purchasing power of Scottish councils, it is reasonable to assume they can secure electricity rates close to this cap or slightly higher. For gas, the Ofgem energy price cap for standard variable tariffs from July 1 to September 30, 2024, is set at 5.48p/kWh, with a daily standing charge of 31.41p. In the preceding time of from

April 1 to June 30, 2024, the gas price was slightly higher at 6.04p/kWh, with a daily standing charge of 31.43p (Ofgem, 2024).

3.2.2 **Model of Solar PV**

In Homer, Photovoltaic (PV) modules are modelled to produce direct current (DC) electricity in direct correlation to the solar radiation they receive. The electrical output from PV panels is affected by several factors, including solar irradiation, module temperature, and geographic location. PV output is calculated using the following formula (Ghenai and Bettayeb, 2020):

$$P = P_{PV} f_{PV} \times \left(\frac{\bar{G}_T}{\bar{G}_{T,STC}}\right)\left[1 + \alpha_p (T_{c-} T_{C\,STC})\right] \qquad (5)$$

PV energy output, denoted as P, depends on multiple factors. Here, P_{PV} represents the optimised size of the PV panel. f_{PV} is the PV derating factor. $\bar{G}_T$ is the solar radiation on the inclined surface measured in W/m², and $\bar{G}_{T,STC}$ signifies the solar radiation at standard test conditions in (W/m²). Additionally, $(T_{c-} T_{C\,STC})$refers to the cell temperature under standard test conditions, and α_p is the power temperature coefficient expressed in %/°C.

3.2.3 **Model of Wind Turbine**

When accounting for wind speed variability in HOMER, the WT power output is determined in three-steps at every time steps, utilising the power curve of the chosen turbine. First, v_{anem} the wind's velocity at the anemometer height is adjusted to the hub height wind speed h_{hub} using either the power or logarithmic law. Afterwards, the turbine's power production is determined by the wind velocity at the centre of the blades. In the end, the power generated is modified to reflect the real air density in the location (Murshed et al., 2023).

$$v_{hub} = v_{anem}\left(\frac{h_{hub}}{h_{nem}}\right) \; or \; v_{anem}\frac{\ln(h_{hub}/h_0)}{\ln(h_{anem}/h_0)} \qquad (6)$$

$$P_{WT} = N_W \times \sum_i f_i\,(v) P_{WT,i}\,\rho(v_{hub}) \times \frac{\rho}{\rho_0} \qquad (7)$$

Where N_W represents the number of WT, f_i is the likelihood of duration at site wind speed $P_{WT,i}$, (is the h_{hub} hub height power production from the turbine from its power curve at the time i (kW), $\rho(v_{hub})$is the actual air density (kg/m3), $\rho_0$the air density at standard temperature and pressure (1.225 kg/m3), α is the wind shear coefficient for the site and h_0 is the surface roughness length (m).

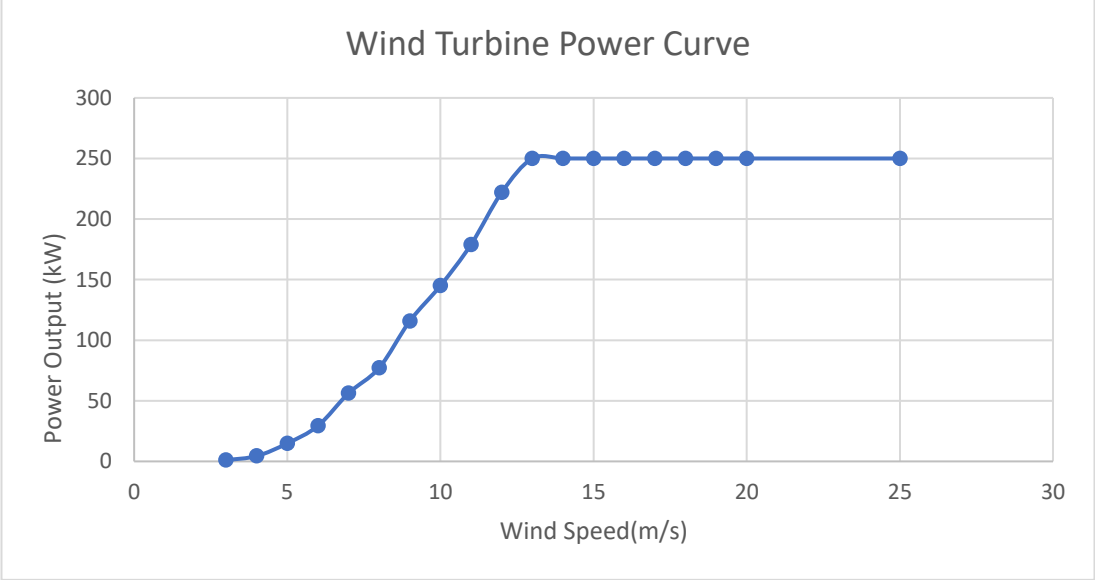

Figure 28: The Wind Turbine Power Curve

Another method for calculating a WT's power output is as follows (Diyoke, 2019):

$$P_{WT}\ (v_{hub}) = N_W \times \frac{1}{2}\ \rho A v_{hub^3}\ C_{p(\lambda,\beta)}\ \eta_{\ m}\ \eta_{\ G} \qquad (8)$$

Where $\eta_{\ m}$and η_G is the efficiency of the wind turbine's mechanical and generator components. C_p (λ, β) is calculated based on the WT blade angel C_p and the tip speed ratio (λ), with A representing the swept area of the WT blades (m^2).

3.2.4 Model of Converter

The converter in a renewable energy system is designed to perform as both a rectifier (AC-DC) and an inverter (DC-AC), facilitating efficient energy flow between AC and DC bus components. HOMER represents converter capacity as a sustainable level that the device can sustain indefinitely. The formula to calculate the converter capacity, ensuring consistent performance, is given by (Ghenai and Bettayeb, 2020):

$$P_{InvIN} = P_{PV} \quad (9)$$

where P_{InvIN} represents the input power to the inverter, also referred to as the converter capacity, and P_{PV} his represents the power output from the photovoltaic panels.

3.3 Components Selection and Validation

3.3.1 Photovoltaic (PV) Scenario and Cost Assumptions

The selection of photovoltaic (PV) modules in this study is guided by manufacturers' specifications, focusing on efficiency and maximum power output. Following a thorough market survey, 330W CanadianSolar MaxPower CS6U-330PPV modules were chosen for their impressive efficiency of 16.97%, reflecting recent technological advancements in the solar industry. These panels are designed to withstand harsh environments, featuring a durable frame rated for high snow loads, ensuring long-term reliability. Their versatility makes them suitable for various applications, including grid-connected commercial/industrial rooftops, residential ground-mount systems, solar power stations, and carports. (Canadian Solar CS6U-330P 330W MAXPOWER Solar Panel, no date). This choice is further supported by Ghenai and Bettayeb (2020), who emphasise the critical role of modelling, simulation, and optimisation methods in designing efficient and cost-effective PV systems.

The price of PV panels has seen a significant decline over the past decade, as illustrated in the price trend graph in figure 15. This sharp decrease in costs makes the 330W panels a financially viable option. For this study, the capital and replacement expensed for the PV array are estimated at £2,300 per kW, with an annual operation and maintenance (O&M) cost of £10. These cost parameters are consistent with those reported by Ahmed et al. (2024), having been converted from US dollars ($) to British pounds (£) to ensure the durability and sustainability of the PV system.

The 330W solar panels are scheduled for installation in the Queen's Quay DHN. The masterplan of Queen's Quay, illustrated in figure 29, includes an analysis of the area designated for this purpose.

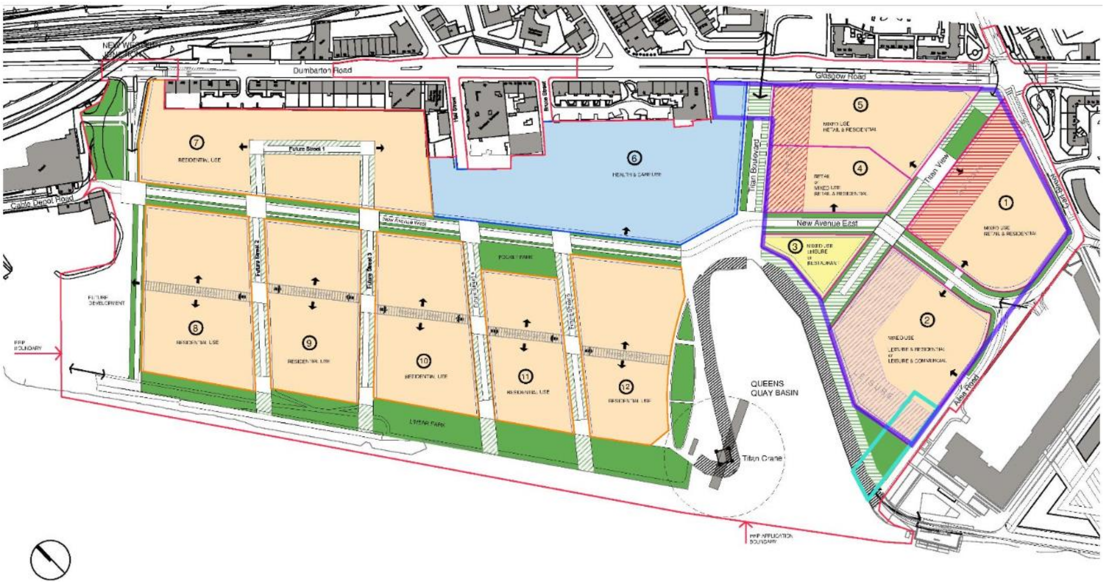

Figure 29: Queens Quay Masterplan, (Local renewables, No date).

The DHN offers seven potential areas for setting up a PV farm, with three of these areas selected for detailed assessment. This evaluation draws on data from a previous project on Queen's Quay (Local Renewables, no date). In these locations, it is assumed that the roof area constitutes 46% of the total floor area. Another standard assumption is that every 1 kWp of installation requires 10 m² of space (Abul et al, 2020). This guideline is crucial for estimating the total roof area available for solar installations and ensuring that the system design is feasible given space constraints. By applying this assumption, it becomes possible to calculate the total number of solar panels that can be installed based on the available roof area, facilitating an efficient and practical layout for the solar PV system (Ghenai and Bettayeb, 2020).

Using these assumptions, the maximum installed capacity at each site is determined in table 5. As a result, the total available roof area can support the installation of up to 1,713.04 kWp, which surpasses the required capacity of 1,709.68 kWp.

Table 5: Capacity and Requirements for Solar Installations Across Multiple Sites

S/n	Site	Floor Area (m^2)	Roof Area (46 % of F.A)	Max Capacity Installable (kWp)	Total Capacity Req. (kW)
1.	Site 1	14,500.00	6,670.00	667.00	1709.68
2.	Site 2	15,600.00	7,176.00	717.60	
3.	Site 3	7,140.00	3,284.40	328.44	
		37,240.00	**17,130.40**	**1,713.04**	

3.3.2 Wind Turbine Scenario and Cost Assumptions

To determine the best wind turbine size, the performance of various turbines in the system is assessed, with capacities varying from 250 kW to 2 MW. This selection reflects the area's diversity of turbine sizes, which range from smaller installations like Findhorn Village to larger ones like white lee Wind Farm (Vavoura, 2019).

Table 6:Comparative Analysis of Wind Turbine Performance using HOMER

Wind Turbine (WT)	WT rated capacity (kw)	Mean output (kw)	Peak load (kw)	Number of WT	Wind Penetration (%)	Max output (kw)
WES 250	250	117	1,709.68	7	19	250
Leitwind 90 1000kW	1,000	721		2	115	999
Enercon E-82 E2 [2MW]	2,000	1,153		1	184	2,049

Table 6 presents an analysis conducted using HOMER to assess the effectiveness and financial viability of various wind turbine options for integration into a hybrid power system. This evaluation aims to compare different turbine models to determine the most suitable option that can efficiently meet energy demands while minimising costs. The input parameters and associated costs for each wind turbine were carefully entered into HOMER to facilitate this comparison (APPENDIX A).

The 2MW wind turbine is the most favourable option for the base system, due to its high capacity and efficiency. However, its installation near the Queen's Quay District Heating Network is complicated by proximity to an airport, raising concerns regarding regulatory compliance and radar interference. Large wind turbines can cause significant radar interference, affecting the detection and tracking of aircraft, and pose visual impacts that are problematic near airports (Wind Turbine Radar Interference, no date). Alam and Jin (2023) suggest that smaller wind turbines, like a 250-kW model, are a better option near airports due to their reduced visual and radar impact.

Given these considerations, the 250-kW wind turbine will be modelled for hybrid WT grid-connected systems. Balancing the need for renewable energy integration with regulatory and safety constraints. The detailed costs for the 250-kW wind turbine include £425,645.00 for capital, £386,950.00 for replacement, and £30,956.00 annually for O&M are derived from a thorough analysis by Farahmand et al (2024). These figures have been precisely converted from US dollars ($) to British pounds (£), ensuring they are both accurate and relevant for the project.

3.3.3 Converters

1 kW converter is chosen for the PV system, with both the capital and replacement costs set at £230 and no annual O&M costs. Which are estimated based on thorough market research and manufacturer data, indicating that these converters are both high-quality and efficient. The inverter inputs are designed to last 15 years with a 95% efficiency, while the rectifier inputs maintain a 100% comparative capacity with the same efficiency.

The PV system's converter of 1 kW capacity is suitable for PV installations of a moderate size, offering flexibility and scalability. Multiple converters can be utilised simultaneously in larger systems, expanding their adaptability to various installation

sizes. Kroposki et al. (2017) emphasise that modular converters provide substantial advantages in scalability and system control, making them perfect for residential and small commercial uses. Converters with a 95% efficiency rate and a lifespan of about 15 years are industry standard, ensuring long-term efficiency and reliability. Flicker and Gonzalez (2015) confirm that modern PV converters typically meet these benchmarks, supporting the assumptions of this study.

3.4 Hybrid Systems Configuration

In this study, the hybrid renewable configurations integrate renewable energy sources with grid connections to efficiently meet heating and electrical demands. These systems are engineered to ensure that the grid can handle peak energy generation, even when heat pumps are off, without compromising its stability or requiring additional infrastructure support.

This section examines various combinations of wind and/or solar energy integrated with the existing grid, which consistently handles a thermal peak load of 1709.68 kW across all scenarios. This approach aims to fulfil energy needs efficiently, uphold grid reliability, and offer valuable insights for future renewable energy integration (Lund et al., 2015).

3.4.1 Baseline Model

The figure 30 illustrates the baseline model for Queen's Quay DHN configuration, showing the connection between the grid and the primary electric load. The system supports an electrical load of 15,026.40 kWh/day, with a peak demand of 1,709.68 kW This setup demonstrates the energy demand and reliance on grid power to meet the heating requirements of the district heating network.

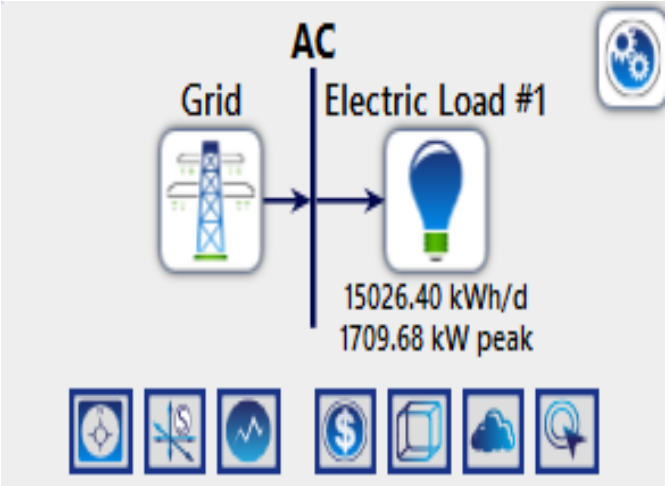

Figure 30:Schematic of the Baseline Model Configuration in HOMER

3.4.2 Photovoltaic (PV) grid-connected Configuration

The image 31 illustrates a hybrid energy system modelled in HOMER, featuring a combination of grid power and photovoltaic (PV) generation. The system includes a grid connection to ensure reliability, particularly during periods of low renewable energy production. The PV system, located on the DC side, harnesses solar energy, contributing to the renewable energy supply. A converter links the AC and DC sides, enabling efficient energy transfer and management between the grid, PV system, and the electric load. Pawar and Nema (2018) advocate for the integration of PV systems with grid support for the DHN, by showcasing the economic and environmental advantages.

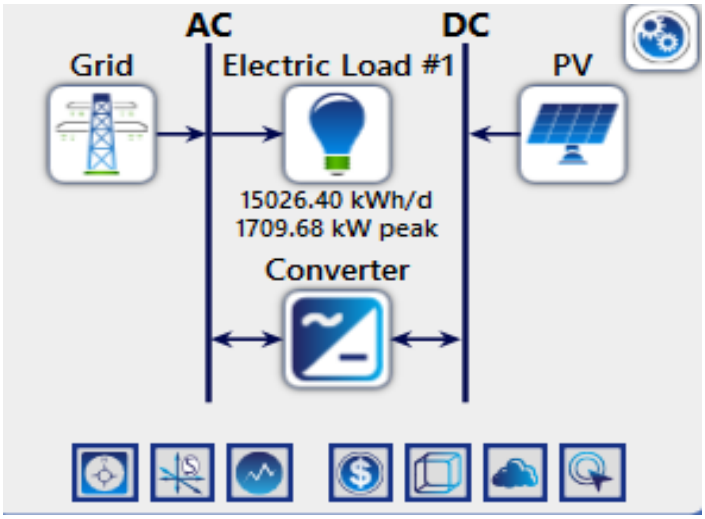

Figure 31:Schematic of the PV grid-connected and Converter system in HOMER

3.4.3 Wind Turbine (WT) grid-connected Configuration

The schematic in Figure 32 demonstrates the integration of WT with the grid to supply power to an electric load. The amount of power generated depends on wind speed and turbine capacity. This configuration is validated by Al-Tajer and Poullikkas (2015), which support the feasibility of the grid combined with WT setup for DHNs.

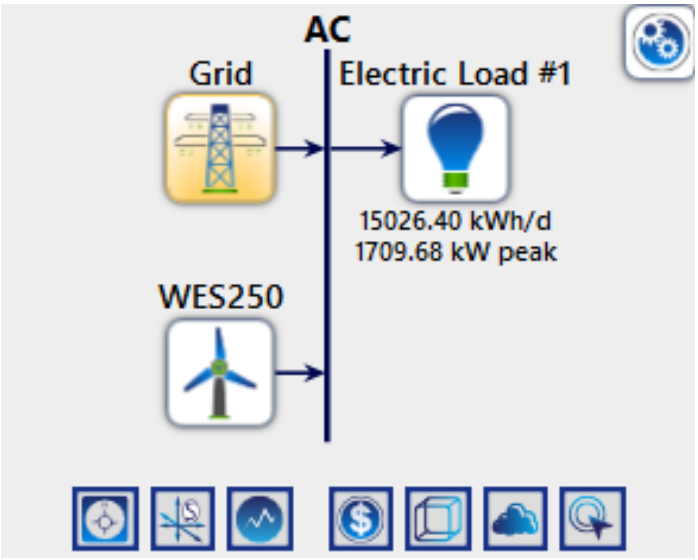

Figure 32:Schematic of WT grid-connected System in HOMER

3.4.4 Combined WT and PV grid-connected Configuration

The figure 33 represents a hybrid renewable energy system where power from WT, PV and the grid to meet the electrical need. The grid and wind turbine provide AC (alternating current) power directly to the AC bus, while the solar PV system generates DC (direct current) power, which is converted to AC via a converter.

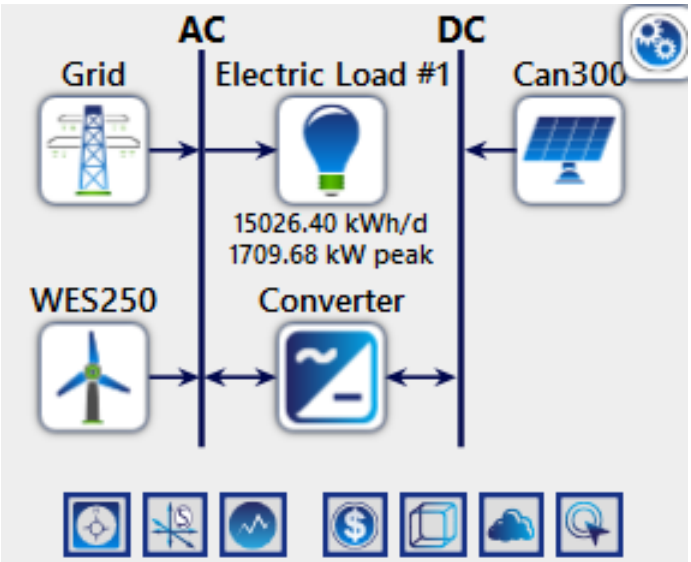

Figure 33: Schematic of the WT and PV grid-connected System in HOMER

The study shown in table 7, aims to evaluate the most efficient integration of WT and PV systems, by varying the number of 250 kW wind turbines while maintaining the total renewable energy capacity within the grid's limits.

Table 7: PV and WT Integration with the grid

S/N	250 kW- WT	PV (kWp)	Peak Load (KW)
1	250 x 1	1459.68	1709.68
2	250 x 2	1209.68	
3	250 x 3	959.68	
4	250 x 4	709.68	
5	250 x 5	459.68	
6	250 x 6	209.68	

3.5 Key Performance Indicators (KPI)

Key Performance Indicators (KPIs) are vital measurements utilised for assessing the effectiveness of systems. They provide quantifiable measurements that reflect the efficiency, effectiveness, and overall progress toward set goals. This study focuses on financial and energy performance KPIs.

The scope of these calculations includes only the expenses associated with the new renewable electricity supply components, excluding costs related to Heat Pumps (HP) and the District Heating Network (DHN). For each electricity supply component, such as the grid, PV, WT, and combined WT and PV systems, the elements considered within this scope are:

- Capital investment
- Operating and maintenance expenses (O&M)
- Heat produced by the heat pumps

3.5.1 Financial KPI

This financial analysis is examined through multiple KPIs, such as the Levelized Cost of Electricity (LCOE) in £/ kWh, Net Present Cost (NPC) in £, Levelized cost of heat (LCOH) in £/ kWh, and Payback period. Analysing the LCOE alongside the LCOH provides a comprehensive understanding of the economic feasibility and efficiency of energy systems. It also enables stakeholders to compare and optimise investments in electricity generation and heating technologies, supports informed energy policy and planning, promotes sustainable choices.

LCOE: Shows the average price per kWh of electricity generated by the system. This measure offers information on how efficiently the energy generated by the system is produced. The calculation is done by utilising the formula provided (Nian et al., 2016):

$$LCOE = \frac{I_0 + \sum_{t=1}^{n} \frac{A_t}{(1+r)^t}}{\sum_{t=1}^{n} \frac{M_{t,el}}{(1+r)^t}} \qquad (9)$$

Where, I_0 is the investment expenditure in £, A_t is the annual total cost in £, $M_{t,el}$ is the produced amount of electricity in kWh per year, r is the real interest rate in %, n is the economic lifetime in years and t is the year of lifetime (1, 2, …..n).

LCOH: Also referred to as the levelized cost of thermal energy, measures the cost of heat generation systems. LCOH calculates the cost per kWh of heat over the system's lifetime, providing a useful metric for determining the long-term cost a household will pay for heating (Nian et al., 2016):

$$LCOH = \frac{I_0 - S_0 \sum_{t=1}^{n} \frac{C_t}{(1+r)^t}}{\sum_{t=1}^{n} \frac{E_t}{(1+r)^t}} \qquad (10)$$

Where, Where, I_0 is the Capital investment (£), S_0 = Subsidies/earnings (£), C_T is the O&M running costs (£), $E_{t,el}$ heat produced in a given year (kWh), r is the discount rate in %, n is the economic lifetime in years and t is the year of lifetime (1, 2, …..n) (Nian et al, 2016).

As per equation (12) and (9), the LCOH can be calculated using this formula:

$$LCOH = \frac{LCOE}{COP} \qquad (11)$$

NPC: Is a crucial economic indicator that represents the total cost of the system over its lifetime, minus the total revenues generated. Revenues are derived from grid sales and recycling earnings (Baghel, Manjunath, and Kumar, 2024):

$$NPC = C_0 + \sum_{i=1}^{N}(OC_i + OM_i + REP_i + PEN_i + EP_i - ES_i - SL_i \qquad (12)$$

where C_0 is the initial capital, OC_i is the operating cost, OM_i is the maintenance and repair cost, REP_i is the renewal fee, PEN_i is the penalty fee, EP_i is the energy purchase cost, ES_i is the energy sales profit, and SL_i is the recycling profit for the i-th year (Baghel, Manjunath, and Kumar, 2024).

The Simple Payback Period: Is an essential metric in assessing the financial viability of investments. It indicates the amount of time required for an investment to generate enough savings or income to cover its initial expenditure. The formula used to calculate the simple payback period is (Baghel, Manjunath, and Kumar, 2024):

$$Simple\ Payback\ Period = \frac{Initial\ Investement}{Annual\ Cash\ Flows} \quad (13)$$

In this context, the 'initial investment' represents the total cost of the project, and the 'annual cash flows' are the yearly financial returns or savings produced by the investment. This calculation provides a clear understanding of how quickly the initial costs can be recovered.

3.5.2 Energy Performance KPI

An additional characteristic that sets an HRPS apart, is its inclination to fully utilise renewable energy components.

The Renewable Fraction (RF): A metric utilised to measure the amount of energy produced from renewables in HRPS. The calculation is determined by the formula provided (Hassan et al., 2022):

$$Renewable\ Fraction = \frac{Total\ Energy\ Produced}{Total\ Energy\ Consumed} \quad (14)$$

Where, Energy from Renewable Sources is 'the total amount of energy generated' from solar and wind. And 'Total Energy Consumption' is the total energy usage of the system, including both renewable and non-renewable sources.

Excess Electricity: Surplus electricity appears when the power produced by the renewables like PV panels or wind turbines, exceeds the immediate consumption needs of the connected load.

This metric becomes even more critical in evaluating the performance of energy systems without storage capabilities, as it directly reflects the mismatch between energy generation and consumption. High levels of excess electricity in such systems may indicate overproduction, poor system sizing, or the need for better load management or alternative ways to use or store the surplus energy (Amole et al., 2023).

$$Excess\ Electricity = Total\ Energy\ Produces - Total\ Energy\ Consumed$$

3.6 Summary of Assumptions and Technical Data (HP, PV and WT)

1. The COP of 3.1 for heat pumps is calculated via theoretical formulae.
2. Efficiency factor is taken as 61% based on typical heat pump performance.
3. System lifetime is assumed to be 25 years with an annual discount and inflation rates set at 8% and 2% respectively and maximum annual capacity shortage of 10% is allowed (Ahmed et al., 2024).
4. Power costs are assumed as follow: Electricity cost of 24 p/kWh, Gas cost of 6.06 p/kWh and compensation rate of 0.14 p/kWh for returning power to the grid.
5. Area required for 1 kWp of PV installation is assumed to be 10 m^2.
6. 46% of the available footprint area is considered as roof area for PV installation.
7. The study assumes a single set of load demand and weather data, with annual variations in wind and solar resources.
8. The cost assumptions of each component, reflect current costs and do not account for potential future changes.

4.0 Results and Discussion

This section evaluates the energy and economic performance of three HRPS configurations compared to a baseline model reliant on grid electricity. The evaluation of electrical performance involves analysing energy production, surplus electricity and the proportion of renewable energy obtained. Economic feasibility is assessed using metrics such NPC, LCOE, LCOH and payback period. Collectively, these indicators offer a thorough comprehension of the overall effectiveness and efficiency of all three configurations. The discussion emphasises the benefits of hybrid systems in achieving lower LCOE and LCOH and acknowledges the constraints of the research, as well as suggesting future research pathways.

The monthly and yearly electrical and economic simulation results for all the hybrid systems architecture using HOMER throughout this section, details various parameters of consumption and production based on the inputs parameters mentioned in the methodology.

The AC Primary Load: Represents the total annual electricity consumption by devices and systems that operate on alternating current (AC).

DC Primary Load: Represents the total annual electricity consumption by devices and systems that operate on direct current (DC).

Deferrable Load: Represents the total annual electricity consumption by loads that can be deferred or shifted to different times without impacting operations.

Total Consumption: Is sum of all types of electrical loads (AC, DC, and deferrable) over the year.

Production (kWh/year)

Grid Purchases**:** Represent the total annual electricity purchased from the grid to meet the system's demand.

Total Production: Sum of all electricity produced or acquired to meet the total consumption

Excess Electricity (kWh/year)

Unmet Electric Load: Represents the amount of electricity demand that was not met over the year.

Capacity shortage: Represents instances where the system's capacity was insufficient to meet the demand, leading to potential power outages.

The initial examination focuses on the simulation and results from HOMER of the '**baseline system'**, where the grid supplies all consumption (Table 8).

Table 8: Simulation Electrical Results for the grid Architecture (HOMER Data)

Consumption	**kWh/year**	**kWh/year**
AC Primary Load	5,484,635	100
DC Primary Load	0	0
Deferrable Load	0	0
Total	5,484,635	100
Production	**kWh/year**	**%**
Grid Purchases	5,484,635	100
Total	5,484,635	100
Excess Electricity	**0**	**0**
Unmet Electric Load	0	0
Capacity Shortage	0	0
Renewable Fraction	-	0

Table 8 presents the simulation's electrical results for the grid architecture using HOMER, indicating that the total annual electricity consumption is 5,484,635 kWh, all of which is attributed to the AC primary load. This demand is entirely met by grid purchases, demonstrating a complete reliance on the grid with no contributions from DC primary load or deferrable load, and no integration of renewable energy sources. The results show a balanced system with no excess electricity, unmet electric load, or capacity shortages.

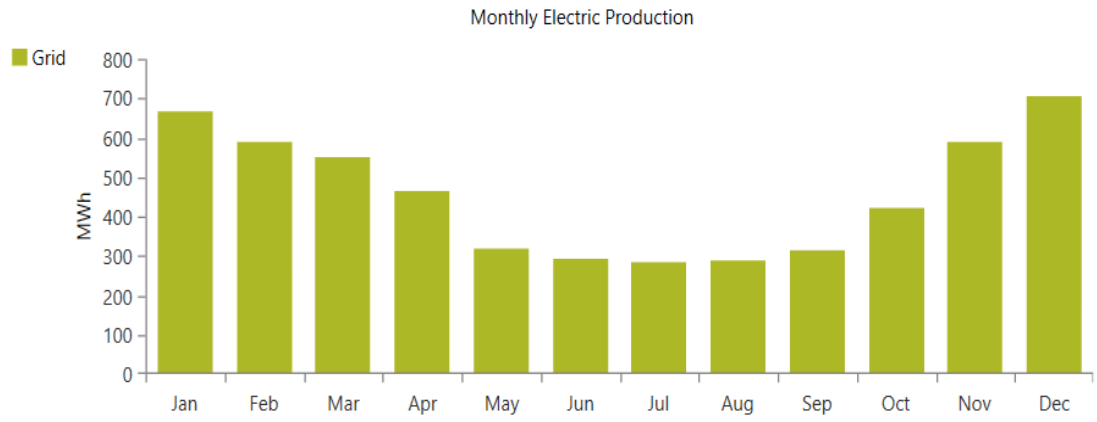

Figure 34: Monthly Electrical Load of the Baseline Model

The graph in figure 34, illustrates monthly electric production from the grid, highlighting significant seasonal variations. Electric production peaks in the winter months of January, November, and December, reaching around 700-800 MWh, likely due to increased heating demands. Conversely, production drops to its lowest in June and July, at about 200-250 MWh, reflecting reduced summer demand. Spring and fall show moderate production levels, marking transitional periods.

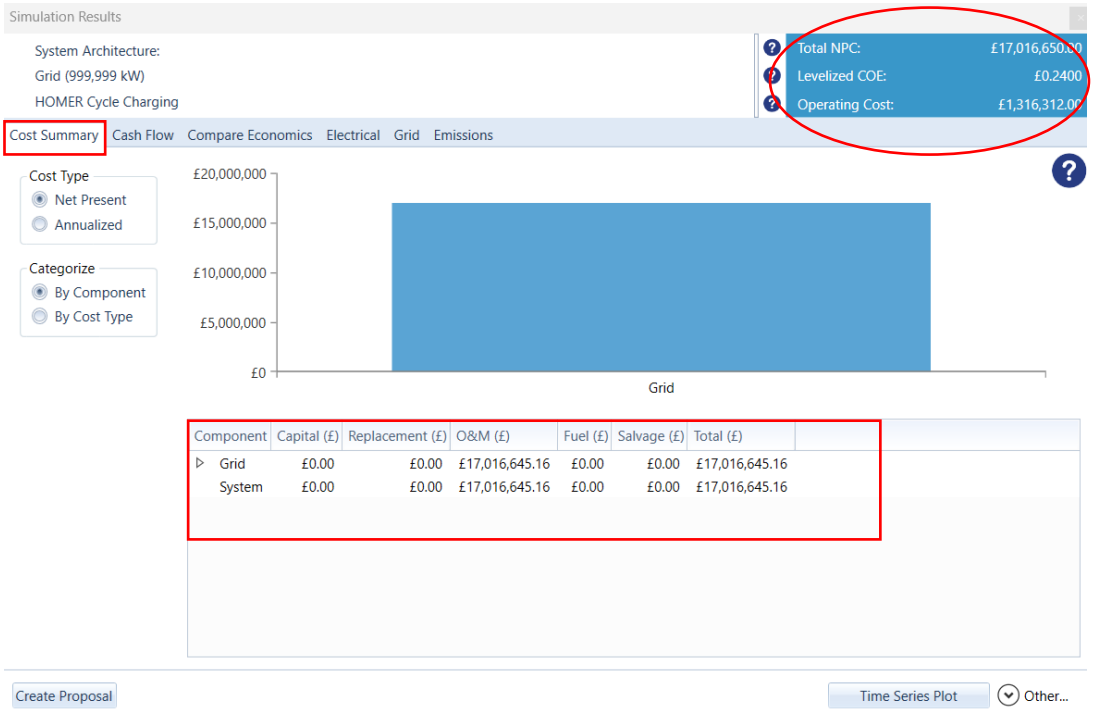

Figure 35:Detailed Cost Summary for a grid-tied Power System

Figure 35 provides a comprehensive cost summary for a grid-tied power system. The financial metrics indicate an **NPC** of £17 million, primarily driven by operational and maintenance expenses, with no costs allocated to capital, replacement, fuel, or salvage.

The model exhibits an **LCOE** of 0.24 £/kWh, and **LCOH** of 0.0774 £/kWh (calculated from equation 11).

4.1 Electrical Analysis of the three HRPS

4.1.1 Grid- connected Photovoltaic (PV) System

Simulations are performed with PV modules in conjunction with the grid in HOMER. According to the methodological analysis in table 5, the maximum PV capacity that can be installed, based on the available roof area in Queen's Quay, is 1,713.04 kWp. Hence, to meet the system's peak load requirement of 1,709.68 kW, approximately 5180 PV panels are needed.

Table 9: Simulation Electrical Results for the PV grid-connected Architecture (Homer Data)

Consumption	**kWh/year**	**%**
AC Primary Load	5,484,635	92.4
DC Primary Load	0	0
Deferrable Load	0	0
Grid Sales	450,564	7.59
Total	5,935,199	100
Production	**kWh/year**	**%**
PV	1,749,634	28.9
Grid Purchases	4,303,110	71.1
Total	6,052,744	100
Excess Electricity	31,646	0.523
Unmet Electric Load	0	0
Capacity Shortage	0	0
Renewable Fraction	-	27.5

Table 9 illustrates the electrical results after HOMER's simulation for the PV grid-connected system. In this scenario, the annual average electricity production from PV

accounts for approximately 29% (1,749,634 kWh/year) of the total generation, with a capacity factor of 11.7%. While the remaining of 71% (4,303,110 kWh/year) is the required power purchased from the grid. Therefore, the grid provides most of the power necessary to satisfy the load requirement, with a renewable fraction of 27.5%. While the excess electricity is 31,646 kWh/year.

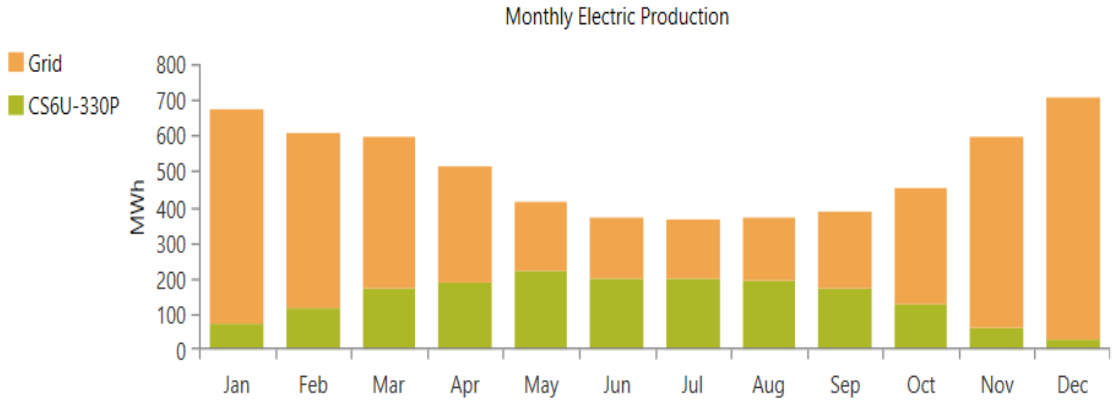

Figure 36:Monthly Average Electrical Production

The graph in figure 36 shows the seasonal variations of energy generation by the PV system and the grid. During the winter months (November to February), there is a marked reliance on the grid, with grid production peaking at approximately 700 MWh in December and around 600 MWh in January, while the PV system contributes a modest 50 MWh. As the seasons transition to sunnier months, the PV system's output significantly increases, reaching a peak of around 200 MWh in May. From April to September, the PV system's enhanced production reduces the grid's share, with grid output dropping to approximately 400 MWh in May and June. This pattern underscores the heavy dependence on grid electricity during the winter and the substantial contribution from the PV system during the sunnier months, highlighting the seasonal dynamics of energy production in the system.

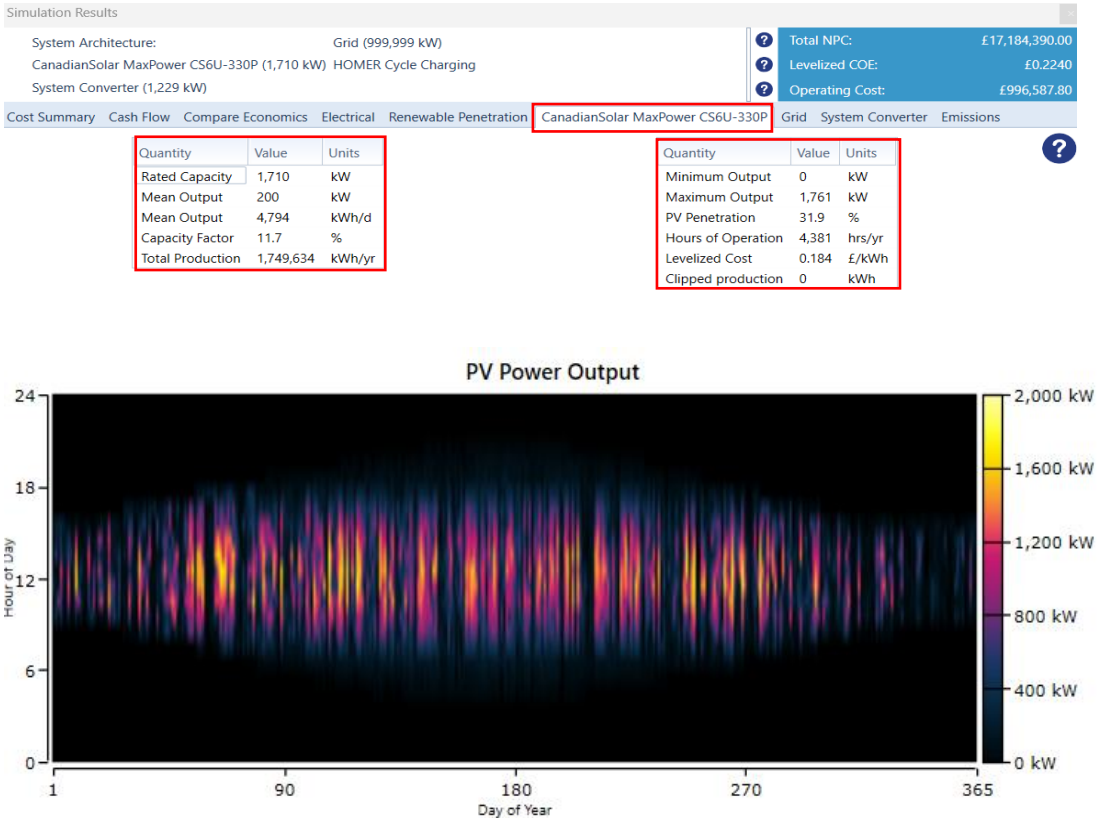

Figure 37: Yearly PV Power Outputs in HOMER

The PV system produces electricity during the daytime, reaching its highest output around noon as shown in figure 37. The system runs for a total 4,381 hours throughout the year. The average and highest power generated by this PV panel is 200 kW (4,794 kWh/day) and 1,761 kW, respectively, at a 31.9% penetration rate.

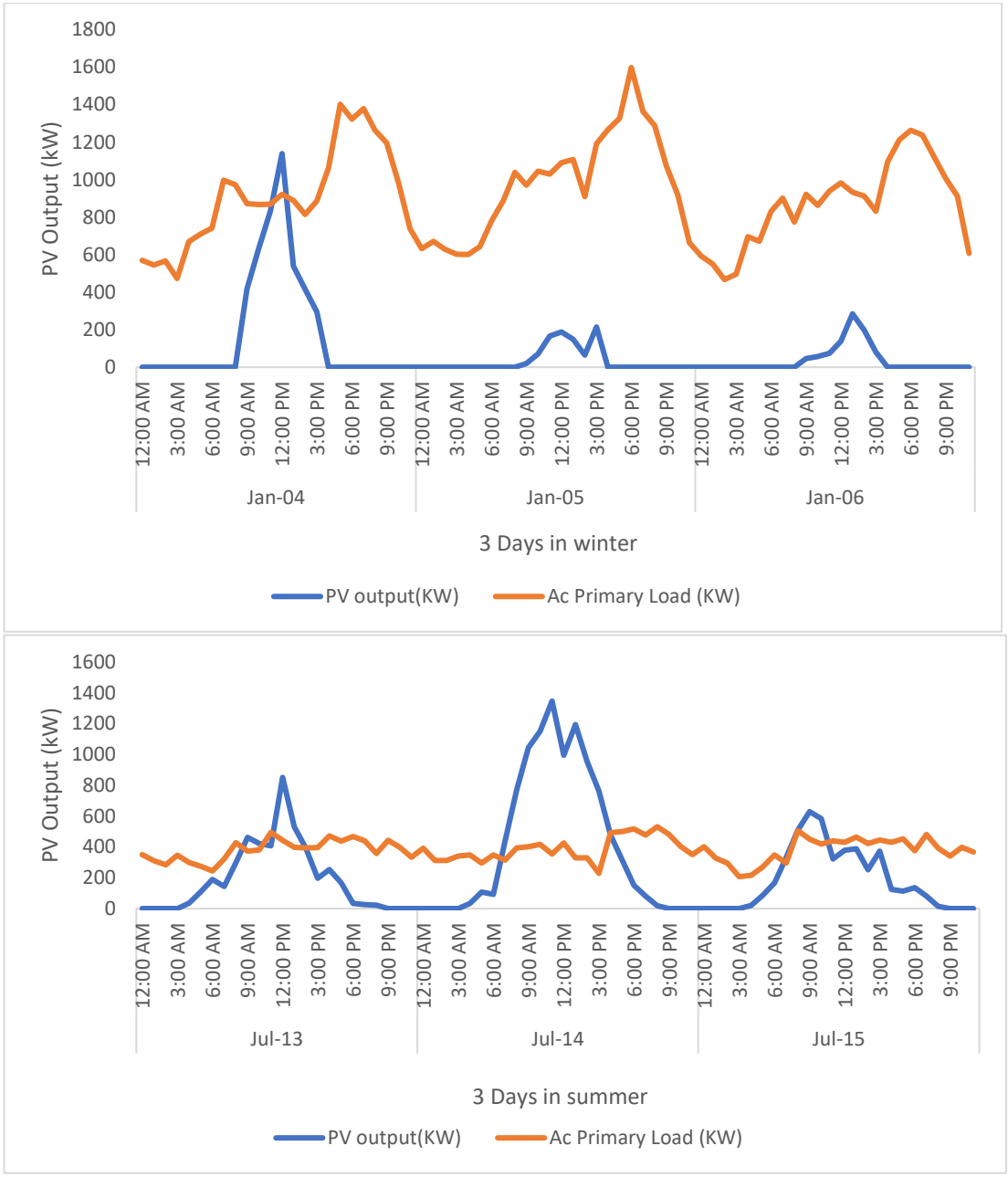

Figure 38: PV Output and Ac primary Load during 3 days in Winter and Summer

Both graphs in figure 38 illustrate the variability of PV output and the relative stability of AC primary load over three-day periods in winter and summer. In winter, the PV output is lower with peaks around midday reaching approximately 600-800 kW and less aligned with the AC primary load. While in summer, the PV output is higher with peaks around midday reaching approximately 1,200-1,400 kW and more closely matches the load during daylight hours.

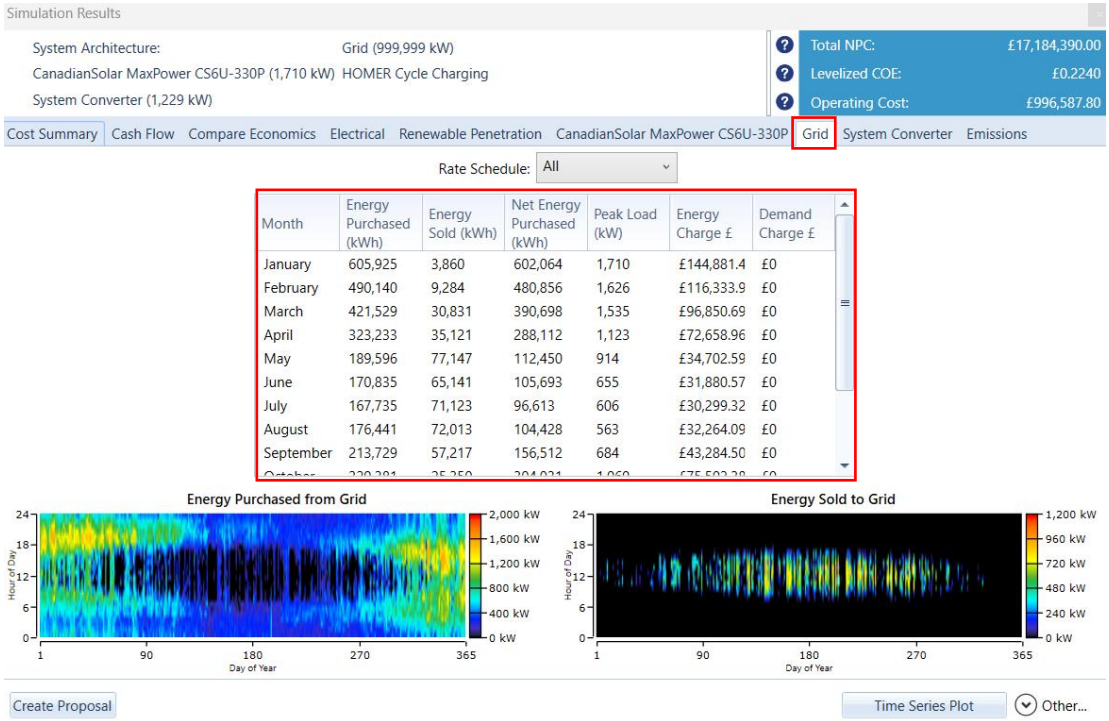

Figure 39:The Energy Purchased and Sold to the grid in HOMER

Figure 39 presents the simulation results for a grid-tied power system with PV panels. The table shown above, details monthly energy purchased and sold to the grid. The heat maps illustrate the hourly and seasonal variations in energy purchased from and sold to the grid.

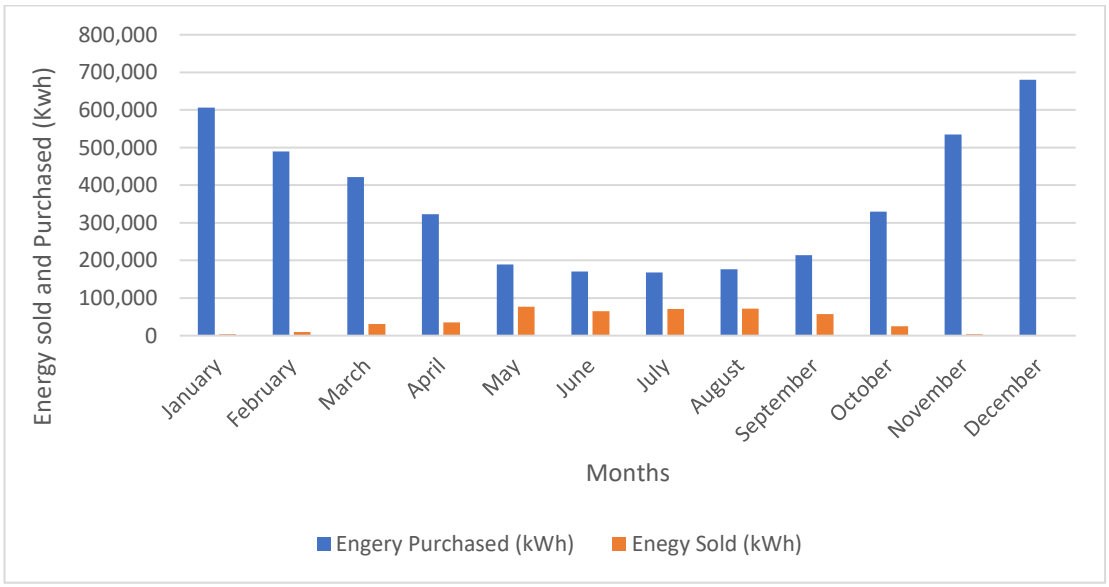

Figure 40: Monthly Energy Sold and Purchased from the grid for PV-grid connected system

The energy bought from the grid to satisfy the load demand in this location and the energy sold to the grid when the generated electricity surpassed the demand is depicted in figure 40. The graph indicates a clear trend of higher energy purchase from the grid, especially during the winter months (November, December, January) show a significant increase in energy purchases, consistent with higher heating demands and reduced PV generation. Summer months (June, July, August) show relatively lower energy purchases and slightly higher energy sold, reflecting better PV generation and lower heating demands.

4.1.2 Grid- connected Wind Turbine (WT) System

After evaluating various turbine sizes and associated costs using HOMER, as detailed in table 10. a 250-kW wind turbine is identified as the most suitable option for the site's conditions, despite its higher LCOE (Table 10). Consequently, it is proposed to install seven 250-kW wind turbines, totalling 1.75 MW of capacity, to enhance the overall system performance.

Table 10: Comparative Analysis of WT Performance and Cost Efficiency using HOMER

WT rated capacity (kW)	Number of WT	Mean output (kW)	Max output (kW)	Peak load (kW)	Wind Penetration (%)	Net LCOE(£/kWh)
250	7	117	250	1,709.68	19	0.4631
1,000	2	721	999		115	0.0355
2,000	1	1,153	2,049		184	0.0134

Table 11:Simulation Electrical Results for the WT grid-connected Architecture (Homer Data)

Consumption	**kWh/year**	**%**
AC Primary Load	5,484,635	62.1
DC Primary Load	0	0
Deferrable Load	0	0
Grid Sales	3,341,768	37.9
Total	8,826,403	100
Production	**kWh/year**	**%**
WT	7,207,808	81.7
Grid Purchases	1,618,595	18.3
Total	8,826,403	100
Excess Electricity	0	0
Unmet Electric Load	0	0
Capacity Shortage	0	0
Renewable Fraction	-	81.6

Table 11 illustrates the electrical results after HOMER's simulation for the WT grid-connected system. In this scenario, wind turbines contribute significantly to the annual electricity production, generating approximately 81.7% of the total energy required, equivalent to 7,207,808 kWh/yr. The remaining 18.3 % (1,618,595 kWh/year) of the necessary power is supplemented by grid purchases. This configuration achieves a renewable energy fraction of 81.6%, highlighting the system's efficiency in leveraging wind power to satisfy most of its energy needs with no excess electricity.

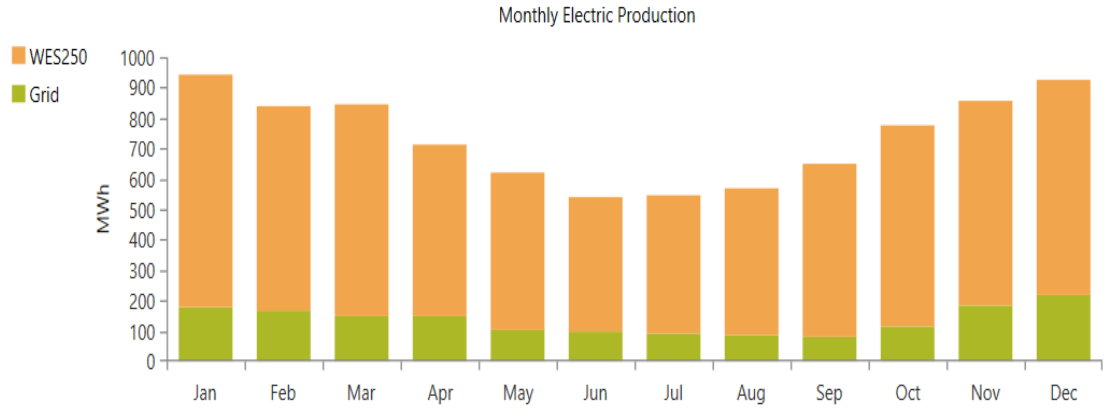

Figure 41: Monthly Average Electrical Production

Figure 41 illustrates the monthly average electrical production of the hybrid system. The wind turbines generate the most electricity during the winter months (January, February, November, December), with production peaking around 800-900 MWh. Production dips slightly during the summer months (June, July, August), where it falls to around 600-700 MWh, likely due to reduced wind speeds or availability. Consequently, the wind turbines primarily meet the load demand, ensuring that the system experiences zero unmet energy.

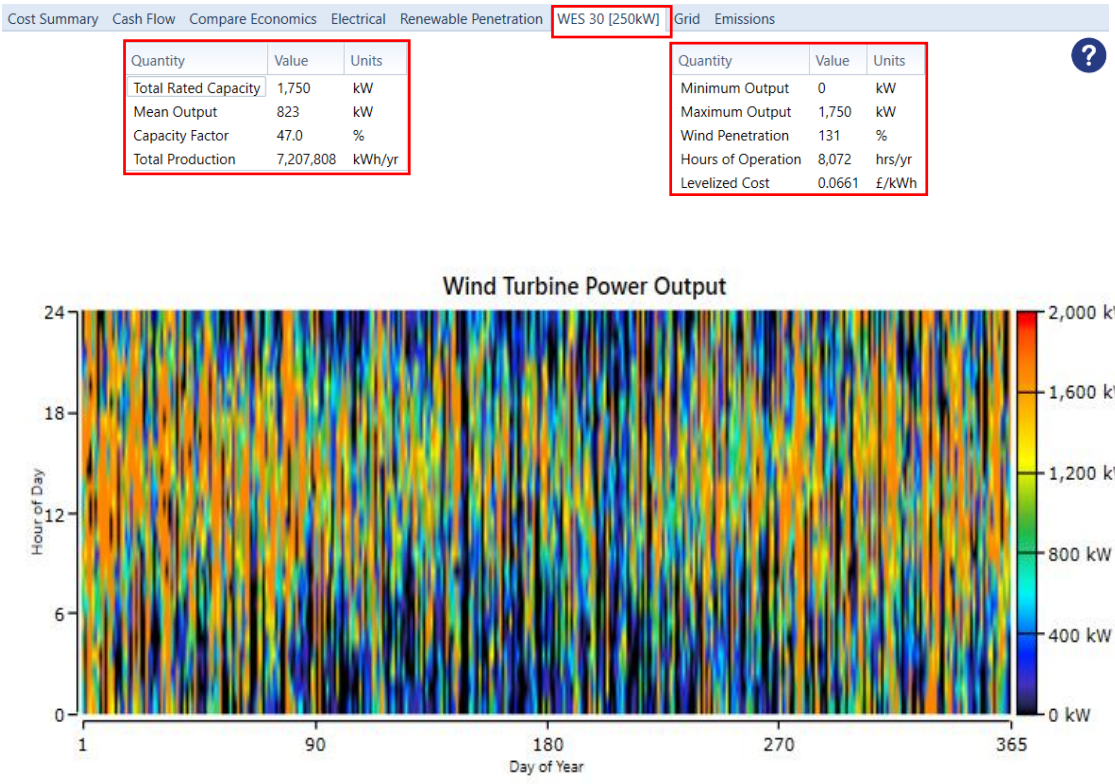

Figure 42:Yearly WT Power Output in HOMER

The graph in figure 42 demonstrates the wind turbines performance. The wind turbines have a mean output of 823 kW and a maximum output of 1,750 kW, with a wind penetration rate of 131%. The system operates efficiently with a high-capacity factor of 47%, and it runs for 8,072 hours a year. This performance highlights the system's efficiency and cost-effectiveness in harnessing wind energy to meet the energy needs.

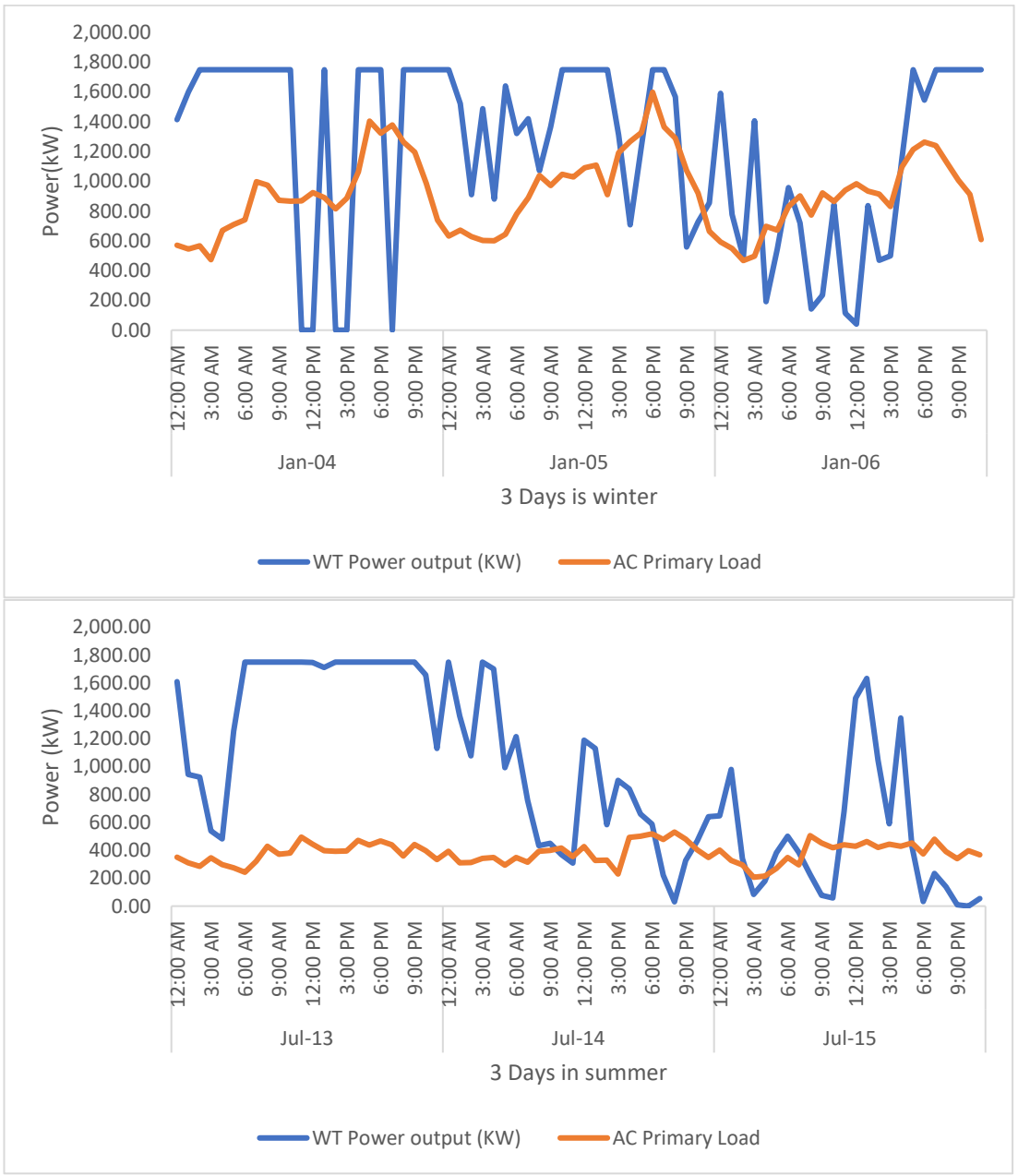

Figure 43:WT Power Output and AC Primary Load during 3 days in Winter and Summer

Both graphs in Figure 43 demonstrate the dynamic nature of wind turbine power output and the relatively stable nature of the AC primary load. In the winter, there are frequent mismatches between wind turbine output and AC primary load, with the load frequently exceeding WT output. The wind turbine power output varies significantly, with peaks of around 1,700 kW. In the summer, wind turbine power output fluctuates but remains high, reaching up to approximately 1,600 kW.

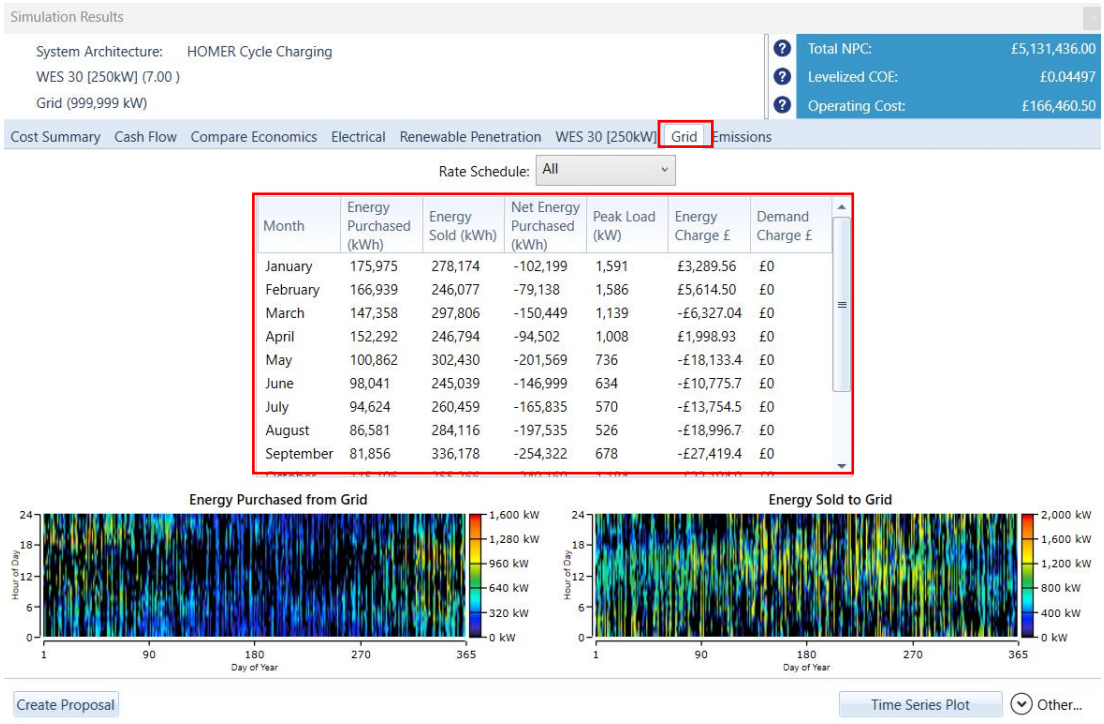

Figure 44:The Energy Purchased and Sold to the grid in HOMER

The figure 44 presents grid simulation results for a grid-tied power system with Wind turbines. Where the table details monthly energy purchased and sold to the grid. The heat maps illustrate the hourly and seasonal variations in energy purchased from and sold to the grid, highlighting peak energy purchases during winter and peak energy sales during summer.

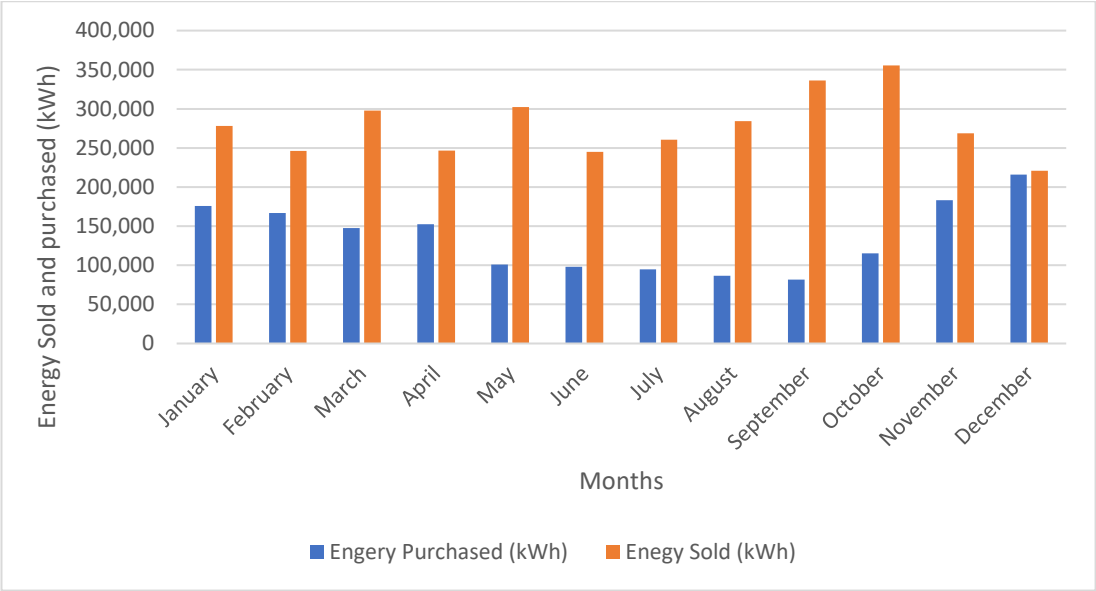

Figure 45:Monthly Energy Sold and Purchased from the grid for the WT-grid connected system

The figure 45, reveals that throughout the year, the energy system consistently exports more energy to the grid than it imports. The energy purchased from the grid is relatively low and consistent throughout the year, with slight increases in the winter months (January, February, November, December) indicating increased energy demand likely due to heating needs during the coldest month. The energy sold back to the grid is consistently low across all months, with small peaks during the summer months (June, July, August). This indicates that surplus energy generation is minimal, reflecting either limited excess production or effective self-consumption of generated energy.

4.1.3 Grid-connected PV and WT System

The optimal combination for minimising costs and excess electricity production while meeting peak load demand, as identified in the methodological analysis (Table 7), is a 209.68 kW peak PV array consisting of 635 PV panels, paired with six 250 kW wind turbines. This configuration achieves the lowest LCOE and NPC obtained after the simulation in HOMER to ensure an efficient and cost-effective energy solution, as shown in figure 46.

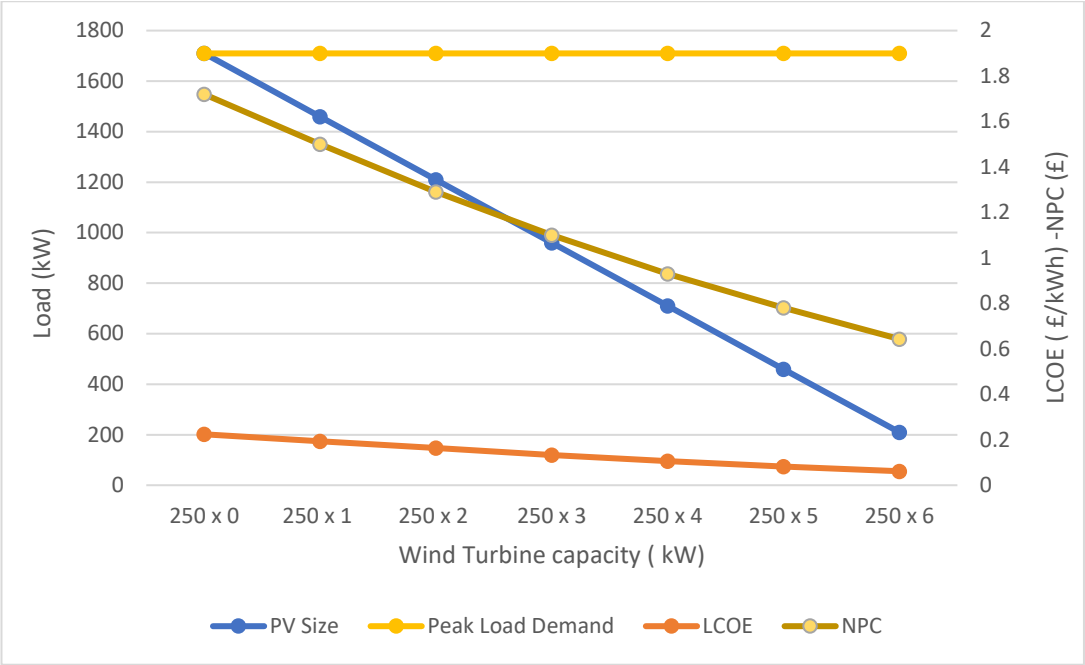

Figure 46:Comparison of WT Capacity with PV Size, Load Demand, LCOE, and NPC

The figure illustrates the relationship between wind turbine capacity (in kW), PV Size (kW), Peak Load Demand (kW), LCOE in (£/kWh), and NPC in (£).

As wind turbine capacity increases, the PV size, represented by the blue line, decreases linearly, indicating a reduced need for PV capacity to meet energy demand. The peak load demand, remains constant at approximately 1700 kW across all scenarios, underscoring the fixed energy requirement. The LCOE, shows a slight decrease with increasing wind turbine capacity, suggesting enhanced economic efficiency per unit of electricity generated. Similarly, the NPC, decreases as wind turbine capacity increases, highlighting a reduction in overall system costs, including installation, operation, and maintenance over the system's lifetime. Overall, the analysis suggests that integrating more wind turbines can reduce the dependence on PV systems and improve the economic efficiency of the Queen's Quay District Heating Network.

Export... Export Details...

Optimization Results

Double click on a system to see its Simulation Details.

Categorized Overall

	Architecture								Cost				System		
					CS6U-330P (kW)	WES250	Grid (kW)	Converter (kW)	Dispatch	NPC (£)	LCOE (£/kWh)	Operating cost (£/yr)	CAPEX (£)	Ren Frac (%)	Total Fuel (L/yr)	
						6	999,999		LF	£6.31M	£0.0615	£290,628	£2.55M	77.8	0	4
					210	6	999,999	160	LF	£6.43M	£0.0616	£258,635	£3.08M	79.0	0	3
					210		999,999	160	LF	£17.0M	£0.239	£1.27M	£530,358	3.68	0	6
							999,999		LF	£17.0M	£0.240	£1.32M	£0.00	0	0	

Figure 47:HOMER Simulation Results for the PV, WT grid-connected System

Figure 47 illustrates the categorised simulation result for the PV, WT and the grid system in HOMER. After simulation, the power system is selected to guarantee a larger percentage of renewable energy, minimal surplus electricity, NPC and LCOE.

Four systems are identified as viable options: WT/grid, PV/WT/grid, PV/grid, and the grid. The hybrid energy system's most reasonable configuration is determined to be the WT and PV grid-connected system.

Table 12: Simulation Electrical Results for the PV and WT grid-connected Architecture (HOMER DATA)

Consumption	**kWh/year**	**%**
AC Primary Load	5,484,635	68
DC Primary Load	0	0
Deferrable Load	0	0
Grid Sales	2,585,660	32
Total	8,070,295	100
Production	**kWh/year**	**%**
PV	214,580	2.65
WT	6,174,561	76.4
Grid Purchases	1,693,854	21
Total	8,082,995	100
Excess Electricity	2,075	0.0257
Unmet Electric Load	0	0
Capacity Shortage	0	0
Renewable Fraction	-	79

In this scenario, the annual average electricity production from PV is about 2.65% (214,580 kWh/year) of the overall generation with at a capacity factor of 11.7%. while the WT annual production forms 76.4% (6,174,561kWh/year) of the total production. The remaining 21% (1,693,854 kWh/year) is purchased energy from the grid as shown in table 12. The system achieves a renewable fraction of 79% with 2,075 kWh/year excess electricity.

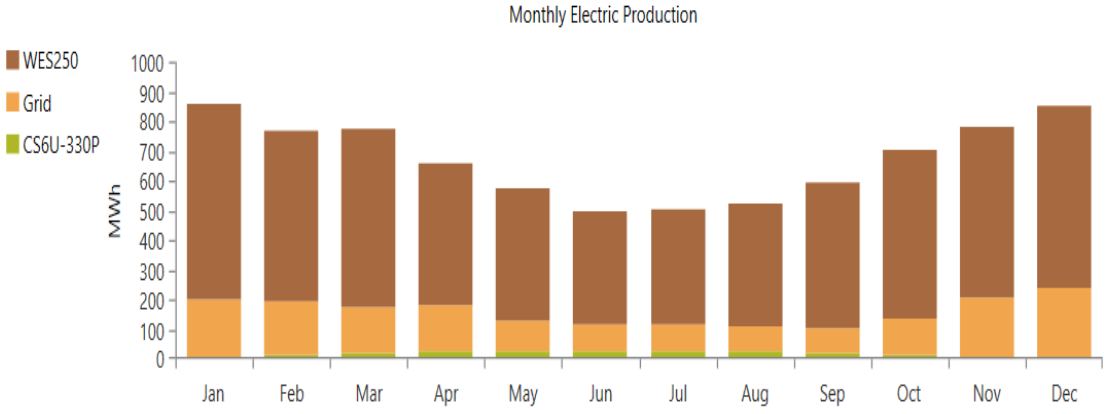

Figure 48: Monthly Average Electrical Production

Figure 48 illustrates the WT monthly electric output, the grid and solar PV panels. The wind turbines consistently generate most of the electricity throughout the year, with production peaking in the winter months (January, February, November, December) at around 800-900 MWh. Grid contributions are relatively stable each month but slightly higher during the winter months to complement the wind production, reaching about 300 MWh. The solar PV panels contribute a small but steady amount of electricity, peaking in the sunnier months (April to August) with a maximum around 100 MWh. This graph highlights the reliance on wind energy for the bulk of production, with grid support more prominent in winter and solar providing additional support in summer, demonstrating a well-balanced hybrid system to meet energy demands throughout the year.

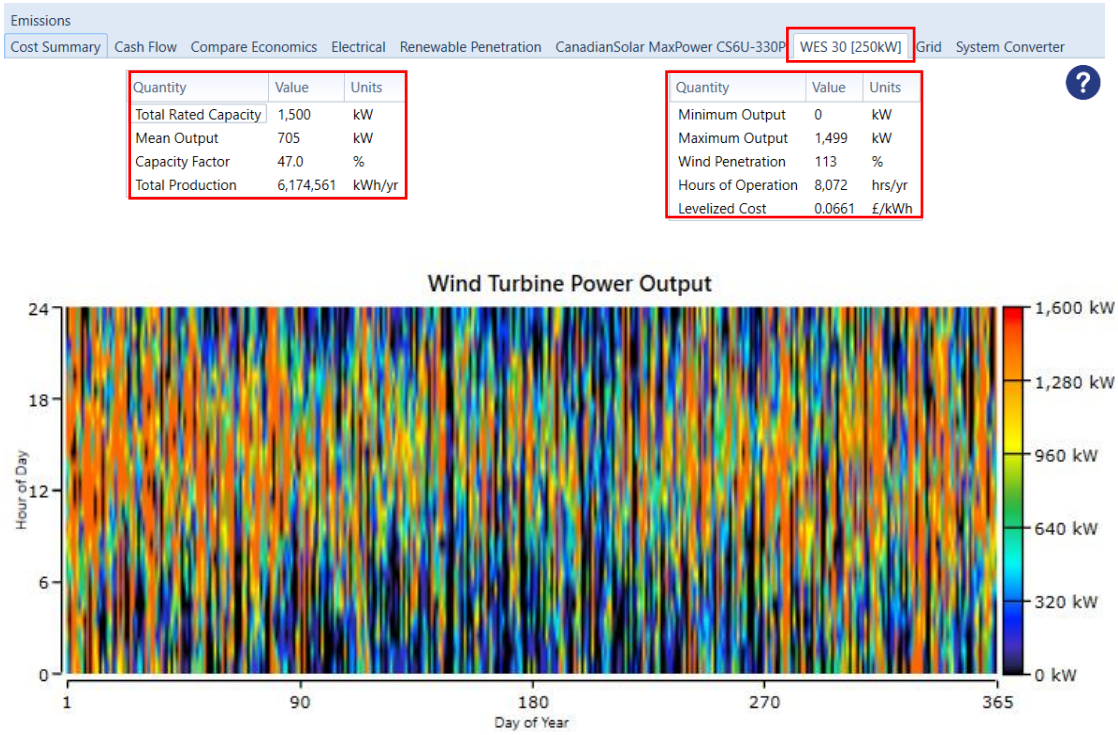

Figure 49: Yearly WT Power Output from HOMER

Figure 49 depicts the wind turbine's power output. The wind turbines have a mean output of 705 kW and a maximum output of 1500 kW, with a wind penetration rate of 113. The wind turbines operate efficiently for 8,072 hours a year. This performance highlights the system's efficiency and cost-effectiveness in harnessing wind energy to meet the energy demands.

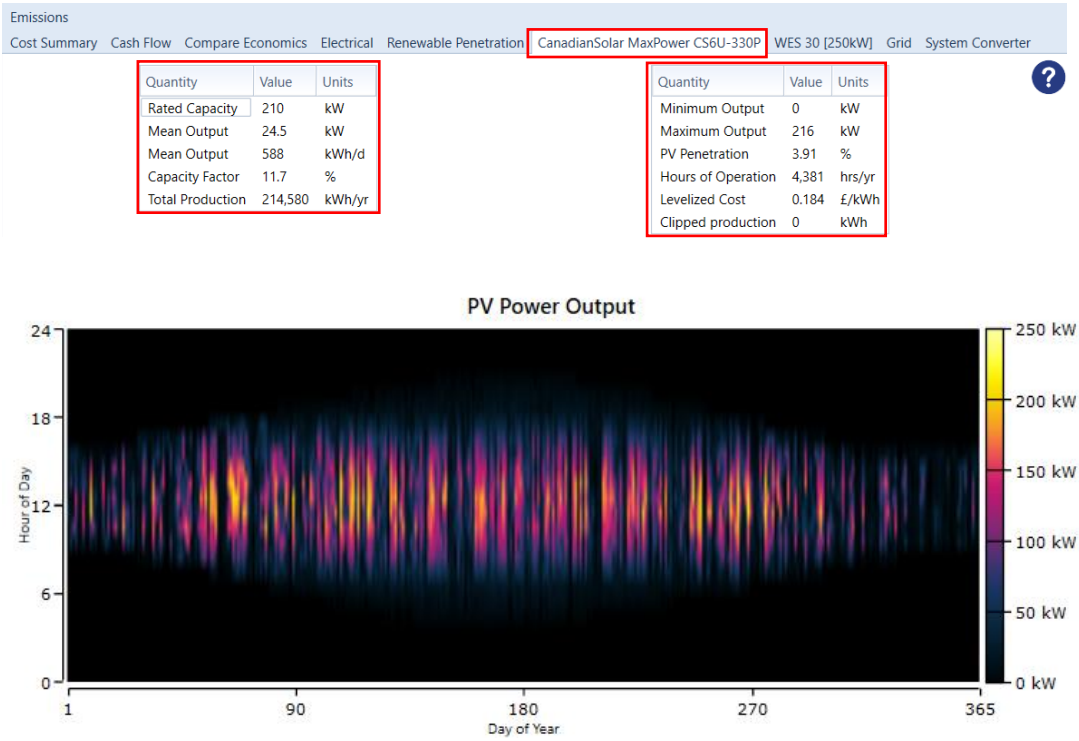

Figure 50: Yearly PV power output from HOMER

Figure 50 shows the PV system's output. It operates 4,381 hours throughout the year. The mean and maximum output of this PV Array is 24.5 kW (588 kWh/day) and 216 kW, respectively, with a penetration rate of 3.91%.

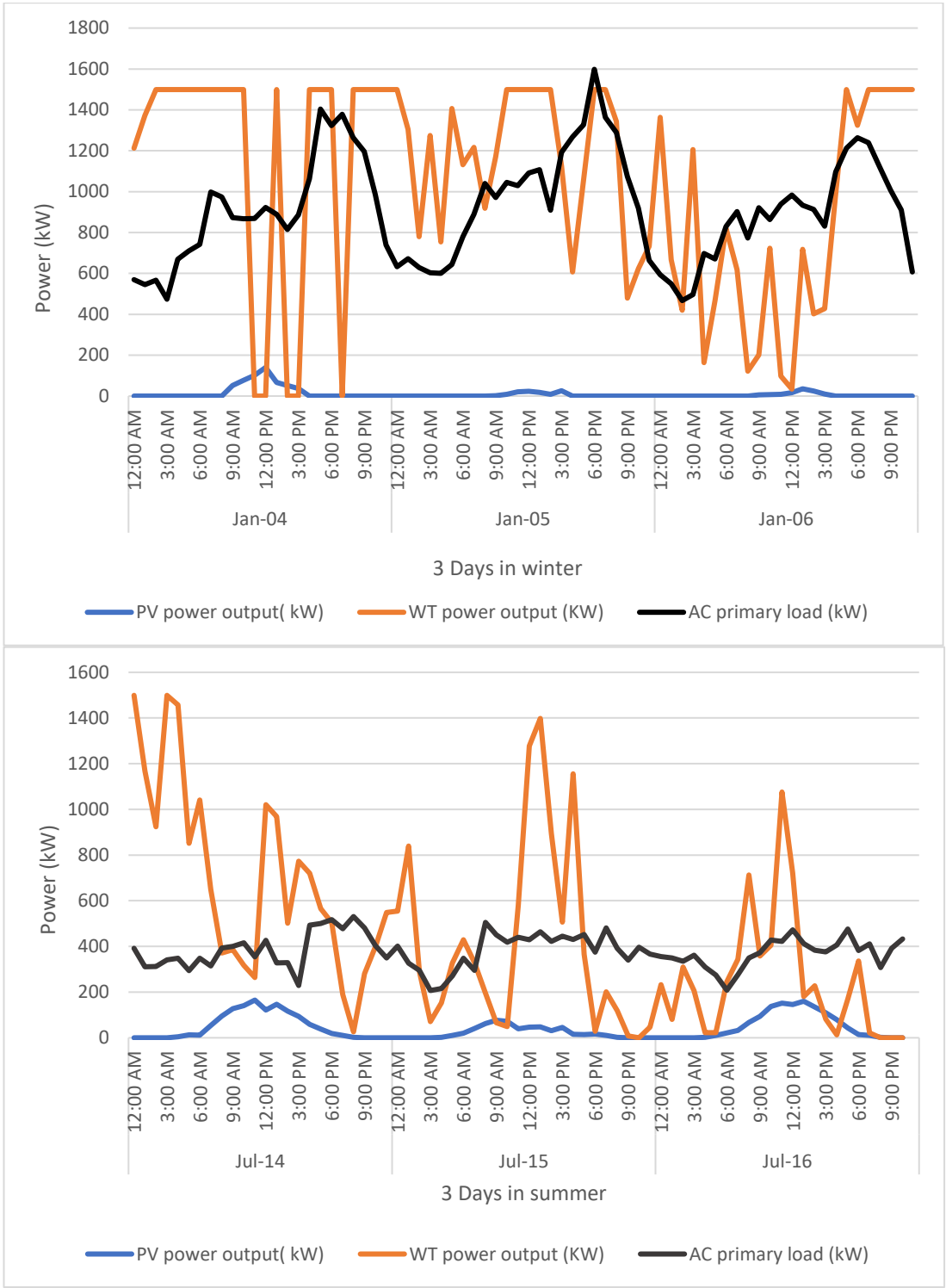

Figure 51:PV + WT Output along with the AC Load during 3 days in Winter and Summer

In figure 51, the graphs illustrate the WT and PV power output along with the AC primary load over a period of three days winter and summer. In winter, the system relies heavily on wind energy, with PV contributing minimally with peaks barely reaching 200 kW due to limited sunlight. The combined output of WT and PV often meets or exceeds the AC primary load, indicating an efficient use of available renewable resources. While in summer, the system benefits from both wind and solar

energy. The PV output is significantly higher with peaks reaching around 400 kW, contributing substantially to meeting the AC primary load. The combined output from WT and PV often exceeds the primary load, especially during daylight hours, ensuring an efficient and balanced supply of renewable energy.

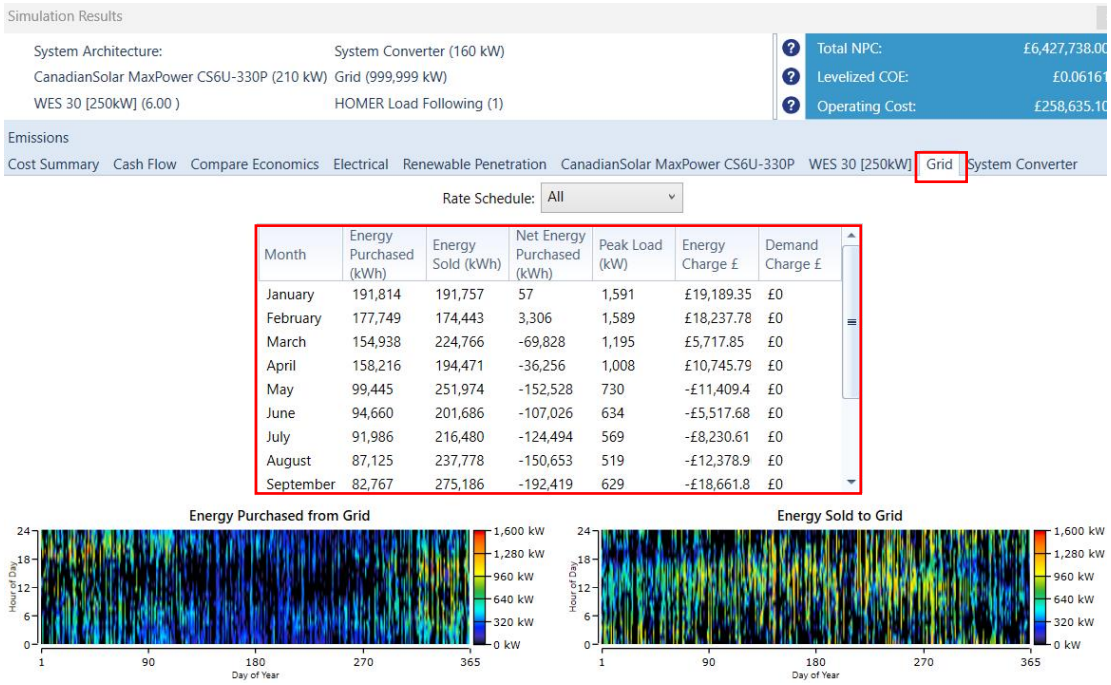

Month	Energy Purchased (kWh)	Energy Sold (kWh)	Net Energy Purchased (kWh)	Peak Load (kW)	Energy Charge £	Demand Charge £
January	191,814	191,757	57	1,591	£19,189.35	£0
February	177,749	174,443	3,306	1,589	£18,237.78	£0
March	154,938	224,766	-69,828	1,195	£5,717.85	£0
April	158,216	194,471	-36,256	1,008	£10,745.79	£0
May	99,445	251,974	-152,528	730	-£11,409.4	£0
June	94,660	201,686	-107,026	634	-£5,517.68	£0
July	91,986	216,480	-124,494	569	-£8,230.61	£0
August	87,125	237,778	-150,653	519	-£12,378.9	£0
September	82,767	275,186	-192,419	629	-£18,661.8	£0

Figure 52:The Energy Purchased and Sold to the grid in HOMER

Figure 52 presents the simulation results for PV, WT and the grid system. Where the table details monthly energy purchased and sold to the grid. The heat maps illustrate the hourly and seasonal variations in energy purchased from and sold to the grid, highlighting peak energy purchases during winter and peak energy sales during summer.

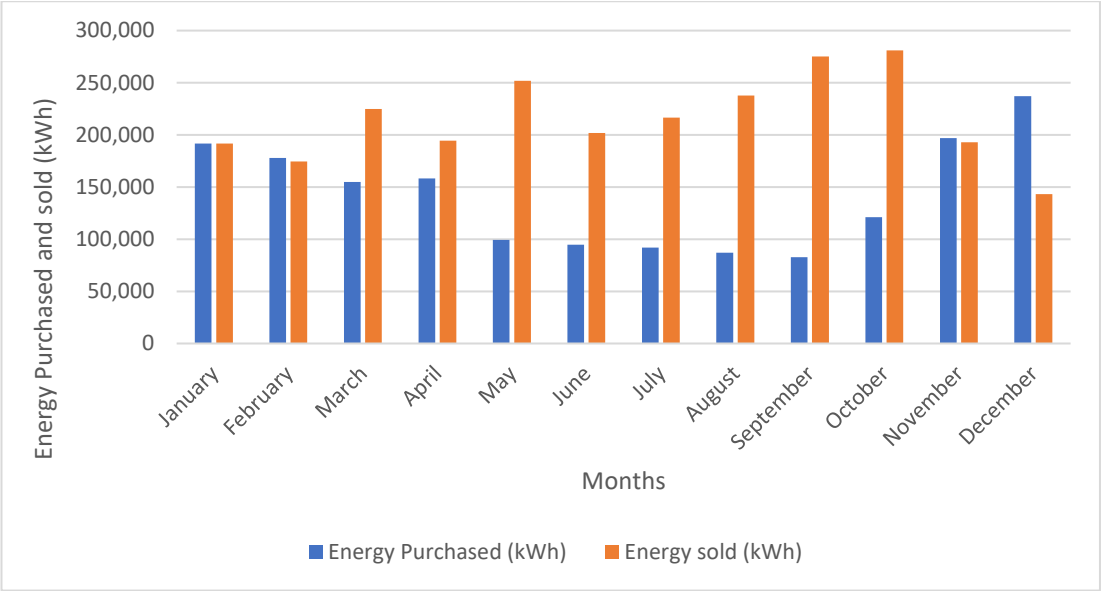

Figure 53:Monthly Energy sold and purchased from the grid for the PV, WT grid-connected System

The graph in figure 53 was generated based on the results obtained from HOMER simulations (figure 52), it illustrates the monthly energy purchased and sold from the grid throughout the year. The energy purchased from the grid remains relatively low and consistent across most months. There is a noticeable peak in December, indicating increased energy demand likely due to heating requirements in winter. The energy sold back to the grid is minimal across all months, with slight increases during the summer months (June, July, August). This suggests that the system generates a small surplus of energy during these months, likely due to higher solar irradiance and wind speeds.

4.2 Economic analysis of the three HRPS

The main goal of the economic assessment is to offer an efficient solution by reducing the NPC, LCOE, and LCOH in the HRPS design.

4.2.1 Grid- connected Photovoltaic (PV) System

Th economic analysis findings of the PV grid-connected system in HOMER is shown in figure 54, that presents a detailed cost summary for a grid-tied power system incorporating a PV system.

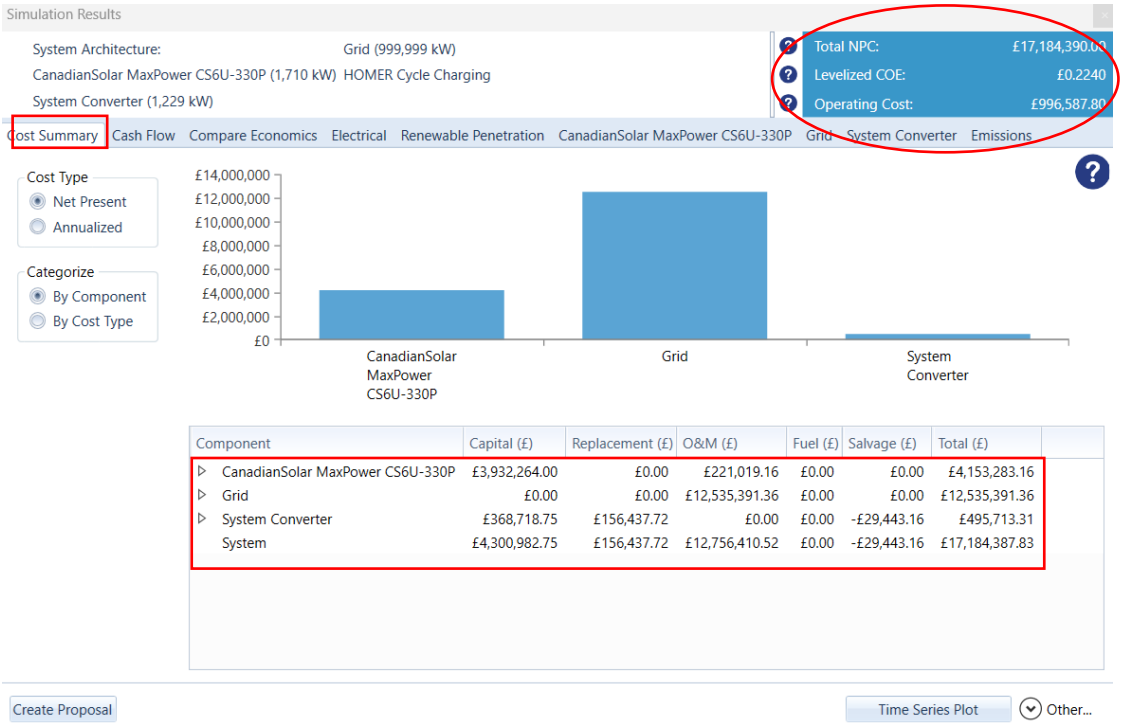

Figure 54: HOMER Financial Results of the PV grid-connected System

The system incurs a total **NPC** of is £17.2 million, driven by grid costs amounting to £12,535,391.36, primarily due to operational and maintenance (O&M) expenses. The PV system contributes £4,153,283.16 to the NPC, which has £3,932,264.00 as capital costs and £221,019.16 for O&M expenses. The system converter adds an additional £495,713.31 to the NPC, consisting of £368,718.75 in capital costs, £156,437.72 in replacement costs. The system has an **LCOE** of 0.2240 £/kWh, an **LCOH** of 0.072 £/kWh with **payback period** of 13 years, indicating that it will generate enough savings to cover the initial investment within this timeframe, subsequently providing net financial benefits.

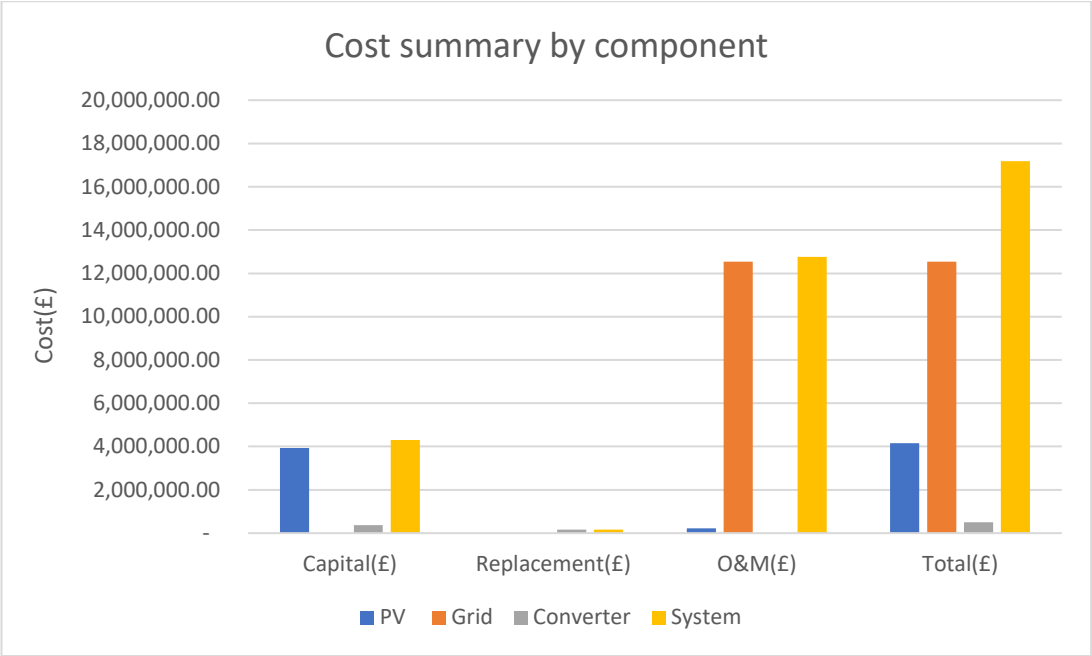

Figure 55: System Summary Cost by Component

The graph in figure 55, provides a cost summary of the Hybrid system (PV grid-connected) by component. It breaks down the costs into categories: Capital (£), Replacement (£), O&M (£), and Total (£) for PV, Grid, Converter, and System components. PV system incurs the highest total costs, driven by significant capital and replacement expenses, followed by substantial O&M costs. The grid also has notable total costs primarily due to high O&M expenses, while the system converter contributes minimally to the overall costs.

4.2.2 Grid- connected Wind Turbine (WT) System

Th WT grid-connected system economic analysis of the in HOMER is shown figure 56.

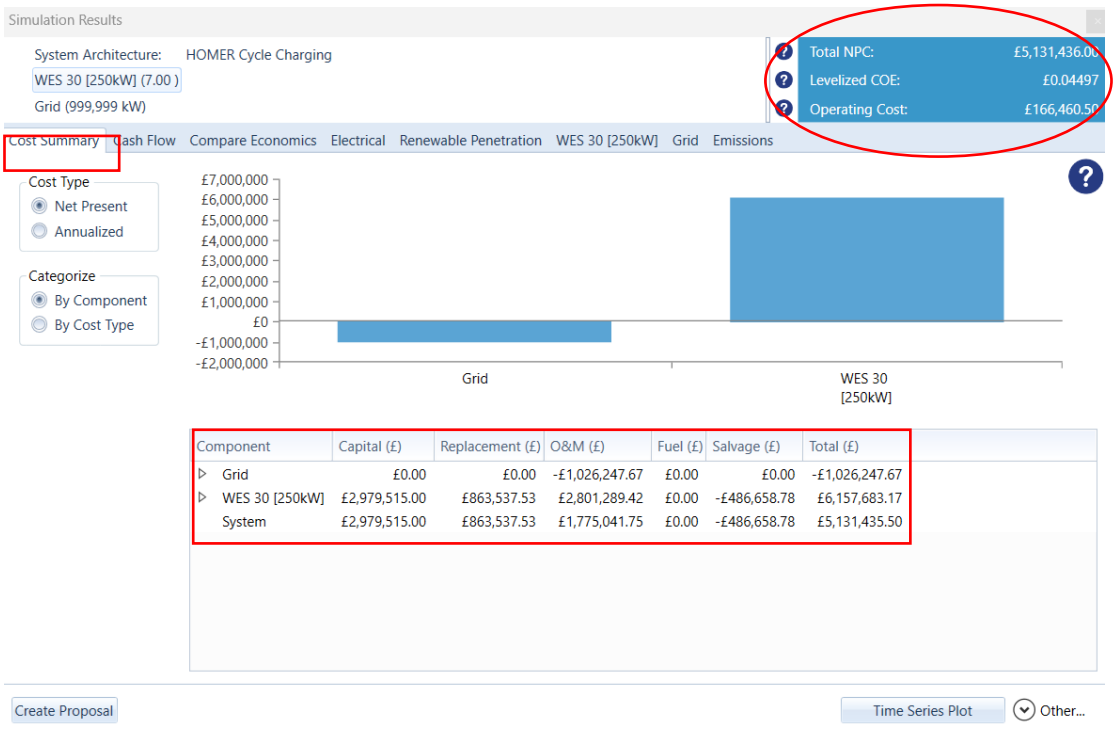

Figure 56: Homer Financial Results of the WT grid-connected System

The economic analysis of the hybrid system comprising seven wind turbines, and a grid connection demonstrates an **NPC** of £5.13 million, that incorporates the initial capital investment of £2.98 million for the wind turbines, replacement costs of £863,537.53, operational and maintenance (O&M) costs of £2.80 million, and a salvage value of -£486,658.78. The grid component contributes a negative O&M cost of -£1.03 million, indicating net savings or revenue from the grid connection. These factors together result in the total NPC. The system achieves an **LCOE** of 0.045 £/kWh, with annual operating expenses of £166,460.50, an **LCOH** of 0.0145 and a rapid **payback period** of just two and a half years.

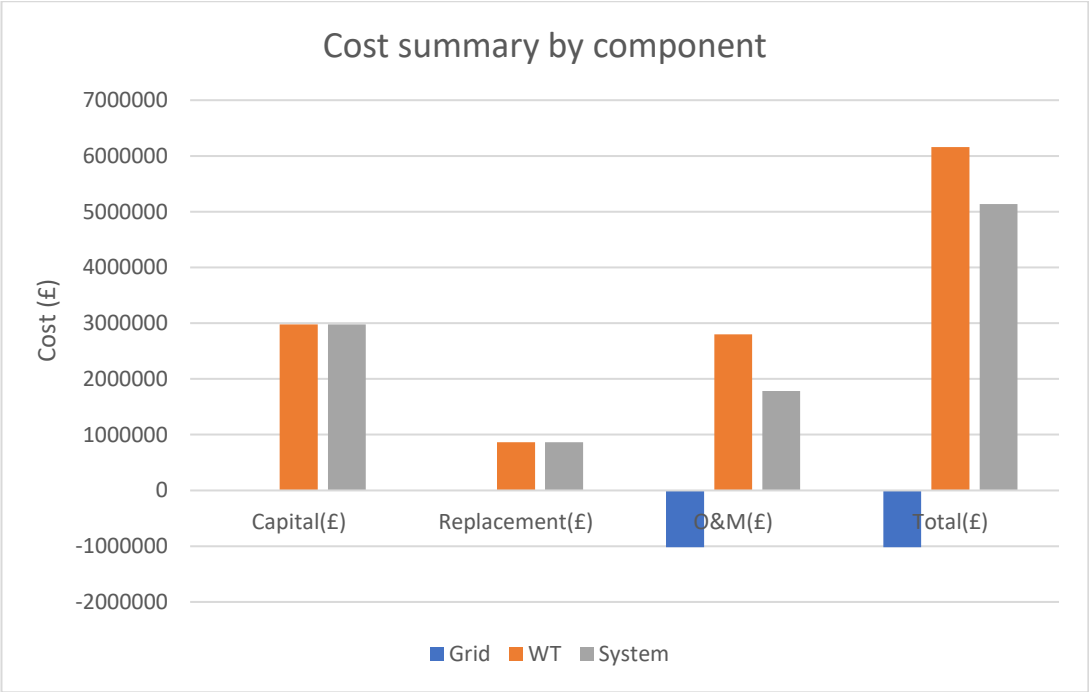

Figure 57:System Summary Cost by Component

The graph in figure 57 highlights the distribution of costs across the components of the proposed system. The wind turbines show substantial capital, replacement, and O&M costs, contributing significantly to the total system costs. The grid component, while having minimal capital costs, reflects negative O&M expenses, indicating potential cost savings. The overall system costs are driven by the combined expenses of all components, providing a detailed financial overview necessary for planning and decision-making.

4.2.3 Grid-connected Photovoltaic (PV)and Wind Turbines (WT) System

Th economic analysis of the PV and WT grid-connected system in HOMER Pro is shown figure 58.

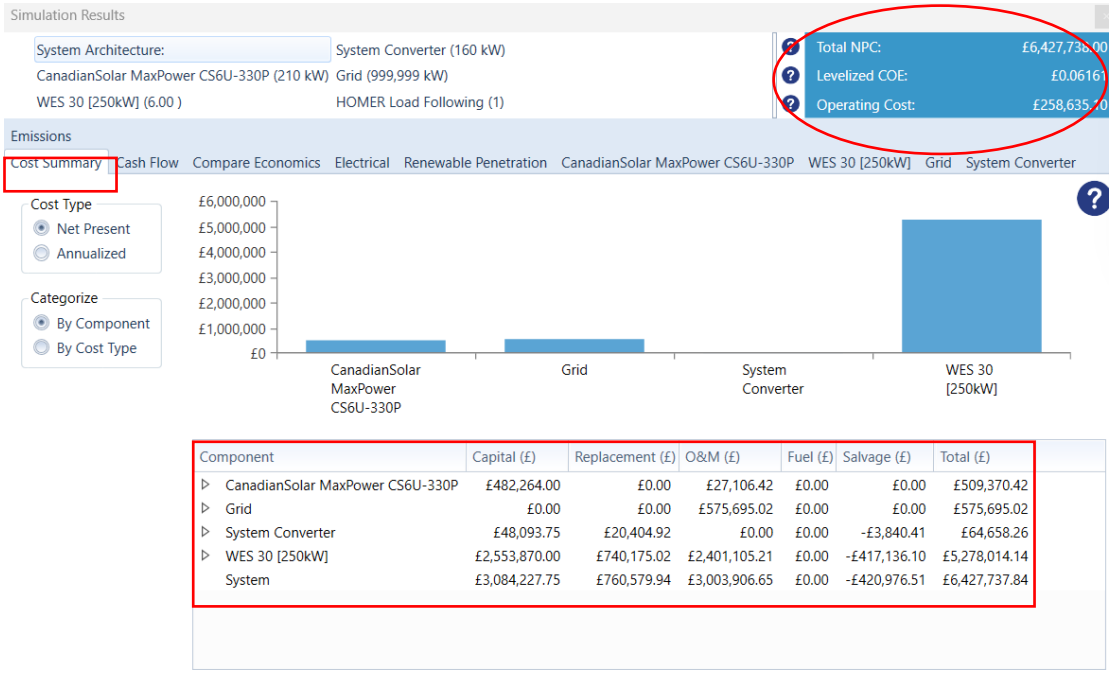

Figure 58: Homer Financial Results of the PV, WT grid-connected System

The economic analysis of the hybrid system reveals an **NPC** of £6,427,738.00. The NPC is derived from various cost components: the capital cost of the solar panels is £482,264.00, with an additional £27,106.42 in O&M costs, totalling £509,370.42. The grid incurs O&M costs of £575,695.02. The system converter has a capital cost of £48,093.75, replacement costs of £20,404.92, and a salvage value of -£3,840.41, summing up to £64,658.26. The wind turbines contribute the most significant portion with a capital cost of £2,553,870.00, replacement costs of £740,175.02, O&M costs of £2,401,105.21, and a salvage value of -£417,136.10, leading to a total of £5,278,014.13. The total system costs, considering all components, are £6,427,737.84. The operating cost is £258,635.10 annually. This cost structure results in a highly competitive **LCOE** of 0.061 £/kWh indicating a cost-effective energy production system, an **LCOH** of 0.0199 £/ kWh and 3 years **payback period**.

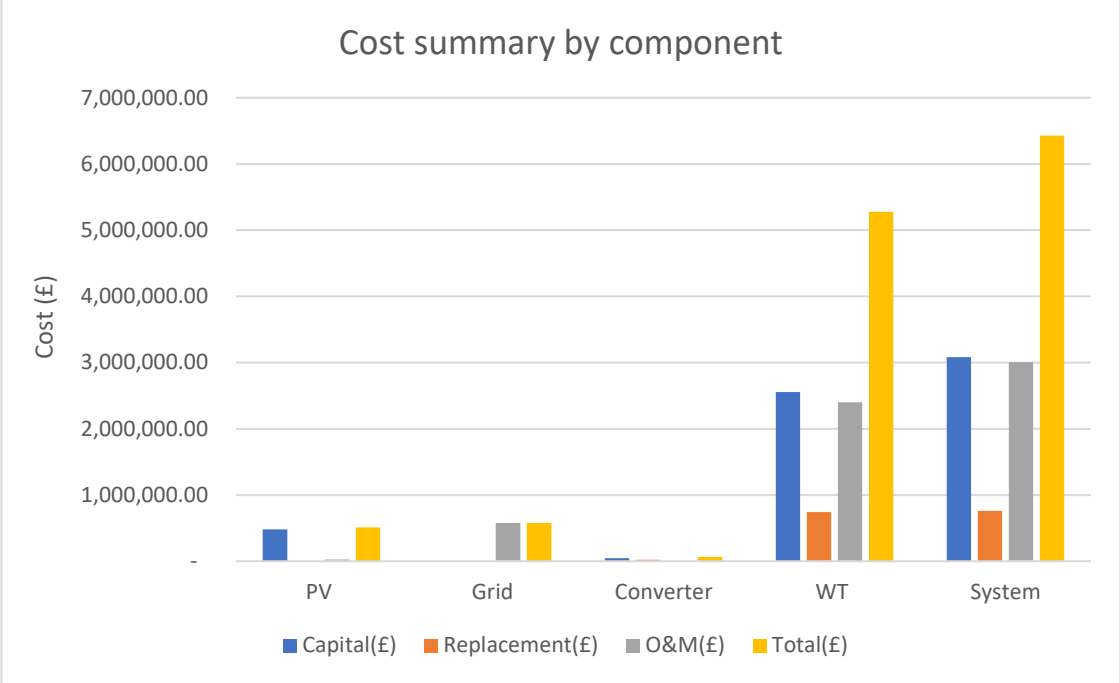

Figure 59: System Summary Cost by Component

Figure 59 demonstrates the cost breakdown of the energy system's components, including PV, grid, converter, wind turbine, and the overall system. The costs are categorised into capital costs, replacement costs, O&M costs, and total costs. The WT show substantial capital, replacement, and O&M costs, making them the most expensive component. The PV system, grid, and system converter have lower costs in all categories. The overall system cost is a combination of these components.

4.3 The Overall Discussion of key Findings

This dissertation has effectively demonstrated the benefits of integrating Wind and Solar renewable energies into the Queen's DHN, achieving significant improvements in energy and economic performance compared to the baseline model reliant on grid electricity alone.

From energy performance perspective, all hybrid configurations significantly increased the proportion of renewable energy utilised within the DHN. The combined WT and PV system achieved the highest renewable fraction, effectively addressing issues related to energy intermittency. This hybrid setup demonstrated superior energy production capabilities, thereby reducing the overall dependence on the grid for electricity supply. In contrast, the baseline model lacked the capacity to harness renewable energy, making it entirely reliant on external grid power. Santiago et al. (2024) state that the implementation of PV systems for self-consumption in urban environments not only contributes to substantial cost savings but also offers environmental benefits. The higher efficiency of larger PV modules, particularly under favourable conditions, further amplifies these economic advantages.

From an economic perspective, the hybrid systems outperformed the baseline model across several key metrics. The configuration combining WT with grid electricity proved to be the most cost-efficient, achieving the lowest NPC, LCOE, and LCOH compared to the baseline model. This configuration translated into reduced operational costs and increased affordability for consumers over the system's lifetime. The inclusion of PV panels further enhanced economic viability, with a notable reduction in both LCOE and NPC. The baseline model, by contrast, maintained higher NPC, LCOE, and LCOH values due to its exclusive reliance on grid electricity, leading to higher long-term costs and less favourable economic outcomes. Murshed et al. (2023) found that integrating WT with systems like Li-ion batteries and converters not only yields considerable economic savings but also bolsters system resilience, aligning with sustainable development goals. This is further supported by Baghel, Manjunath, and Kumar (2024), who highlighted the effectiveness of HRES in enhancing reliability and reducing costs. Their study, which included solar PV, WT, and additional components like hydrogen fuel cells and electrolysers, underscores the potential of such systems in achieving competitive pricing for DHNs.

These outcomes underscore the hybrid system's crucial role in minimising costs for the DHN, enabling it to provide heat at more competitive prices. This promotes the adoption of renewable energy solutions and supports long-term sustainability objectives.

4.3.1 Limitations and Future Work of the Study

While the dissertation offers important insights on incorporating renewable energy sources into the Queen's Quay DHN, further research and practical testing is needed to ensure the effectiveness and scalability of the proposed solutions.

The study primarily relies on simulated data and models, which may not fully capture the complexities and variations of real-world scenarios. It is important to acknowledge that this project is based on a single load profile and a single weather year, which may not represent future conditions. Obtaining actual input data for weather conditions, load demand, and component performance is crucial for improving accuracy and validation. Real-world variations in these factors could significantly impact system performance and financial outcomes.

The investigation focused on PV panels and wind turbines, excluding other potential renewable technologies such as biomass, geothermal energy, and advanced energy storage systems. Future studies can explore the integration of a wider range of renewable energy sources and storage technologies that could diversify energy solution, enhancing overall system resilience and efficiency.

Beyond the scope of this thesis, is the lack of storage solutions that were initially investigated but ultimately found to be costly and challenging to control within HOMER, resulting in their exclusion. Without energy storage, the system relies heavily on grid support to balance supply and demand, which can reduce overall efficiency and reliability. The forthcoming studies should focus on modelling energy storage technologies, such as batteries, using alternative software tools to overcome these constraints. Additionally, thermal storage is essential for achieving balance between supply and demand, enhancing system efficiency, and minimising operational costs by storing surplus heat during periods of low demand and releasing it during

periods of high demand. Therefore, it is necessary that future investigation gives priority to incorporating thorough thermal storage modelling.

The financial input data was collected to be as accurate as possible to match current market prices. However, assumptions were necessary when data were unavailable. The economic analysis is based on estimated electricity, gas and components prices for 2024, which may not reflect future costs. Future projects should consider grid rate schedules with day and night import and export tariffs to conduct a comprehensive economic analysis and determine the optimal financial configuration. Likewise, future component costs are expected to decrease due to technological advancements and economies of scale, introducing uncertainties in financial projections.

To summarise, time constraints limited the scope of the study, preventing a more in-depth examination of additional renewable energy sources and storage alternatives. Later studies should attempt to undertake a comprehensive and extensive analysis that encompasses a wider range of renewable energy sources and storage technologies, along with an in-depth examination of their economic and technical viability.

5.0 Conclusion

This dissertation has examined the integration and modelling of hybrid renewable power systems (HRPS) within the Queen's Quay District Heating Network (DHN). By leveraging the capabilities of photovoltaic (PV) panels and wind turbines (WT), the study aimed to reduce electricity and heating costs, thereby increasing end-user connectivity to the DHN system.

Through a comprehensive methodology encompassing resource assessment, load estimation, and system simulation, the study has demonstrated that HRPS can significantly improve both economic and energy performance metrics.

The findings showed that grid-connected HRPS offer substantial benefits. The system combining wind turbines with the grid emerged as the most cost-effective solution, while the combination of PV panels and WT provided a balanced and reliable energy supply. These configurations notably improved NPC, LCOE and LCOH, underscoring their economic viability and potential to attract interest and investment in these solutions.

Nevertheless, the research also highlighted several limitations that need to be addressed to enhance the reliability and scalability of the proposed systems. The reliance on simulated data and models does not entirely capture the complexities and variations of real-world conditions, which could affect the system's performance and financial outcomes. Moreover, the assumptions made regarding input parameters, component costs, and the use of a single weather and load profile further restrict the applicability of the findings. Future research should focus on incorporating comprehensive real-world data for weather patterns, load demands, and component performance to enhance accuracy.

In summary, this thesis provides a foundation for integrating renewable energy sources into district heating networks. Demonstrating the significant potential of HRPS to lower electricity, heating costs and enhance the reliability of energy supply. Addressing the identified limitations through further research and practical implementation will be crucial to fully harnessing the benefits of these systems and promoting sustainable energy practices.

6.0 References

1. Aberilla, J.M., Gallego-Schmid, A., Stamford, L. and Azapagic, A. (2020) 'Design and environmental sustainability assessment of small-scale off-grid energy systems for remote rural communities. *Applied Energy*, *258*, p.114004. available at: https://www.sciencedirect.com/science/article/pii/S0306261919316915 (accessed: 01 August 2024)

2. Abul, S.B., Muhammad, E.H., Tabassum, M., Muscat, O., Molla, M.E., Ashraf, A. and Ahmed, J. (2020) 'Feasibility study of solar power system in residential area'. *International Journal of Innovation in Computational Science and Engineering (IJICSE)*, *1*(1), pp.10-17. Available at: https://www.researchgate.net/profile/Mujahid-Tabassum/publication/341580054_Feasibility_Study_of_Solar_Power_System_in_Residential_Area/links/5ec839d0458515626cc301bca/Feasibility-Study-of-Solar-Power-System-in-Residential-Area.pdf (accessed: 03 August 2024)

3. Ahmed, A.A., Didane, D.H., Hussein, B.A., Al-Alimi, S., Manshoor, B. and Saif, Y. (2024) 'Techno-Economic Analysis of Off-Grid PV Solar System for Residential Building Load: A Case Study in Baidoa, Somalia'. International Journal of Integrated Engineering, 16(1), pp.178-188. Available at: https://penerbit.uthm.edu.my/ojs/index.php/ijie/article/view/14217 (accessed: 09 August 2024)

4. Alam, F. and Jin, Y. (2023) 'The Utilisation of Small Wind Turbines in Built-Up Areas: Prospects and Challenges'. *Wind*, *3*(4), pp.418-438. Available at: https://www.mdpi.com/2674-032X/3/4/24 (accessed: 03 August 2024)

5. Al-Tajer, Y. and Poullikkas, A. (2015) 'Parametric analysis for the implementation of wind power in United Arab Emirates'. *Renewable and Sustainable Energy Reviews*, *52*, pp.635-644. Available at: https://www.sciencedirect.com/science/article/abs/pii/S1364032115008163 (accessed: 31 July 2024)

6. Amole, A.O., Oladipo, S., Olabode, O.E., Makinde, K.A. and Gbadega, P. (2023) 'Analysis of grid/solar photovoltaic power generation for improved village energy supply: A case of Ikose in Oyo State Nigeria'. *Renewable Energy Focus*, *44*, pp.186-211. available at: https://www.sciencedirect.com/science/article/abs/pii/S1755008423000030 (accessed: 31 July 2024)

7. An introduction to river water ammonia heat pumps for district heating, Star Renewable Energy. (No date) Available at: https://www.neatpumps.com/blog/an-introduction-to-river-water-ammonia-heat-pumps-for-district-heating/ (accessed: 01 August 2024)

8. *Applied energy*, *87*(12), pp.3611-3624. Available at: https://www.sciencedirect.com/science/article/abs/pii/S030626191000228X (accessed: 01 August 2024)

9. Aragon, V., James, P.A. and Gauthier, S. (2022) 'The influence of weather on heat demand profiles in UK social housing tower blocks'. *Building and Environment*, *219*, p.109101. available at: https://www.sciencedirect.com/science/article/pii/S0360132322003389 (accessed: 01 August 2024)

10. Auer, M. (2019) 'Renewable Energy Supplied District Heating for a Scottish Community Utilising Heat Pumps: Isle of Barra Future Heating Case Study

(Doctoral dissertation, Master Thesis, University of Strathclyde, 2019'. available at: https://www.researchgate.net/profile/Markus-Auer-4/publication/361742758_Renewable_Energy_Supplied_District_Heating_for_a_Scottish_Community_Utilising_Heat_Pumps_Isle_of_Barra_Future_Heating_Case_Study/links/62c301249a17145f5f45f099/Renewable-Energy-Supplied-District-Heating-for-a-Scottish-Community-Utilising-Heat-Pumps-Isle-of-Barra-Future-Heating-Case-Study.pdf (accessed: 31 July 2024)

11. Awan, A.B., Zubair, M., Sidhu, G.A.S., Bhatti, A.R. and Abo-Khalil, A.G. (2019) 'Performance analysis of various hybrid renewable energy systems using battery, hydrogen, and pumped hydro-based storage units'. *International Journal of Energy Research*, *43*(12), pp.6296-6321. Available at: https://onlinelibrary.wiley.com/doi/full/10.1002/er.4343?casa_token=hud0svtcmhUAAAAA%3A6tSvfbHLezwt_5VdxVSyHL8_Xkzdp8pobzru0lKSlSw1q_qw75lZlvrvoOaLBSB15F2pvmlItUxe8N1C&fbclid=IwY2xjawEbal9leHRuA2FlbQIxMAABHXxCgBTspaK0BzTiDRm2kJFxcNWsMB51dNePtX0BU95BXPSi1qN1-J3kXw_aem_Zb8d0k-nnJxcVTyPGfe1BQ (accessed: 03 August 2024)

12. Ayub, Z. (2016) 'World's largest ammonia heat pump (14 MWh) for district heating in Norway—a case study. *Heat Transfer Engineering*, *37*(3-4), pp.382-386'. Available at: https://www.tandfonline.com/doi/abs/10.1080/01457632.2015.1052716 (accessed: 01 August 2024)

13. Baghel, N., Manjunath, K. and Kumar, A. (2024) 'Techno-economic analysis of hybrid renewable power generation system under different climatic zones in India'. *Electrical Engineering*, pp.1-16. Available at: https://link.springer.com/article/10.1007/s00202-024-02318-7 (accessed: 02 August 2024)
14. Bazdar, E. and Shirzadi, N. (2017) 'Economic Analysis and Simulation of Solar PV, Wind Turbine Hybrid Energy System Using HOMER pro'. *Journal*

of Solar Energy Research, *2*(3), pp.53-58. Available at: https://jser.ut.ac.ir/article_63944.html (accessed: 01 August 2024)

15. Brown, A., Foley, A., Laverty, D., McLoone, S. and Keatley, P. (2022) 'Heating and cooling networks: A comprehensive review of modelling approaches to map future directions'. Energy, 261, p.125060. available at: https://www.sciencedirect.com/science/article/pii/S0360544222019557 (accessed: 31 July 2024)

16. Buffa, S., Cozzini, M., D'antoni, M., Baratieri, M. and Fedrizzi, R. (2019) '5th generation district heating and cooling systems: A review of existing cases in Europe'. Renewable and Sustainable Energy Reviews, 104, pp.504-522. available at: https://www.sciencedirect.com/science/article/pii/S1364032118308608 (accessed: 31 July 2024)

17. Canadian Solar CS6U-330P 330W MAXPOWER Solar Panel. (No date). Available at: https://www.solarelectricsupply.com/canadian-solar-cs6u-330p-330w-maxpower-solar-panel?fbclid=IwY2xjawEbZ9NleHRuA2FlbQIxMAABHfKuH4a0W3fmROzjk2BoBk-aSkpmYuFmI7OjHKvfdJNV2d2h75LukQwXjw_aem_h4Gc67NfaxsXvHunMlV8gw (accessed: 03 August 2024)

18. Carroll, P., Chesser, M. and Lyons, P. (2020) 'Air Source Heat Pumps field studies: A systematic literature review'. *Renewable and sustainable energy reviews*, *134*, p.110275. available at: https://www.sciencedirect.com/science/article/pii/S1364032120305621 (accessed: 01 August 2024)

19. Chmiel, Z. and Bhattacharyya, S.C. (2015) ‘Analysis of off-grid electricity system at Isle of Eigg (Scotland): Lessons for developing countries’. *Renewable Energy*, *81*, pp.578-588. Available at: https://www.sciencedirect.com/science/article/pii/S0960148115002438 (accessed: 03 August 2024)

20. Chua, K.J., Chou, S.K. and Yang, W.M. (2010) ‘Advances in heat pump systems: A review’.

21. Cui, Y., Zhu, J., Zoras, S., Qiao, Y. and Zhang, X. (2020). Energy performance and life cycle cost assessments of a photovoltaic/thermal assisted heat pump system. *Energy*, 206, p.118108. available at: https://www.sciencedirect.com/science/article/abs/pii/S0360544220312159 (accessed: 09 August 2024)

22. Clydebank (West Dunbartonshire) weather. (2024). Available at: https://www.metoffice.gov.uk/weather/forecast/gcuy5b33x#?date=2024-07-18 (Accessed: 18 June 2024).

23. Cosla. (2024) ‘New pay offer for Scotland’s council workforce. Available at: https://www.cosla.gov.uk/news/2024/new-pay-offer-for-scotlands-council-workforce (Accessed: 22 July 2024)

24. Cutting, E. (2020) The Integration of Renewable Technologies to Provide Domestic Heat: Grid Demand, Carbon and Financial Impacts. available at: https://www.esru.strath.ac.uk/Documents/MSc_2020/Cutting.pdf (accessed: 31 July 2024)
25. Danish district heating – The heat of the moment (2020) available at: https://www.cibsejournal.com/technical/europes-hottest-city/ (accessed: 03 August 2024)

26. De Bartolo, C. (2015) Strategies for harnessing and integrating renewables into electricity consumption and their application to ecovillages. Available at: https://www.esru.strath.ac.uk/Documents/MSc_2015/DeBartolo.pdf accessed: 31 July 2024)
27. Department for Energy Security and Net Zero (2024) Heat networks, GOV.UK. Available at: https://www.gov.uk/government/collections/heat-networks (Accessed: 17 July 2024).
28. Deshmukh, M.K. and Deshmukh, S.S. (2008) 'Modeling of hybrid renewable energy systems'. Renewable and sustainable energy reviews, 12(1), pp.235-249. Available at: https://www.sciencedirect.com/science/article/abs/pii/S1364032106001134 (accessed: 31 July 2024)
29. Diyoke, C. (2019) 'A new approximate capacity factor method for matching wind turbines to a site: case study of Humber region, UK'. *International Journal of Energy and Environmental Engineering*, *10*(4), pp.451-462. Available at: https://link.springer.com/article/10.1007/s40095-019-00320-5 (accessed: 03 August 2024)
30. Djurić Ilić, D. (2020) 'Classification of measures for dealing with district heating load variations—a systematic review'. Energies, 14(1), p.3. available at: https://www.mdpi.com/1996-1073/14/1/3 (accessed: 01 August 2024)
31. El-Houari, H., Allouhi, A., Rehman, S., Buker, M.S., Kousksou, T., Jamil, A. and El Amrani, B. (2019) 'Design, simulation, and economic optimization of an off-grid photovoltaic system for rural electrification'. Energies, 12(24), p.4735. Available at: https://www.mdpi.com/1996-1073/12/24/4735 (accessed: 31 July 2024)
32. Ewing, G. (2020) '5th generation district heating and cooling retrofit a case study'. *The University of Strathclyde*. available at: https://www.esru.strath.ac.uk/Documents/MSc_2020/Ewing.pdf (accessed: 31 July 2024)
33. Fadlallah, S.O., Serradj, D.E.B. and Sedzro, D.M. (2021) 'Is this the right time for Sudan to replace diesel-powered generator systems with wind turbines?'. *Renewable Energy*, *180*, pp.40-54. Available at: https://www.sciencedirect.com/science/article/abs/pii/S0960148121011782 (accessed: 31 July 2024)

34. Farahmand, F., Kotian, S., Maliat, A. and Ghahremanlou, D. (2024) 'Hybrid Energy System Development for Natuashish'. European Journal of Electrical Engineering and Computer Science, 8(2), pp.71-76. Available at: https://www.ejece.org/index.php/ejece/article/view/613 (accessed: 04 August 2024)

35. Fitzgerald, N., Foley, A.M. and McKeogh, E. (2012) 'Integrating wind power using intelligent electric water heating'. *Energy*, *48*(1), pp.135-143. Available at: https://www.sciencedirect.com/science/article/abs/pii/S0360544212002058 (accessed: 31 July 2024)
36. Flicker, J. and Gonzalez, S. (2005) 'June. Performance and reliability of PV inverter component and systems due to advanced inverter functionality'. In *2015 IEEE 42nd Photovoltaic Specialist Conference (PVSC)* (pp. 1-5). IEEE. Available at: https://ieeexplore.ieee.org/abstract/document/7355978 (accessed: 04 August 2024)
37. Get energy price cap standing charges and unit rates by region. (No date). Available at: https://www.ofgem.gov.uk/energy-advice-households/get-energy-price-cap-standing-charges-and-unit-rates-region (accessed: 01 August 2024)
38. Ghenai, C. and Bettayeb, M. (2020) 'Design and optimization of grid-tied and off-grid solar PV systems for super-efficient electrical appliances'. Energy Efficiency, 13(2), pp.291-305. Available at: https://link.springer.com/article/10.1007/s12053-019-09773-3 (accessed: 31 July 2024)
39. Givler, T. and Lilienthal, P. (2005) '*Using HOMER software, NREL's micropower optimization model, to explore the role of gen-sets in small solar power systems; case study: Sri Lanka* (No. NREL/TP-710-36774)'. National Renewable Energy Lab.(NREL), Golden, CO (United States). Available at: https://www.nrel.gov/docs/fy05osti/36774.pdf (accessed: 03 August 2024)
40. Global solar atlas. (No date). Available at: https://globalsolaratlas.info/downloadhttps://globalsolaratlas.info/download (Accessed: 17 June 2024).

41. Global wind atlas. (No date). Available at: https://globalwindatlas.info/fr (Accessed: 18 June 2024).

42. Grassi, W. (2017) '*Heat pumps: fundamentals and applications*'. Springer. Available at: https://books.google.co.uk/books?hl=en&lr=&id=h5wwDwAAQBAJ&oi=fnd&pg=PR5&dq=Grassi,+W.+(2018)+Heat+pumps:+Fundamentals+and+applications.+Cham:+Springer+International+Publishing%E2%80%AF:+Imprint%E2%80%AF:+Springer.+&ots=ra92EW8liM&sig=I0qhnTHfztikVfI7iHpP5cWLWh0#v=onepage&q&f=false (accessed: 01 August 2024)

43. Hassan, Q., Jaszczur, M., Hafedh, S.A., Abbas, M.K., Abdulateef, A.M., Hasan, A., Abdulateef, J. and Mohamad, A. (2022) 'Optimizing a microgrid photovoltaic-fuel cell energy system at the highest renewable fraction'. International Journal of Hydrogen Energy, 47(28), pp.13710-13731. Available at: https://www.sciencedirect.com/science/article/abs/pii/S0360319922007200 (accessed: 09 August 2024)

44. Hedegaard, K. (2013) 'Wind power integration with heat pumps, heat storages, and electric vehicles'. *Energy Syst Anal Modell*. Available at: https://orbit.dtu.dk/en/publications/wind-power-integration-with-heat-pumps-heat-storages-and-electric (accessed: 31 July 2024)

45. Hong, L., Lund, H., Mathiesen, B.V. and Möller, B. (2013) '2050 pathway to an active renewable energy scenario for Jiangsu province'. Energy Policy, 53, pp.267-278. Available at: https://www.sciencedirect.com/science/article/abs/pii/S0301421512009408 (accessed: 31 July 2024)

46. Jensen, J.K., Ommen, T., Markussen, W.B. and Elmegaard, B. (2017) 'Design of serially connected district heating heat pumps utilising a geothermal heat source'. Energy, 137, pp.865-877. available at:

https://www.sciencedirect.com/science/article/abs/pii/S0360544217305728 (accessed: 31 July 2024)

47. Jensen, J.K., Ommen, T., Reinholdt, L., Markussen, W.B. and Elmegaard, B. (2018) 'Heat pump COP, part 2: Generalized COP estimation of heat pump processes'. In 13th IIR Gustav Lorentzen Conference on Natural Refrigerants (GL2018) (pp. 1136-1145). International Institute of Refrigeration. available at: https://orbit.dtu.dk/en/publications/heat-pump-cop-part-2-generalized-cop-estimation-of-heat-pump-proc (accessed: 01 August 2024)
48. Kamel, R.S., Fung, A.S. and Dash, P.R. (2015) 'Solar systems and their integration with heat pumps: A review'. *Energy and buildings*, *87*, pp.395-412. Available at: https://www.sciencedirect.com/science/article/abs/pii/S037877881400961X (accessed: 01 August 2024)
49. Kansara, B.U. (no date) 'Feasibility investigation of dispatch strategies and energy storage systems of microgrid in islanded and grid connected modes'. Available at: http://hdl.handle.net/10603/34708 (accessed: 09 August 2024)
50. Khan, F.A., Pal, N. and Saeed, S.H. (2021) 'Stand-alone hybrid system of solar photovoltaics/wind energy resources: an eco-friendly sustainable approach'. In *Renewable Energy Systems* (pp. 687-705). Academic Press. Available at: https://www.sciencedirect.com/science/article/pii/B9780128200049000309 (accessed: 01 August 2024)
51. Khalil, L., Bhatti, K.L., Awan, M.A.I., Riaz, M., Khalil, K. and Alwaz, N. (2021) 'Optimization and designing of hybrid power system using HOMER pro'. *Materials Today: Proceedings*, *47*, pp.S110-S115. Available at: https://www.sciencedirect.com/science/article/abs/pii/S2214785320345016 (accessed: 01 August 2024)
52. Kroposki, B., Johnson, B., Zhang, Y., Gevorgian, V., Denholm, P., Hodge, B.M. and Hannegan, B. (2017) 'Achieving a 100% renewable grid: Operating electric power systems with extremely high levels of variable renewable energy'. *IEEE Power and energy magazine*, *15*(2), pp.61-73. Available at:

https://ieeexplore.ieee.org/abstract/document/7866938 (accessed: 04 August 2024)

53. Lambert, T., Gilman, P. and Lilienthal, P. (2006) 'Micropower system modeling with HOMER'. *Integration of alternative sources of energy*, *1*(1), pp.379-385. Available at: https://www.pspb.org/e21/media/HOMERModelingInformation.pdf (accessed: 03 August 2024)
54. Li, C., Zhou, D., Wang, H., Lu, Y. and Li, D. (2020) 'Techno-economic performance study of stand-alone wind/diesel/battery hybrid system with different battery technologies in the cold region of China'. *Energy*, *192*, p.116702. available at: https://www.sciencedirect.com/science/article/abs/pii/S0360544219323977 (accessed: 01 August 2024)
55. Lindström, H.O. (1985) 'Experiences with a 3.3 MW heat pump using sewage water as heat source'. *Journal of heat recovery systems*, *5*(1), pp.33-38. Available at: https://www.sciencedirect.com/science/article/abs/pii/0198759385901195 (accessed: 01 August 2024)
56. Liu, G., Rasul, M.G., Amanullah, M.T.O. and Khan, M.M.K. (2012) 'Techno-economic simulation and optimization of residential grid-connected PV system for the Queensland climate'. *Renewable Energy*, *45*, pp.146-155. available at: https://www.sciencedirect.com/science/article/abs/pii/S0960148112001796 (accessed: 31 July 2024)
57. Local renewables. (No date). Available at: https://www.esru.strath.ac.uk/EandE/Web_sites/18-19/cleanheat/renewables.html (accessed: 03 August 2024)
58. Lund, H. (2007) 'Renewable energy strategies for sustainable development'. energy, 32(6), pp.912-919. Available at: https://www.sciencedirect.com/science/article/abs/pii/S036054420600301X (accessed: 31 July 2024)

59. Lund, H., Østergaard, P.A., Chang, M., Werner, S., Svendsen, S., Sorknæs, P., Thorsen, J.E., Hvelplund, F., Mortensen, B.O.G., Mathiesen, B.V. and Bojesen, C. (2018) 'The status of 4th generation district heating: Research and results'. Energy, 164, pp.147-159. Available at: https://www.sciencedirect.com/science/article/abs/pii/S0360544218317420 (accessed: 31 July 2024)
60. Lund, H., Werner, S., Wiltshire, R., Svendsen, S., Thorsen, J.E., Hvelplund, F. and Mathiesen, B.V. (2014) '4th Generation District Heating (4GDH): Integrating smart thermal grids into future sustainable energy systems'. *energy*, *68*, pp.1-11. available at: https://www.sciencedirect.com/science/article/abs/pii/S0360544214002369 (accessed: 31 July 2024)
61. Lyden, A., Flett, G. and Tuohy, P.G. (2021) PyLESA: A Python modelling tool for planning-level Local, integrated, and smart Energy Systems Analysis. SoftwareX, 14, p.100699. Available at: https://www.sciencedirect.com/science/article/pii/S2352711021000443 (accessed: 09 August 2024)
62. Lyden, A., Pepper, R. and Tuohy, P.G. (2018) 'A modelling tool selection process for planning of community scale energy systems including storage and demand side management'. Sustainable cities and society, 39, pp.674-688. Available at: https://www.sciencedirect.com/science/article/pii/S2210670717309824 (accessed: 03 August 2024)
63. Lyden, A. and Tuohy, P. (2019) 'November. Heat pump and thermal storage sizing with time-of-use electricity pricing'. In *The 13th International Renewable Energy Storage Conference 2019 (IRES 2019)* (pp. 29-40). Atlantis Press. Available at: https://pureportal.strath.ac.uk/en/publications/heat-pump-and-thermal-storage-sizing-with-time-of-use-electricity (accessed: 03 August 2024)
64. McKeown, C. (2020) 'Investigation into Decarbonising the District Heating Network at West Whitlawburn Housing Co-operative'. Dissertation. Available at: https://www.esru.strath.ac.uk/Documents/MSc_2020/McKeown.pdf (accessed: 01 August 2024)

65. Millar, M.A. (2022) *Delivering district energy for a net zero society* (Doctoral dissertation, University of Glasgow). Available at: https://theses.gla.ac.uk/82897/ (accessed: 31 July 2024)
66. Millar, M.A., Elrick, B., Jones, G., Yu, Z. and Burnside, N.M. (2020) 'Roadblocks to low temperature district heating'. *Energies*, *13*(22), p.5893. available at: https://www.mdpi.com/1996-1073/13/22/5893 (accessed: 01 August 2024)
67. Mokheimer, E.M., Al-Sharafi, A., Habib, M.A. and Alzaharnah, I. (2015) 'A new study for hybrid PV/wind off-grid power generation systems with the comparison of results from homer'. *International Journal of Green Energy*, *12*(5), pp.526-542. Available at: https://www.tandfonline.com/doi/abs/10.1080/15435075.2013.833929 (accessed: 01 August 2024)
68. Mondal, M.A.H. and Islam, A.S. (2011) 'Potential and viability of grid-connected solar PV system in Bangladesh'. *Renewable energy*, *36*(6), pp.1869-1874. available at: https://www.sciencedirect.com/science/article/abs/pii/S096014811000546X (accessed: 31 July 2024)
69. Moran, L. (2021) A new era for heat: Queens Quay heat pump. Available at: https://www.cibsejournal.com/case-studies/a-new-era-for-heat-queens-quay-heat-pump/ (accessed: 01 August 2024)
70. Murshed, M., Chamana, M., Schmitt, K.E.K., Bhatta, R., Adeyanju, O. and Bayne, S. (2023) 'Design and Performance Analysis of a Grid-Connected Distributed Wind Turbine'. *Energies*, *16*(15), p.5778. Available at: https://www.mdpi.com/1996-1073/16/15/5778 (accessed: 02 August 2024)
71. Nian, V., Sun, Q., Ma, Z. and Li, H. (2016) 'A comparative cost assessment of energy production from central heating plant or combined heat and power plant'. Energy Procedia, 104, pp.556-561. Available at: https://www.sciencedirect.com/science/article/pii/S1876610216316526 (accessed: 09 August 2024)
72. Roser, M. (2024) 'Why did renewables become so cheap so fast?'. Our World in Data. Available at: https://ourworldindata.org/cheap-renewables-growth?utm_source=substack&utm_medium=email (accessed: 09 August 2024)

73. Olabi, A.G., Mahmoud, M., Obaideen, K., Sayed, E.T., Ramadan, M. and Abdelkareem, M.A. (2023) 'Ground source heat pumps: Recent progress, applications, challenges, barriers, and role in achieving sustainable development goals based on bibliometric analysis'. *Thermal Science and Engineering Progress*, *41*, p.101851. available at: https://www.sciencedirect.com/science/article/abs/pii/S2451904923002044 (accessed: 01 August 2024)

74. Oyedepo, S.O. (2012) 'Energy and sustainable development in Nigeria: the way forward'. *Energy, Sustainability and Society*, *2*, pp.1-17. Available at: https://doi.org/10.1186/2192-0567-2-15 (Accessed: 16 July 2024)

75. Pamuk, N. (2024) 'Techno-economic feasibility analysis of grid configuration sizing for hybrid renewable energy system in Turkey using different optimization techniques'. *Ain Shams Engineering Journal*, *15*(3), p.102474. Available at: https://www.sciencedirect.com/science/article/pii/S2090447923003635 (accessed: 01 August 2024)

76. Pawar, N. and Nema, P. (2018) 'December. Techno-economic performance analysis of grid connected PV solar power generation system using HOMER software'. In *2018 IEEE International Conference on Computational Intelligence and Computing Research (ICCIC)* (pp. 1-5). IEEE. Available at: https://ieeexplore.ieee.org/abstract/document/8782411 (accessed: 01 August 2024)

77. Pieper, H., Ommen, T., Jensen, J.K., Elmegaard, B. and Markussen, W.B. (2020) 'Comparison of COP estimation methods for large-scale heat pumps used in energy planning'. Energy, 205, p.117994. available at: https://www.sciencedirect.com/science/article/abs/pii/S0360544220311014 (accessed: 31 July 2024)

78. Purlu, M.İ.K.A.İ.L. and Ozkan, U. (2023) 'Economic and environmental analysis of grid-connected rooftop photovoltaic system using HOMER'. *Turk. J. Electr. Power Energy Syst*, *3*(1), pp.39-46. available at: https://tepesjournal.org/Content/files/sayilar/7/TEPES_February_2023-39-46.pdf (accessed: 31 July 2024)

79. Qiu, K. and Entchev, E. (2024) 'Modeling, design and optimization of integrated renewable energy systems for electrification in remote communities'. *Sustainable Energy Research*, *11*(1), p.10. Available at: https://link.springer.com/article/10.1186/s40807-024-00103-5 (accessed: 02 August 2024)

80. Queens Quay Heat Network. (No date). Available at: https://www.vitalenergi.co.uk/our-work/queens-quay-heat-network-design/ (Accessed: 16 May 2024).

81. Queens Quay: Water Source Heat Pump Scheme in Scotland (no date) available at: https://www.vitalenergi.co.uk/our-work/queens-quay-heat-network-design/ (16 may 2024)

82. Rahman, M.M., Baky, M.A.H. and Islam, A.S. (2017) 'Electricity from wind for off-grid applications in Bangladesh: a techno-economic assessment'. *International Journal of Renewable Energy Development*, *6*(1), pp.55-64. Available at: https://d1wqtxts1xzle7.cloudfront.net/73310532/8da575019ece160eeaacd946e484fcbdb8ad-libre.pdf?1634836036=&response-content-disposition=inline%3B+filename%3DElectricity_from_Wind_for_Off_Grid_Appli.pdf&Expires=1722530195&Signature=NTP79O73DaVwNti2uFwIxhLfK0obHvB0U4w75X-HfnFyuy4Tn4AlvyIR~W2KSGCMZc0VbM3gjlqGs1IUGjlpCj1IVpUF1xtRLn5~loWKrHvcTXK6YhTPMBjywyKpeGLbOrrOR4acTzvzHkny3zTUNlE8MuVpufcIxZis8vUWRiBW29YhBdJgGvGk3-ZzPLfgNaciWzpHYSUba07G8mHSC1eUM4GYLIeYeppPwt9WyajyP59K~k~uhB3caMENLxNBCcPNVEtsyHVT2nUN69JwqZ5~dip3YWyMoz7tqxhrAcJIQLJbZ~noq1wEQ01RgrHWfT0ukIoj7QBSUYdvBmzKZw__&Key-Pair-Id=APKAJLOHF5GGSLRBV4ZA (accessed: 01 August 2024)

83. Ram, P. (2017) '*Investigation of Renewable Power house by 2030 in Cuba using Homer*'. Thesis. Available at: https://www.esru.strath.ac.uk/Documents/MSc_2017/Ram.pdf (accessed: 01 August 2024)

84. Rehman, S. (2004) 'Wind energy resources assessment for Yanbo, Saudi Arabia', *Energy Conversion and Management*, 45(13–14), pp. 2019–2032. Available at:

https://www.sciencedirect.com/science/article/abs/pii/S0196890403003467 (accessed: 31 July 2024)

85. Reiners, T., Gross, M., Altieri, L., Wagner, H.J. and Bertsch, V. (2021) 'Heat pump efficiency in fifth generation ultra-low temperature district heating networks using a wastewater heat source'. *Energy*, *236*, p.121318. available at: https://www.sciencedirect.com/science/article/abs/pii/S0360544221015668 (accessed: 01 August 2024)
86. Roy, D. (2023) 'Modelling an off-grid hybrid renewable energy system to deliver electricity to a remote Indian island'. *Energy Conversion and Management*, *281*, p.116839. Available at: https://www.sciencedirect.com/science/article/abs/pii/S0196890423001851 (accessed: 02 August 2024)
87. Said, T.R., Kichonge, B. and Kivevele, T. (2024) 'optimal design and analysis of a grid-connected hybrid renewable energy system using HOMER Pro: A case study of Tumbatu Island, Zanzibar'. *Energy Science & Engineering*, *12*(5), pp.2137-2163. Available at: https://scijournals.onlinelibrary.wiley.com/doi/full/10.1002/ese3.1735 (accessed: 02 August 2024)
88. Sarbu, I., Mirza, M. and Muntean, D. (2022) 'Integration of renewable energy sources into low-temperature district heating systems: a review'. *Energies*, *15*(18), p.6523. available at: https://www.mdpi.com/1996-1073/15/18/6523 (accessed: 01 August 2024)
89. Scotland's carbon footprint 1998-2020. (2024) Available at: https://www.gov.scot/publications/scotlands-carbon-footprint-1998-2020-2/pages/material-footprint-for-scotland-experimental-statistics/ (Accessed: 30 June 2024).
90. Scottish Energy Statistics Hub. (2024) available at: https://scotland.shinyapps.io/Energy/?Section=RenLowCarbon&Subsection=RenElec&Chart=RenElecSources (accessed: 31 July 2024)
91. ScottishPower Tariffs, Prices & Reviews. (2024). Available at: https://www.electricityprices.org.uk/scottishpower-tariffs/ (accessed: 01 August 2024)
92. Scottish renewables (no date) STATISTICS. Energy Consumption by Sector. Available at: https://www.scottishrenewables.com/our-industry/statistics (accessed: 31 July 2024)

93. See, I., Lale, A., Marquez, P., Streiff, M.B., Wheeler, A.P., Tepper, N.K., Woo, E.J., Broder, K.R., Edwards, K.M., Gallego, R. and Geller, A.I. (2022) 'Case series of thrombosis with thrombocytopenia syndrome after COVID-19 vaccination—United States, December 2020 to August 2021'. *Annals of internal medicine*, *175*(4), pp.513-522. Available at: https://www.acpjournals.org/doi/full/10.7326/M21-4502 (accessed: 03 August 2024)
94. Sen, R. and Bhattacharyya, S.C. (2014) 'Off-grid electricity generation with renewable energy technologies in India: An application of HOMER'. *Renewable energy*, *62*, pp.388-398. Available at: https://www.sciencedirect.com/science/article/abs/pii/S0960148113003832 (accessed: 31 July 2024)
95. Shahzad, S.J.H., Kumar, R.R., Zakaria, M. and Hurr, M. (2017) 'Carbon emission, energy consumption, trade openness and financial development in Pakistan: a revisit'. *Renewable and Sustainable Energy Reviews*, *70*, pp.185-192. Available at: https://www.sciencedirect.com/science/article/abs/pii/S1364032116308401 (accessed: 03 August 2024)
96. Sinha, S. and Chandel, S.S. (2014) 'Review of software tools for hybrid renewable energy systems'. *Renewable and sustainable energy reviews*, *32*, pp.192-205. Available at: https://www.sciencedirect.com/science/article/abs/pii/S136403211400046X (accessed: 03 August 2024)
97. Slaihem, W.G. (2021) To Investigate Possibilities for Decarbonizing Glasgow Heating Systems. Available at: https://www.esru.strath.ac.uk/Documents/MSc_2021/Slaihem.pdf (accessed: 02 August 2024)
98. SNP. (2022) *Our bold plan to make Scotland net zero by 2045*, *Scottish National Party*. Available at: https://www.snp.org/net-zero-by-2045/ (Accessed: 16 July 2024).
99. Soloha, R., Pakere, I. and Blumberga, D. (2017) 'Solar energy use in district heating systems. A case study in Latvia'. Energy, 137, pp.586-594. Available at: https://www.sciencedirect.com/science/article/abs/pii/S0360544217307272 (accessed: 31 July 2024)

100. Türkay, B.E. and Telli, A.Y. (2011) 'Economic analysis of standalone and grid connected hybrid energy systems'. *Renewable energy*, *36*(7), pp.1931-1943. Available at: https://www.sciencedirect.com/science/article/abs/pii/S0960148110005616 (accessed: 01 August 2024)

101. UK's largest residential air -source heat pump halves the cost of energy for flats in hillpark. (No date). Available at: https://www.star-ref.co.uk/wp-content/uploads/2020/04/hillpark-air-source-heat-pump.pdf (accessed: 03 August 2024)

102. Vavoura, E. (2019) Exploring the potential of small-scale District Heating schemes based on renewable sources: A modelling approach based on an existing scheme at Findhorn Ecovillage. Available at: https://www.esru.strath.ac.uk/Documents/MSc_2019/Vavoura.pdf (accessed: 03 August 2024)

103. Viggers, H., Keall, M., Wickens, K. and Howden-Chapman, P. (2017) 'Increased house size can cancel out the effect of improved insulation on overall heating energy requirements'. *Energy Policy*, *107*, pp.248-257. Available at: https://www.sciencedirect.com/science/article/abs/pii/S0301421517302707 (accessed: 04 August 2024)

104. Wind Turbine Radar Interference. (No date). Available at: https://windexchange.energy.gov/projects/radar-interference?fbclid=IwY2xjawEbXa9leHRuA2FlbQIxMAABHb1DBaZuGn5scHNqhr8dV3p3SzN6WV9uw2YQMjQPMdzMrg1_MZB0f4vDTg_aem_QvmulRNvABzyv6tzPPZh_A (accessed: 03 August 2024)

7.0 Appendices

Appendix A: Wind Turbines Data sheets

WES 30/250

Start / Turbines / WES / 30/250

Pictures Datasheet Power curve Marketplace Spare

250 kW

Datasheet

Power

Rated power:	250.0 kW
Flexible power ratings:	-
Cut-in wind speed:	3.5 m/s
Rated wind speed:	13.0 m/s
Cut-out wind speed:	25.0 m/s
Survival wind speed:	60.0 m/s
Wind zone (DIBt):	-
Wind class (IEC):	Ib

Rotor

Diameter:	30.0 m
Swept area:	707.0 m²
Number of blades:	2
Rotor speed, max:	-
Tipspeed:	-
Type:	13.4m blade
Material:	carbon fiber reinforced epoxy
Manufacturer:	-
Power density 1:	353.6 W/m²
Power density 2:	2.8 m²/kW

LTW90 500 | 900 | 1,000 kW

DESIGN DATA

Rated power	500 | 900 | 1,000 kW
Hub height	60 / 65 / 80 / 97.5* m
Tip height max (upper end)	105 / 110 / 125 / 142 m
Wind class	IIIA / IIIA+ / S
Cut-in wind speed	3 m/s
Cut-out wind speed	25 m/s
Concept	Direct Drive 3-bladed upwind turbine with horizontal axis, variable speed and automatic pitch and yaw regulation

TOWER

	Segmented tubular steel tower
	Transformer and converter station in tower bottom

ROTOR

Rotor diameter	90 m
Swept area	6,404 m^2
Rotational speed	15 rpm
Tip speed	71 m/s
Blade material	GFRP-EP
Power and rotor speed control	Active pitch control

AEP - ESTIMATED ANNUAL ELECTRICAL PRODUCTION

	LTW90 500 kW	LTW90 900 kW	LTW90 1.000 kW
m/s	MWh/y	MWh/y	MWh/y
4.5	1,608	2,141	2,194
5.0	1,920	2,660	2,749
5.5	2,195	3,150	3,283
6.0	2,437	3,601	3,781
6.5	2,646	4,007	4,238
7.0	2,827	4,365	4,650
7.5	2,980	4,670	5,020

Enercon E-82 E2 2.000

2 MW

Datasheet

Power

Rated power:	2,000.0 kW
Flexible power ratings:	-
Cut-in wind speed:	2.0 m/s
Rated wind speed:	12.5 m/s
Cut-out wind speed:	34.0 m/s
Survival wind speed:	-
Wind zone (DIBt):	III
Wind class (IEC):	IIa

Rotor

Diameter:	82.0 m
Swept area:	5,281.0 m²
Number of blades:	3
Rotor speed, max:	18.0 U/min
Tipspeed:	77 m/s
Type:	AERO E-82
Material:	GFK / Epoxy
Manufacturer:	Enercon
Power density 1:	378.7 W/m²
Power density 2:	2.6 m²/kW

Appendix B: Carbon Intensity

The carbon intensity of the Scottish grid has been maintained below 0.050 kgCO2/kWh since 2017(Climate Change Plan Monitoring, 2023). Current forecast data shows the carbon intensity for South Scotland at 0.031 kgCO2/kWh and North Scotland at 0.032 kgCO2/kWh, both categorised as very low (Carbon Intensity, 2024). This reflects Scotland's successful integration of renewable energy sources into the grid, minimising the need for fossil fuels.

#	Region	Forecast Carbon Intensity (gCO_2/kWh)	Index
1	North East England	9	very low
2	South Scotland	31	very low
3	North Scotland	32	very low
4	North West England	64	low
5	North Wales & Merseyside	71	low
6	East England	84	low

CI current forecast (Carbon Intensity, 2024).